# EOS Contributions by the Earth Sciences Directorate Goddard Space Flight Center

Michael D. King, Editor
EOS Senior Project Scientist

August 28, 2003

# TABLE OF CONTENTS

Abstract

In 1991, NASA launched a comprehensive program to study the Earth as an environmental system, now called the Earth Science Enterprise. By using satellites and other tools to intensively study the Earth, we hope to expand our understanding of how natural processes affect us, and how we might be affecting them. Such studies will yield improved weather forecasts, tools for managing agriculture and forests, information for fishermen and local planners, and, eventually, the ability to predict how the climate will change in the future.

The Earth Science Enterprise has three main components: a series of Earth-observing satellites, an advanced data system, and teams of scientists who will study the data. Key areas of study include clouds; water and energy cycles; oceans; chemistry of the atmosphere; land surface; water and ecosystem processes; glaciers and polar ice sheets; and the solid Earth.

Phase I of the Earth Science Enterprise was comprised of focused, free-flying satellites, Space Shuttle missions, and various airborne and ground-based studies. Phase II began in December of 1999 with the launch of the first Earth Observing System (EOS) satellite Terra (formerly AM-1). EOS is the first observing system to offer integrated measurements of the Earth's processes. It consists of a science component and a data system supporting a coordinated series of polar-orbiting and low-inclination satellites for long-term global observations of the land surface, biosphere, solid Earth, atmosphere, and oceans. We have initiated an era of unprecedented observational capability for understanding the planet.

This document highlights the depth and breadth of scientific contributions made to the EOS program by the Earth Sciences Directorate at Goddard Space Flight Center. As such, it highlights the many contributions made in the area of algorithm development for various instruments onboard the EOS spacecraft, interdisciplinary science investigations, calibration facilities, validation activities, project scientist activities, and outreach.

## 1. Algorithm Development

### *a. MODIS*

#### 1) CALIBRATION AND CHARACTERIZATION OF MODIS (X. Xiong, W. L. Barnes, V. V. Salomonson)

Comprehensive efforts have been made by the MODIS Calibration Support Team (MCST) to operate, calibrate, and characterize the Terra and Aqua MODIS, to maintain the Level 1B (L1B) algorithms, to update the calibration parameters and to remove any artifacts due to instrument degradation or configuration changes. Overall, both instruments are performing according to their design characteristics. The L1B calibration algorithms are mature and stable and meeting or exceeding basic specifications; namely 5% absolute accuracy in radiances and 2% reflectance accuracy relative to the sun for the reflected solar bands and 1% accuracy in radiances for the thermal infrared bands. Based fundamentally on the rigor of these instrument calibration and characterization efforts (Salomonson et al. 2002, Barnes et al. 2002, Xiong et al. 2003), a wide variety of MODIS products for land, ocean, and atmospheric studies have been produced and validated and are being successfully utilized by the Earth science community. Details on the specific efforts and the attendant accomplishments are described below.

*Terra On-orbit Performance*

Adjustments made during the first few post-launch months enabled a optimal operational configuration that eliminated or substantially reduced the pre-launch identified crosstalk among the SMIR detectors. Terra MODIS has subsequently operated on-orbit in the following configurations:

- "A-side" electronics: from launch to October 31, 2000 (at launch setting)
- "B-side" electronics: from October 31, 2000 to June 15, 2001 (for more stable electronics)
- "A-side" electronics: from July 02, 2001 to September 17, 2002 (due to "B-side" power supply failure)
- "A-side" electronics with "B-side" formatter: September 17, 2002 to present (due to "A-side" formatter reset errors)

Over three and half years of on-orbit solar observations have revealed decreases in the wavelength dependent reflectance of the solar diffuser (SD) of 9.5% at 0.41 micrometer, 6% at 0.46 micrometer, and 3.5% at 0.55 micrometer. The degradation is determined using data from the SD stability monitor (SDSM) observations performed during each SD calibration sequence. The effect due to the change in SD reflectance is removed when computing the calibration coefficients. Recent spacecraft yaw maneuvers have been used to validate the SD degradation uniformity. The scan mirror has also experienced a wavelength dependent loss of reflectance. This loss is mirror side and angle of incidence (AOI) dependent. The

mirror has shown decreases of 11% (side 1) and 15% (side 2) at 0.41 micrometer and 6.5% (side 1) and 8.3% (side 2) at 0.44 micrometer respectively. These effects are corrected via the L1B look-up tables (LUTs).

Though it's in its 4th year of on-orbit operation, the Terra MODIS continues to perform at or above its signal-to-noise (SNR) specifications for most of the reflected solar band (RSB) detectors. In the current L1B software, two correction algorithms are used for RSB calibration: one removes the SWIR bands' thermal leak using B28 as a surrogate (or sending band) and the other reduces the crosstalk striping in B26 by assuming B5 is the primary source.

The thermal emissive bands' (TEBs') responses have shown good short- and long-term stability except for the expected changes at different operational configurations (Figure 1). On-orbit measurements of the TEB detectors' noise-equivalent-difference-in-temperature (NEdT) have also shown consistent results. Several detectors became noisy post launch (see band 30 detector 8 in Figure 1). The on-orbit TEB calibration is performed on a scan-by-scan basis using a blackbody (BB), except for B21 that uses fixed gains provided in the LUTs. An optical leak from B31 into B32-36 is also corrected in the L1B.

Recent spacecraft pitch maneuvers have provided data for updating the TEB response vs. scan angle (RVS). Radiometry for several bands will improve with the

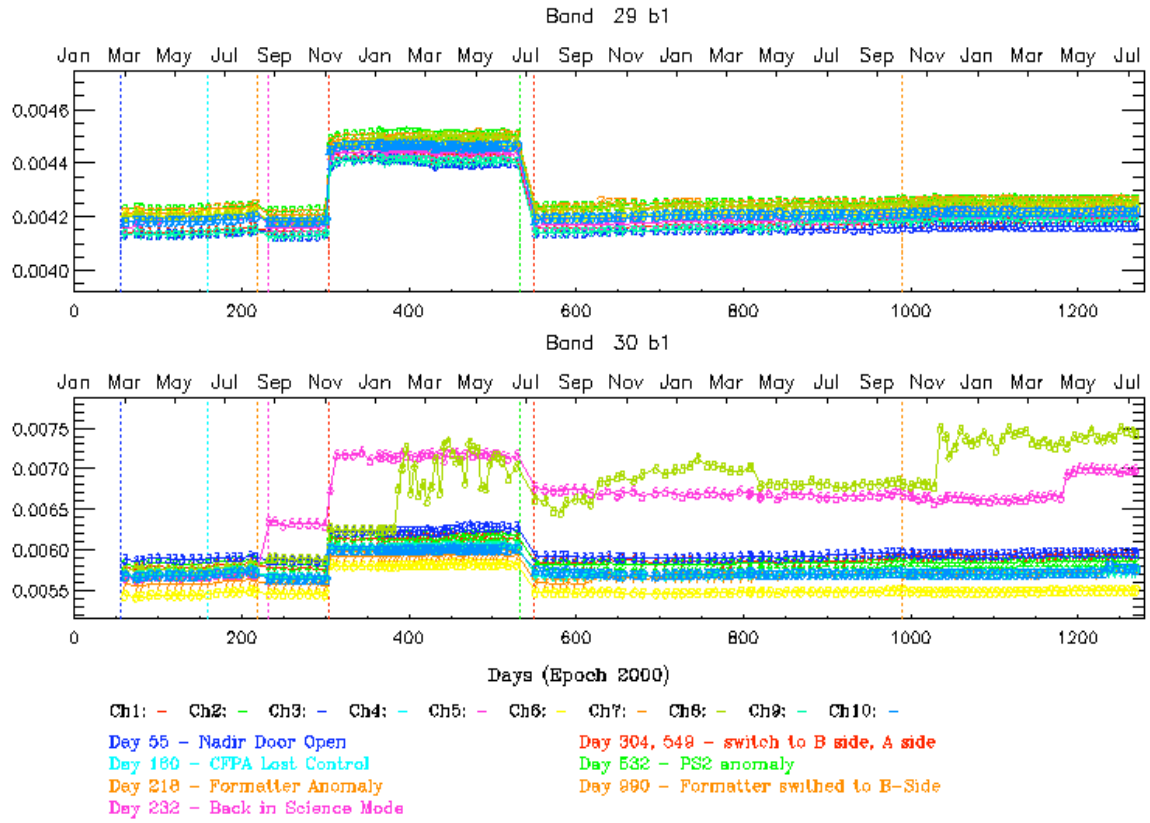


Figure 1. Terra MODIS bands 29 and 30 responses trending. Vertical lines mark the configuration changes and key instrument events.

newly derived RVS from the deep space pitch maneuvers. The band-to-band registration along scan and along track have been very stable since three months after launch. On-orbit spectral characterization results indicate the center wavelength shifts are less than 1nm, compared with pre-launch values for all reflective solar bands (Xiong et al. 2002a, b, c).

*Aqua On-orbit Performance*

Extensive pre-launch calibration and characterization together with improvements made based on the lessons learned from the PFM instrument have resulted in improved performance of the Aqua MODIS. Key improvements include better characterization of RVS, removal of the PC optical leak, and reduction of the SWIR thermal leak and electronic crosstalk among SMIR detectors. In addition, the gains of the 11 and 12 $\mu$m bands (B31 and B32) have been reduced to increase the resolution in the sea surface temperature measurements. This change, coupled with the high quality on-orbit calibration, has led to the quick validation of the Aqua SST product by the ocean science group.

Aqua MODIS concerns include the inoperable detectors in B6 and the out of specification band-to-band registration (BBR) for most bands as identified during pre-launch characterization. For the Aqua MODIS, there are three bands (33, 35, 36) that saturate when the blackbody temperature is above a certain value: 290K for B33, 295K for B35, and 300K for B36. To maintain continuous calibration during BB thermal cycling from the instrument ambient of 270K to 315K, a modification to the calibration approach, like the one used for B21 calibration through the use of LUT values, has been designed and implemented in the L1B code for the Aqua MODIS.

The same "B-side" electronics configuration has been used since Aqua launch. The instrument calibration and characterization efforts are similar to those made for the Terra MODIS. One of the noticeable differences in the trending is that the mirror side dependent degradation is much smaller in Aqua MODIS (Figure 2). In the Aqua L1B software update, a new SWIR band thermal leak correction al-

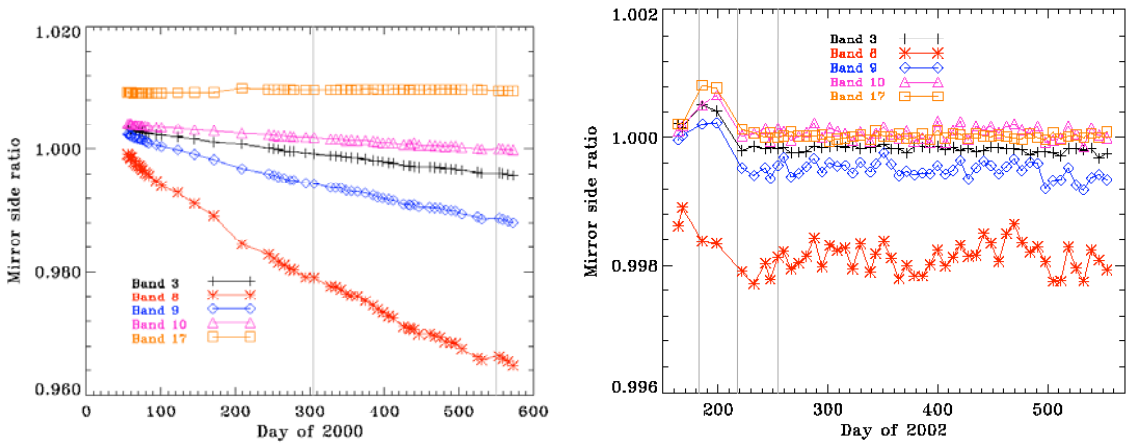


Figure 2. Ratios of the responses from mirror side 1 to that from mirror side 2 (Left for Terra MODIS and right for Aqua MODIS) for several MODIS reflective solar bands.

gorithm using B25 as the sending band has been implemented based on the on-orbit studies.

2) GLOBAL DISTRIBUTION OF AEROSOL OPTICAL PROPERTIES (M. D. King, Y. J. Kaufman, L. A. Remer, B. N. Holben, O. Dubovik)

MODIS has produced the first global distribution of atmospheric aerosols over both land and ocean, with a separation between fine mode aerosols (anthropogenic sources of urban pollution and biomass burning) and natural aerosols (sea salt over the ocean and, especially, dust sources from the land). This is a major accomplishment that has received considerable attention in the international scientific community. The land aerosol algorithm was developed by Yoram Kaufman, Lorraine Remer, and colleagues, while the ocean algorithm was developed by Didier Tanré, the Director of the Laboratoire d'Optique Atmosphérique, Université des Sciences et Technologies de Lille, Villeneuve d'Ascq, France, a MODIS Science Team Member and frequent visitor to the Earth Sciences Directorate.

Figure 3 shows the global distribution of aerosol optical thickness (at 0.56 $\mu$m) of both coarse and fine aerosols for the month of September 2000 derived from Terra data (adapted from Kaufman et al. 2002). These figures show the predominance of fine mode aerosol arising from industrial pollution in North America, Europe and, especially China and the Indian subcontinent. In addition, vegetation fires in South America and southern Africa during September (the dry season in these regions) is most apparent. Coarse aerosol is largely a natural phenomenon, and is most apparent in the dust plumes in the North Atlantic and Arabian Sea and sea salt from wind generated particles in the southern ocean. The latter particles may, in part, be artifacts of cloud contamination in this cloudy region of the roaring 40s, but the strong winds also contribute sea salt and sea spray when cloud free occasions occur.

In addition to the global analysis and sophisticated algorithm development, much work has been done in validating the accuracy, and limitations, of the current algorithm. Of particular importance is the Aerosol Robotic Network (AERONET) of sun/sky radiometers operated as a global, federated network by Brent Holben and colleagues in the Earth Sciences Directorate. Currently there are approximately 120 sunphotometers operating at any one time around the world, and these data are transmitted via satellite and analyzed, cloud screened, inverted for aerosol optical thickness, single scattering albedo, and size distribution, all at Goddard using a consistent set of algorithms. These data are posted on a web site accessible to the global Earth science community, and can be used in model development, validation of satellite observations, and process studies. The AERONET system, funded almost exclusively by the EOS program, is widely cited in any climate change discussion where aerosols are considered as a moderating influence on greenhouse gases in the Earth's atmosphere.

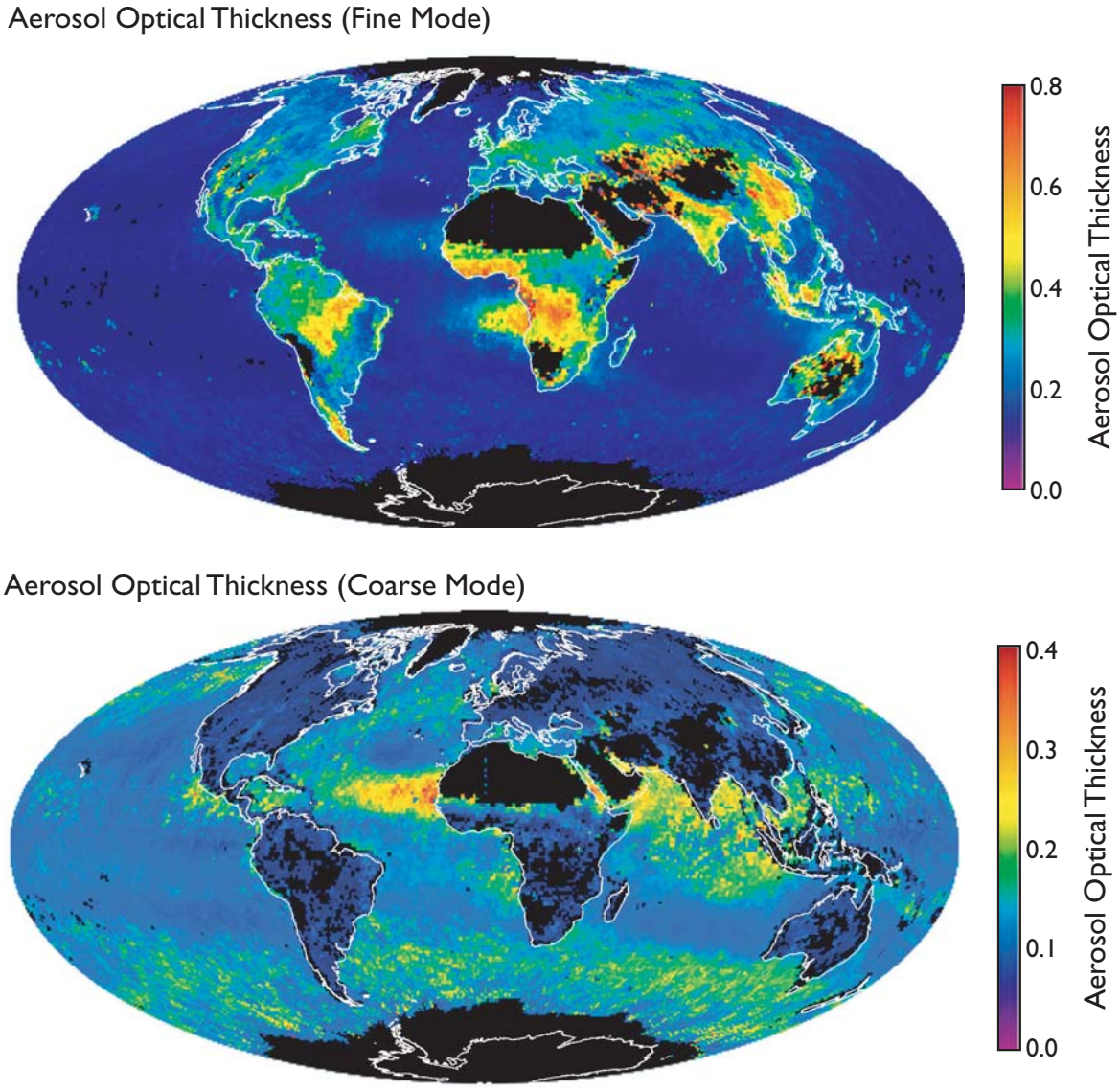


Figure 3. Global distribution of fine (upper panel) and coarse (lower panel) aerosol optical thickness derived from MODIS measurements on the Terra platform for September 2000 (adapted from Kaufman et al. 2002).

The AERONET network is described by Holben et al. (1998), the cloud screening algorithm by Smirnov et al. (2000), and the aerosol size distribution and single scattering albedo inversion algorithm by Dubovik and King (2000). These aerosol optical properties have been used to validate the satellite-derived optical properties of atmospheric aerosols by MODIS (Chu et al. 2002, Remer et al. 2002) and MISR (Diner et al. 2001).

In addition to the validation of MODIS and MISR aerosol optical thickness and size distribution, AERONET has also been used to derive the climatology of aerosol optical thickness, a measure of column concentration (Holben et al. 2001), and to determine the optical properties of aerosol particles in selected worldwide locations. Figure 4 (Dubovik et al. 2002) shows the spectral single scattering al-

bedo (a measure of aerosol absorption, with 1.0 being pure scattering and 0.0 being complete absorption), and aerosol size distribution of particles in urban/industrial regions (Goddard, Paris, Mexico City, and the Maldives), biomass burning regions (Amazonian forest, South American cerrado, African savanna, and boreal forest), desert dust (Bahrain, Saudi Arabia, and Cape Verde Island), and oceanic aerosol (Hawaii).

These results clearly demonstrate that Goddard and Paris are relatively clean environment, with somewhat more absorption in Paris (due to diesel automobiles) than Goddard. Both regions have mostly fine mode particles as shown in the lower panel. In contrast, Mexico City and the dirty environmental air over the Maldives off the Indian subcontinent are far more absorbing with more coarse particles. In biomass burning regions, it is readily apparent that these particles are uniformly small (fine mode particles as shown in Figure 3). Furthermore, Af-

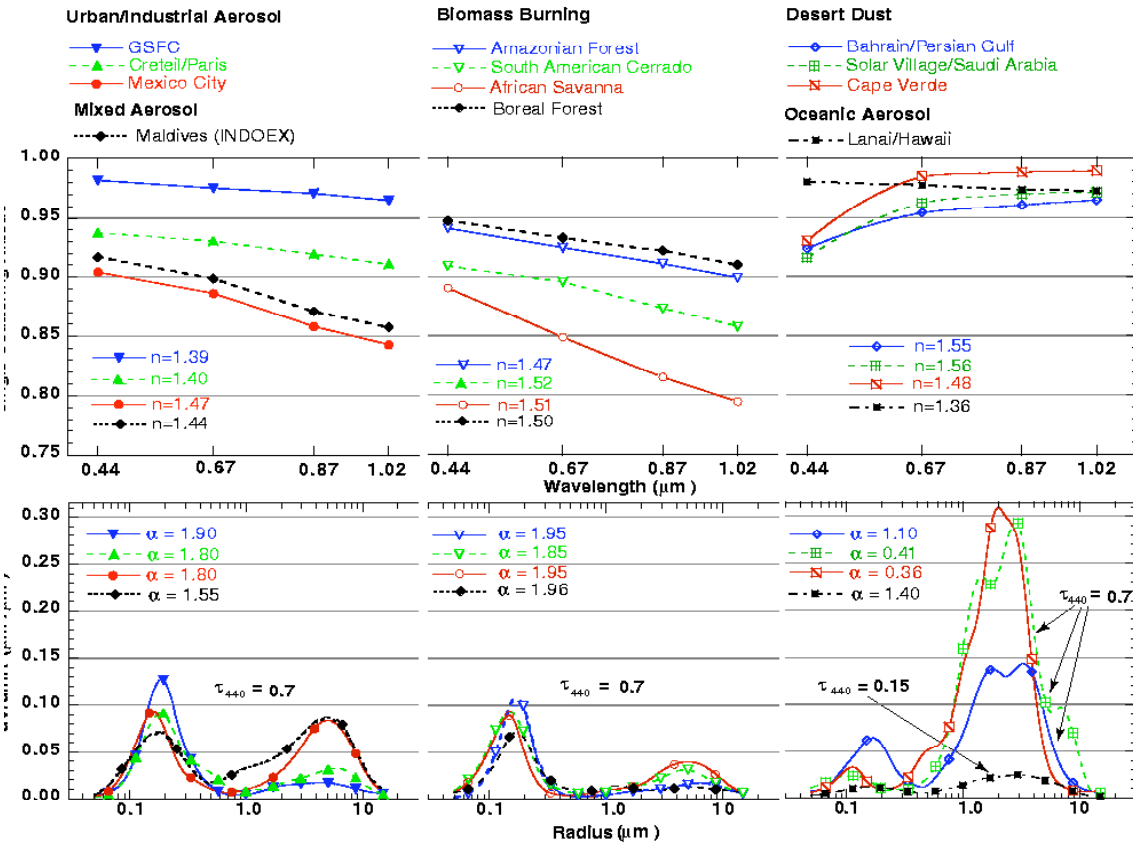


Figure 4. The averaged optical properties of different types of tropospheric aerosol retrieved from AERONET. Urban/industrial, biomass burning and desert dust aerosols are shown for $\tau_{ext}(440) = 0.7$. Oceanic aerosol is shown for $\tau_{ext}(440) = 0.15$ since oceanic background aerosol loading does not often exceed 0.15. Also, $\omega_0(\lambda)$ and the refractive index n shown for Bahrain were obtained only for the cases when $\alpha \leq 0.6$ (for higher $\alpha$, $\omega_0(\lambda)$ and refractive index $n$ were very variable due to a significant presence of urban/industrial aerosol). However, we show the particle size distribution representing all observations in Bahrain (complete range of $\alpha$). Ångström parameter $\alpha$ is estimated using optical thickness at two wavelengths 0.440 and 0.870 nm (adapted from Dubovik et al. 2002).

rican smoke is more absorbing (lower single scattering albedo) than south American and Canadian boreal smoke, largely due to the grassland fires with flaming combustion dominant in Africa (Zambia in this case). Desert dust, which consists largely of coarse (large particles) absorbs primarily in the blue (short) wavelengths, with little absorption in the visible. This is the basis of the TOMS aerosol index for observing aerosol properties over desert regions. Oceanic aerosol consists only of large, coarse, particles and is relatively nonabsorbing.

AERONET measurements were also used to link the EOS measurements of aerosol to the analysis of aerosol forcing of climate. Terra and Aqua measure aerosol at a specific time of the day—about 10:30 am and 1:30 pm, respectively. A natural question arises as to whether these measurements represent the daily average aerosol concentration and properties. The daily AERONET measurements from sunrise to sunset were used to answer this question positively (Kaufman et al. 2000), that is to say morning and afternoon observations are not substantially different from the diurnal average over a wide variety of locations worldwide. AERONET was also used to find the baseline aerosol that is present over the oceans with dust or man-made aerosol intrusions. This baseline is needed to derive the anthropogenic forcing on climate from the total aerosol radiative effects measured by EOS (Kaufman et al. 2001).

These EOS-sponsored results are valuable in and of themselves, and are contributing to studies of the human health impact of aerosols as well as the climatic effect of particles in different geographic locations.

3) GLOBAL DISTRIBUTION OF CLOUD OPTICAL AND MICROPHYSICAL PROPERTIES (M. D. King, S. Platnick)

MODIS has produced the first global distribution of cloud optical thickness and microphysical properties (effective particle radius) of both liquid water and ice clouds. This makes use of the rather sophisticated sensor characteristics and wide spectral range available in MODIS that enables both clouds to be better identified, even in the difficult polar regions over snow and sea ice surfaces, and to distinguish their thermodynamic phase. The cloud optical properties algorithm was developed by Michael King and Steven Platnick, with contributions from Steve Ackerman, Ping Yang, and Kuo-Nan Liou, frequent visitors to the Earth Sciences Directorate.

Figure 5 shows the global distribution of optical thickness (at 0.66 $\mu$m) of both liquid water and ice clouds for the month of April 2003 derived from Terra data (adapted from algorithms described by Platnick et al. 2003 and King et al. 2003a). These panels show the predominance of optically thick ice clouds in the Intertropical Convergence Zone, liquid water clouds in the marine stratocumulus regions off Angola, Namibia, and Peru, ice clouds in the tropical Indian Ocean during this storm season, and the complex multi-phase clouds in the roaring 40s of the southern hemisphere.

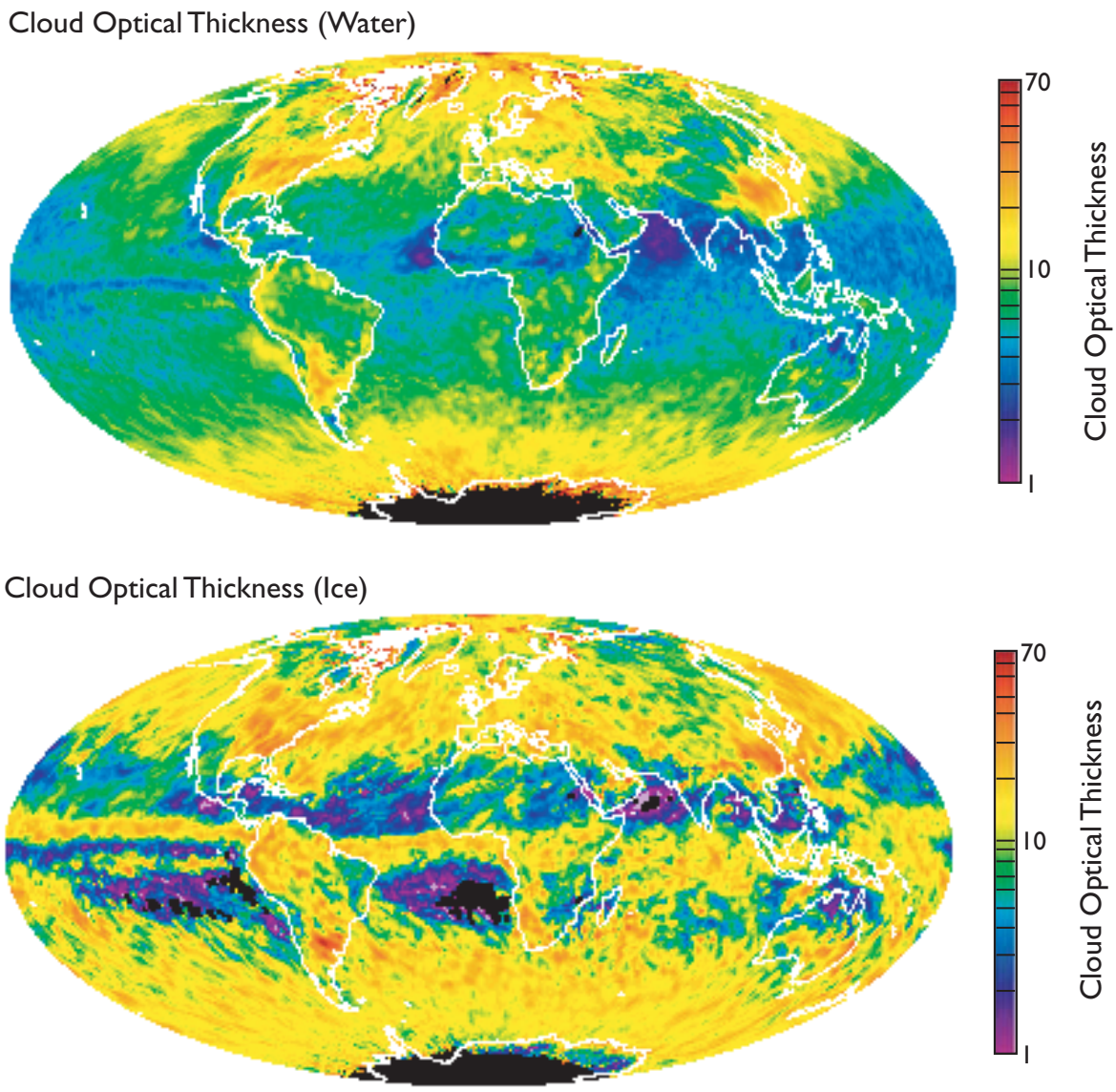


Figure 5. Global distribution of liquid water (upper panel) and ice (lower panel) cloud optical thickness derived from MODIS measurements on the Terra platform for April 2003.

Figure 6 shows the corresponding effective particle radius of spherical water droplets and nonspherical ice crystals for April 2003. The much larger effective radius of liquid water clouds over oceans than land, and in the southern hemisphere vs. the northern hemisphere, is indicative of the much more extensive cloud condensation nuclei over land.

4) GLOBAL DISTRIBUTION OF SNOW COVER (D. K. Hall, V. V. Salomonson, A. T. C. Chang)

There is a pressing need to estimate snow extent and volume at regional and global scales to effectively constrain climate models. MODIS has produced global, daily snow maps at ~5.5 km resolution (Figure 7) that provide the fraction of snow cover within a cell on a geographic (lat/long) grid suitable for use in

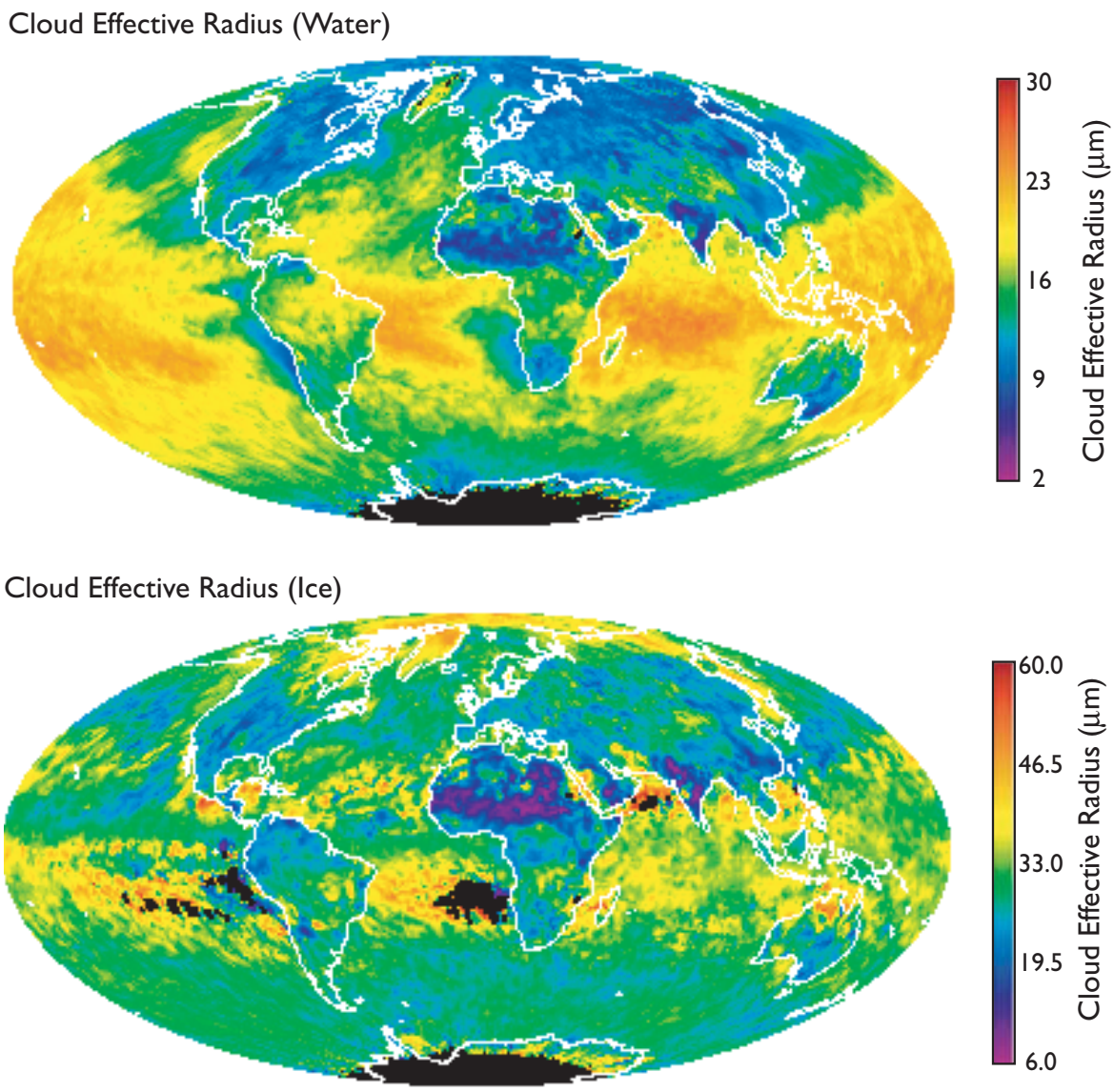


Figure 6. Global distribution of liquid water (upper panel) and ice (lower panel) cloud effective radius ($\mu$m) derived from MODIS measurements on the Terra platform for April 2003.

general-circulation models. This product complements the 500 m resolution snow-cover products that are also available from MODIS that include daily snow albedo (Figure 8) and will include fractional-snow cover (Salomonson and Appel 2003), a parameter needed in basin-scale modeling. AMSR has also produced global snow depth maps (Figure 9) at a resolution of ~25 km (Kelly et al. 2003). Together, these important new global datasets will enable the analysis of snow-covered area and volume globally.

When snow-covered area and depth are known, snow volume may be estimated; snow pack volume globally has been a critical unknown quantity in the global hydrologic cycle. Snow volume is needed for a variety of hydrological uses (determination of water supply and flood potential) as well as for such diverse reasons as monitoring changes in the Earth's oblateness (Cox and Chao 2002) due to

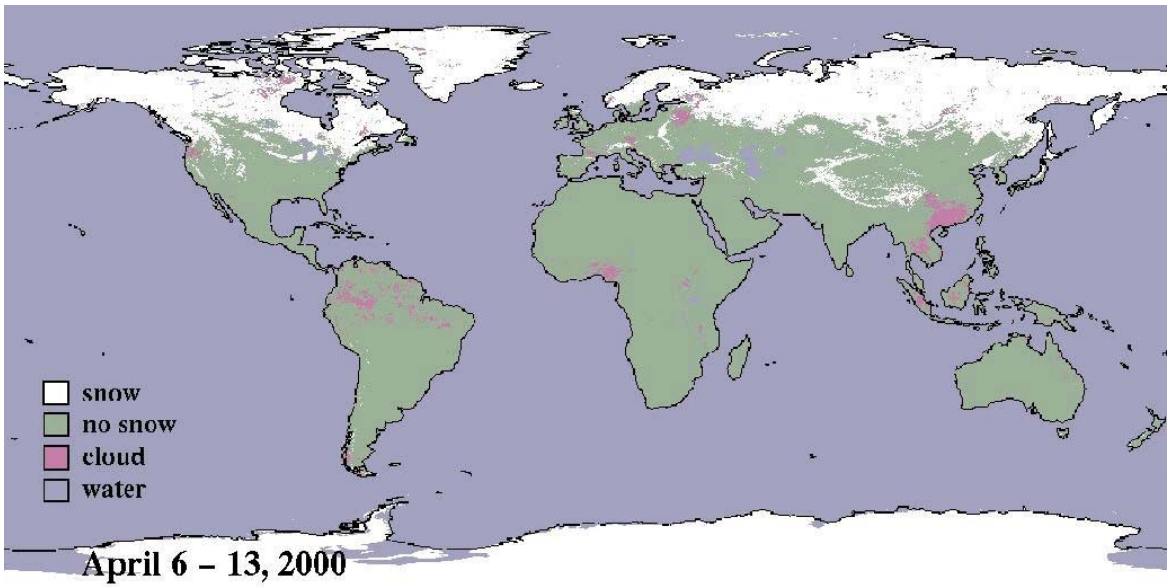


Figure 7. Eight-day composite snow climate-modeling grid snow-cover product from MODIS.

large-scale snow and ice mass redistribution.

Figure 7 shows the global distribution of snow cover from an 8-day composite MODIS snow-cover product from April 6–13, 2000 (Hall et al. 2002a). Because this is a composite map, cloud cover is minimized and snow cover for the period is maximized; while the daily maps contain a large amount of cloud cover, the 8-day composites generally contain very little.

Daily snow albedo (Figure 8) is a recent enhancement to the daily snow product and will be available at a resolution of 500 m. This will be the first global, daily automated snow albedo product and should be available to the public by the

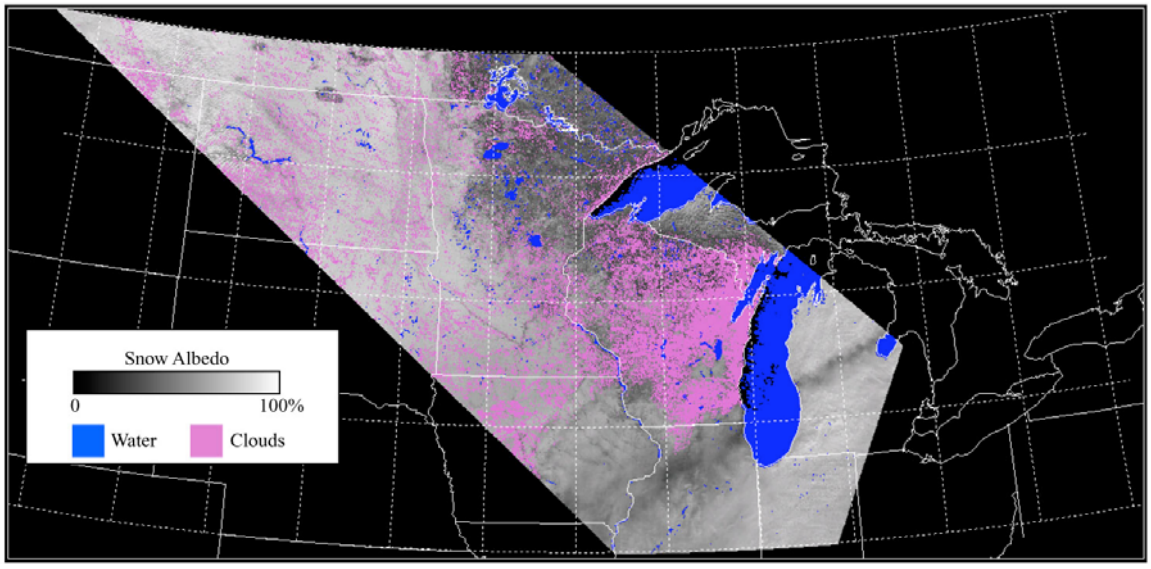


Figure 8. Prototype of snow albedo product - north central United States and southern Canada - February 16, 2001 (courtesy of Andrew G. Klein/Texas A&M University).

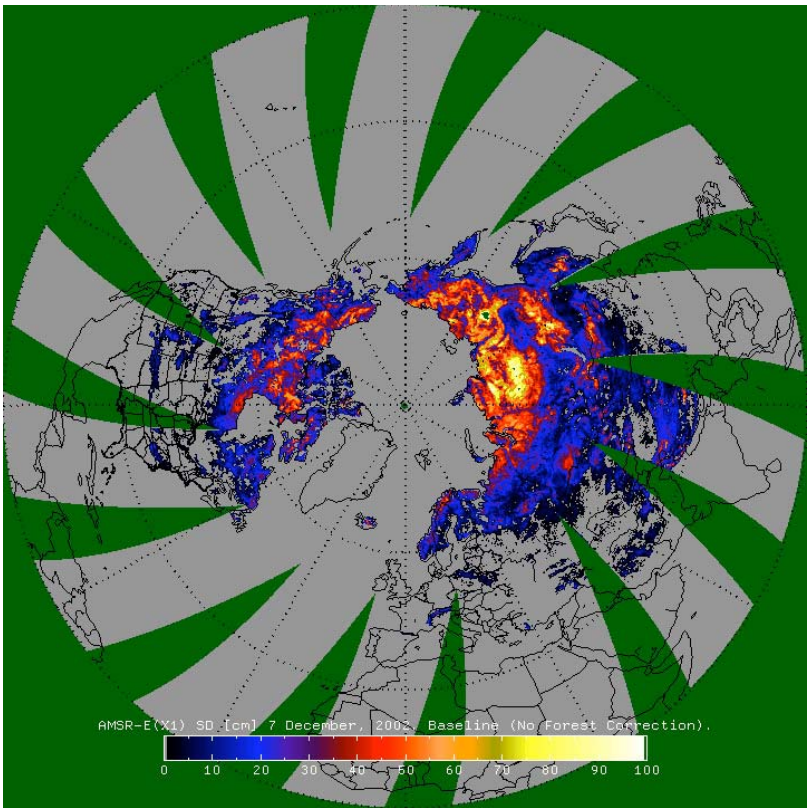


Figure 9. Estimated snow depth for the Northern Hemisphere from AMSR-E data for 7 December 2002 (from R. E. J. Kelly and A. T. C. Chang, unpublished data).

summer of 2003. A broadband snow albedo measurement is provided for snow pixels and a narrow-to-broadband conversion scheme (Liang 2000) is used to combine the MODIS narrow-band albedos into a single broadband albedo estimate (Klein and Stroeve 2002).

The MODIS snow-cover maps compare well with NOAA's operational snow maps (Hall et al. 2002b; Mauer et al. 2003; Klein and Barnett, 2003), but provide improved resolution and snow/cloud discrimination. The MODIS 500 m resolution snow map was compared with the 1 km resolution National Operational Hydrologic Remote Sensing Center (NOHRSC) operational snow map over the Columbia River and the Missouri River basins during winter and spring of 2000-2001 by Mauer et al. (2003). With the MODIS maps, 15% more of the Columbia basin area could be classified as to presence or absence of snow, and the MODIS maps misclassified 4% and 5% fewer pixels overall (for the two basins) as compared to the NOHRSC maps. Improvements in snow mapping translate into better predictions of water supply and flooding potential.

The development of a snow depth retrieval algorithm for the Advanced Microwave Scanning Radiometer – EOS (AMSR-E) has proceeded from current applications of snow depth retrievals from the Special Sensor Microwave/Imager (SSM/I) (Kelly et al., 2003; Kelly and Chang 2003). An improved dynamic method to estimate snow depth using passive microwave observations has been determined. Results indicate that for the 1992-1995 data set, the global snow

depth estimates for 52 stations have an average error of 11.7 cm, which is 7.7 cm better than the Chang et al. (1987) estimates. For the more spatially intensive and globally widespread data set of 2000/2001, the error is 22.1 cm, which is 4.0 cm lower than the errors from the standard 1.59 algorithm. This spatially dynamic approach to estimating snow depth is an improvement on the original retrieval algorithm of Chang et al. (1987); not only is the total average global seasonal error less for the new dynamic approach, but for the 2000-2001 season, daily global average snow depth errors generally are smaller.

Compared with the SSM/I configuration, AMSR-E has twice the spatial resolution and two extra low-frequency channels that will assist with sub-nivean state quantification (frozen/wet/dry soil). These two factors alone should help to improve both snow pack detection accuracy and snow depth/SWE retrieval accuracy when the AMSR-E calibration is finalized.

Global snow cover has an important influence on climate through its effect on the global water cycle and energy budgets at the surface and lower atmospheric levels. Instantaneous snow cover and temporal variations in snow cover must be represented accurately in climate models that are used to predict global climate change. It is known that large spatial and temporal variations exist in global and local snow cover extent and volume and characterization of these variations is of vital importance for effective climate prediction. In addition, water resource managers of snow-covered river catchments need timely information about snow pack extent, volume and state.

Work toward combining MODIS and AMSR snow algorithms will produce snow products that will give an improved delineation of snow-covered area as well as information about snow depth and volume that is needed for hydrological applications.

5) FIRE MONITORING (C. O. Justice, L. Giglio, D. P. Roy, J. Descloitres, J. E. Schmaltz, E. F. Vermote, Y. J. Kaufman, S. Korontzi, D. Davies)

A collaborative research activity has been developed between scientists at NASA/GSFC and the University of Maryland to monitor global fire distributions and their characteristics using EOS data. A robust global algorithm has been developed and tested and global products generated from both the Terra and Aqua instruments (Justice et al. 2002; Roy et al. 2002; Kaufman et al. 2003; Korontzi et al. 2003). The global products are currently being validated using data from the Terra/ASTER and BIRD instruments. An experimental burned area product has been developed and is being tested for different regions of the World. Earth science investigations using these fire data products are underway, examining the diurnal cycle and distribution of fires, the relationship between fires and climate interannual variability, the contribution of fires to regional trace gas emissions and the relationship between smoke, clouds and radiative forcing. Operational research and development is also being performed in the framework of the ESE Applications Division. The MODIS Fire Rapid Response has been developed and is providing near real time MODIS fire data and imagery to fire managers

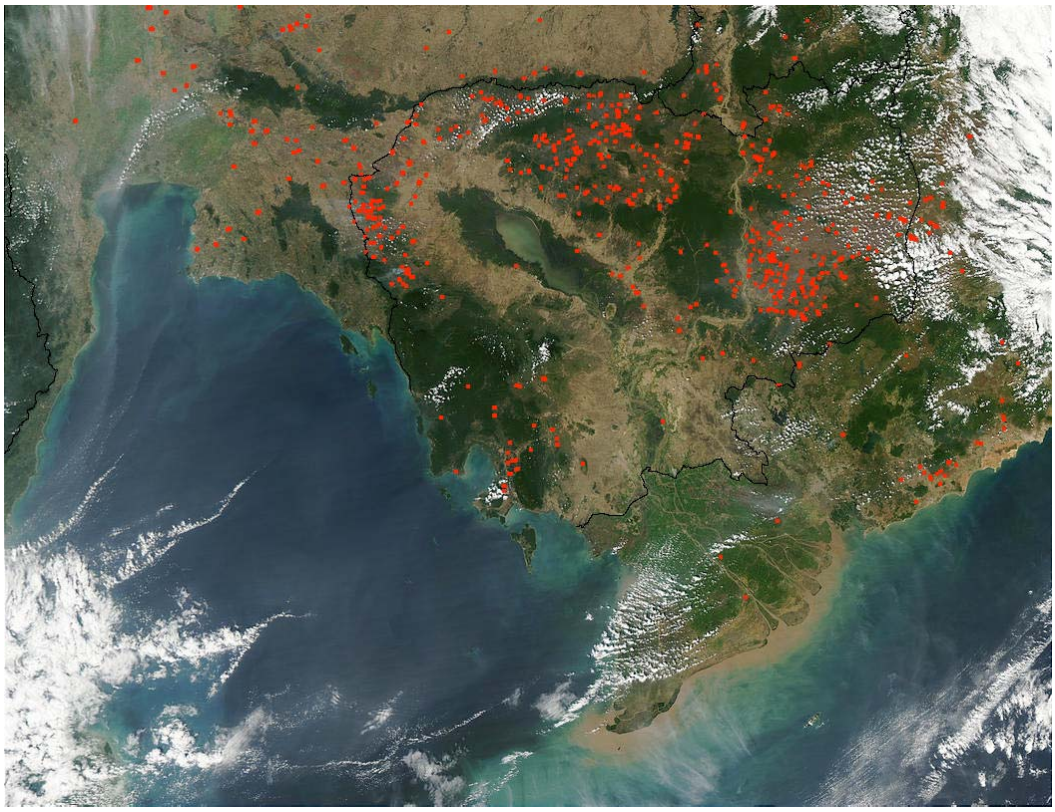

Figure 10. Fires in Indochina January 17, 2003 observed by the Aqua/MODIS instrument.

(cf. Figure 10). The fire location data are also provided as text files and are incorporated in a web mapping system providing fire information in a web-based geographic information system to various research and fire management groups around the World.

6) LAND SURFACE REFLECTANCE (E. F. Vermote, N. Z. Saleous, C. O. Justice)

The MODIS instrument provides major advances in moderate resolution Earth observation. Improved spatial resolution for land observation at 250 m and 500 m and improved spectral band placement provides new remote sensing opportunities. NASA has invested in the development of improved algorithms for MODIS, which will provide new data sets for global change research. Surface reflectance is one of the key products from MODIS and is used in developing several higher-order land products (Vermote et al. 2002a, 2002b; Petitcolin and Vermote 2002). The surface reflectance algorithm builds on the heritage of the AVHRR and SeaWiFS algorithms, taking advantage of the new sensing capabilities of MODIS. Atmospheric correction, by the removal of water vapor and aerosol effects, provides improvements over previous coarse resolution products and the basis for a new time-series, which will extend through to the NPOESS generation of imagers. The algorithm is being validated by comparison to atmospherically corrected high spatial resolution data (ETM+) at AERONET sites validated themselves against ground measurements. In addition, MODIS middle infrared, longwave infrared, and cirrus (1.38 $\mu$m) bands are used in a state of the art cloud/cloud shadow detection algorithm, which is critical in the downstream

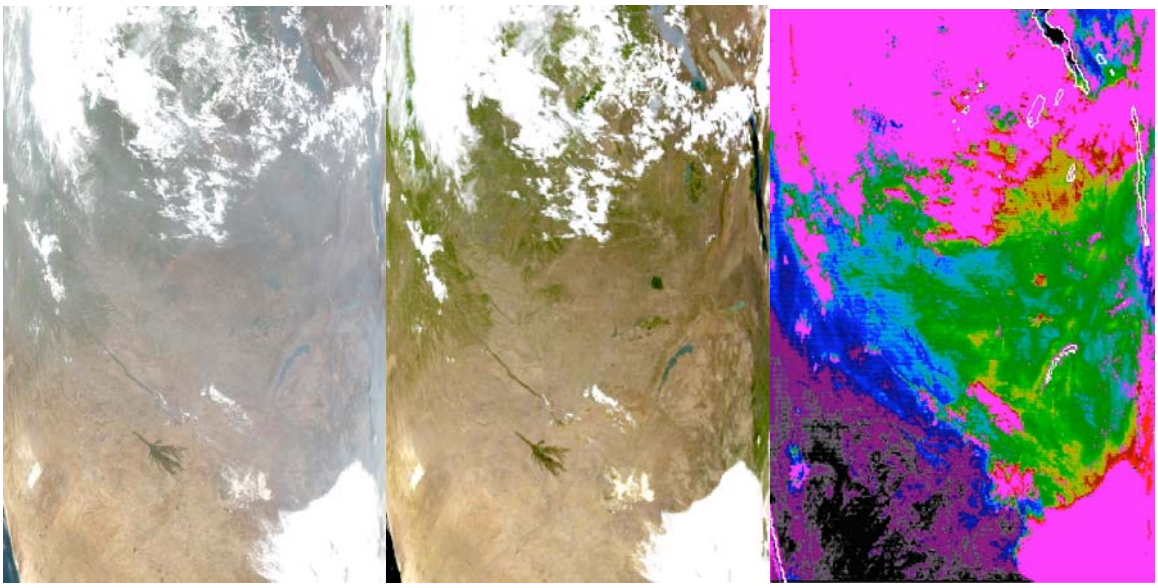

Figure 11. The impact of aerosols and their correction for a Terra/MODIS granule acquired over southern Africa on September 13, 2001 at 8:45 UTC: (a) RGB image of the MODIS bands 1,4,3 not corrected for the aerosol effect (b) RGB image of the surface reflectance in bands 1,4,3 (corrected for aerosol effect), (c) the aerosol optical thickness at 670 nm used in the correction displayed with a rainbow color scale (from0.0: black to 1.0 and above: red). Clouds are masked in magenta and water bodies are outlined in white.

use the generated products.

Figure 11 shows an example of one granule of MODIS data collected over South America, where the figure on the left is the true color composite of raw data, the middle figure shows the same image after being corrected for atmospheric aerosols and water vapor, and the figure on the right is the aerosol optical thickness at 0.67 $\mu$m, where the clouds are masked in magenta and water bodies are white. Note the strong haze over Zambia, just north of the Okavango Delta of northern Botswana, that is dramatically improved after correcting for atmospheric scattering effects.

7) OCEANIC NET PRIMARY PRODUCTIVITY (W. E. Esaias)

Determining the magnitude and variability of oceanic Net Primary Productivity is necessary for understanding variability of the Earth's marine ecosystems, and how the marine ecosystems respond to and provide feedback to changes in the Earth's climate and carbon systems. It is of great interest for understanding how coastal ecosystems and fisheries change and react over time to climate and human perturbations such as eutrophication and fishing pressure. Global primary production, or the initial production of organic matter through the process of photosynthesis, is apportioned relatively equally between terrestrial vegetation and aquatic plants. Net production is that portion which exceeds respiration on a daily basis for aquatic systems. About 40-50% of the atmospheric oxygen we breathe has resulted from marine production. About 99.5% of the carbon on the Earth is sequestered in sediments of marine origin, the final repository following millennia of oceanic NPP (ONPP) and the workings of the oceanic biological car-

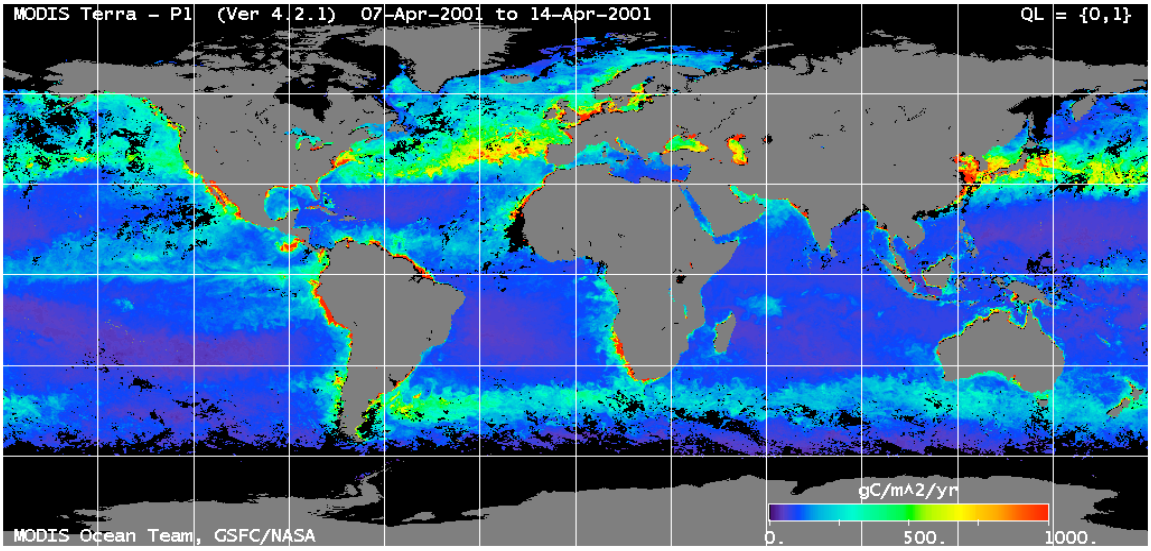


Figure 12. MODIS oceanic net primary productivity (ONPP), based on the Behrenfeld-Falkowski model (from mqabi.gsfc.nasa.gov/terra4).

bon pump. Oceanic NPP provides the base of the complex marine food web, and so is the primary source of energy (food) needed by marine life from zooplankton, fish, and marine mammals.

Estimating oceanic NPP using traditional ship-board techniques has been very difficult, due in large part to the fact that very few measurements can be obtained with sufficient frequency over the broad expanses of the highly variable ocean to address the natural spatial and temporal variations, much less the climate and human induced changes. Unlike terrestrial systems, the marine phytoplankton drift with the oceanic currents, and their biomass can change very rapidly (carbon doubling times are on the order of a few days) in response to environmental forcings. Routine satellite estimates easily encompass this tremendous spatial and temporal variability, and even though the accuracy of individual estimates is still somewhat coarse, the satellite-derived measurements provide the primary global and regional integrations of oceanic NPP, and are used extensively for studying temporal changes on these scales.

We provide routine estimates of ONPP using MODIS data at 4.6 km resolution and averaged over 8 day periods, using two models relating phytoplankton chlorophyll-a concentration, temperature, photosynthetically active radiation (PAR), and the depth of the upper mixed ocean layer. An example is illustrated in Figure 12. These models were developed with ocean color data from the Coastal Zone Color Scanner and SeaWiFS, and have been applied to both Terra/MODIS and Aqua/MODIS observations. Comparisons with estimates from SeaWiFS show that the Terra/MODIS estimates differ by about 1%, or about 2 petagrams (= gigaton) of carbon per year, or about 1/3 of the anthropogenic input of $CO_2$, and the accuracy is increasing with time as MODIS products become more mature. More advanced MODIS chlorophyll algorithms would indicate that ONPP has been underestimated, especially in the Southern Ocean, by about 10%. This underestimation is about the same order of magnitude as current estimates of

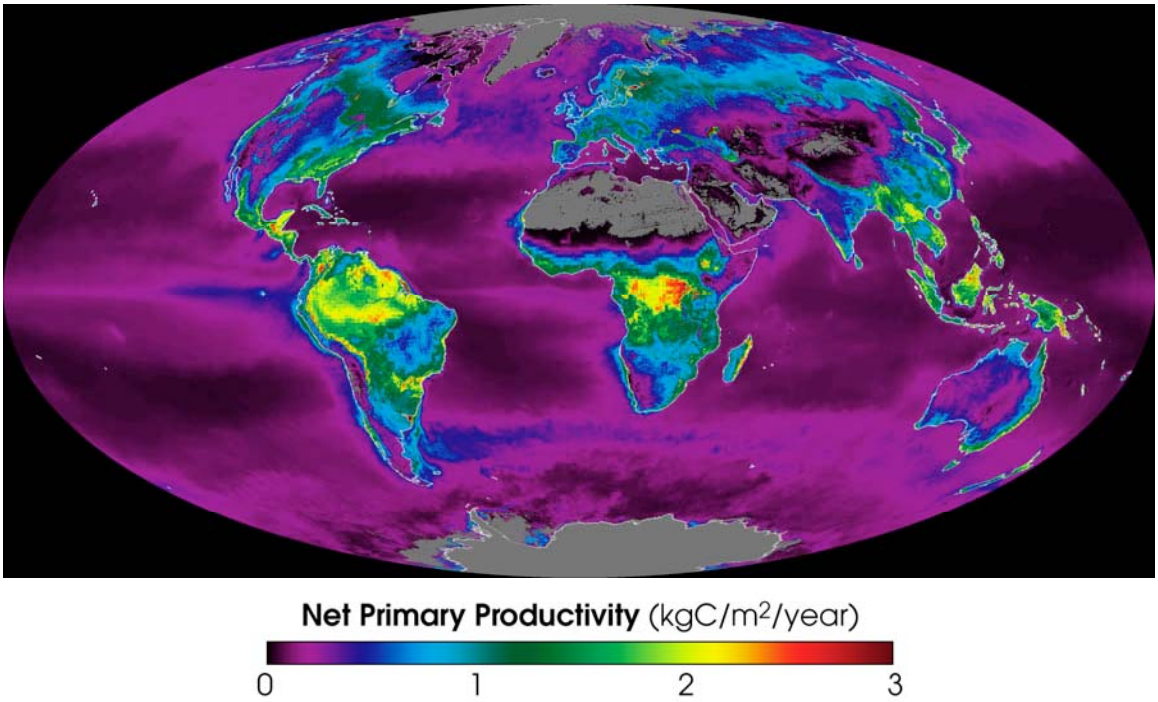


Figure 13. This false-color map represents the Earth's carbon "metabolism"—the rate at which plants absorbed carbon from the atmosphere. The map shows the global, annual average of the net productivity of vegetation on land and in the ocean during 2002, as derived from Terra/MODIS data. The yellow and red areas show the highest rates, ranging from 2 to 3 kg of carbon taken in per square meter per year. The green, blue, and purple shades show progressively lower productivity (visualization by R. Stöckli; see earthobservatory.nasa.gov/Newsroom/NPP/npp.html).

anthropogenic $CO_2$ emissions, and is therefore significant in terms of understanding the global carbon budget. Animations of these data are available on the MODIS ocean website at modis-ocean.gsfc.nasa.gov.

Within MODIS, we have coordinated with Steve Running, University of Montana, who is responsible for the Land NPP product, to assure common units, temporal and spatial resolutions, and to simplify integrations of Global NPP. In April NASA released the first animation of Global NPP on weekly, 5 km scales for 2001-2002 (cf. Figure 13).

*b. Global Sea Ice* (C. L. Parkinson, D. J. Cavalieri, D. K. Hall)

Sea ice has major impacts on polar climates through a multitude of processes, including its reflection of most of the solar radiation incident on it and its insulation of the ocean from the atmosphere and vice versa (e.g., Parkinson and Cavalieri 2002). Sea ice could also have impacts beyond the polar regions, as suggested strongly in a study with the GISS global climate model indicating that 37% of the global warming simulated for a doubling of atmospheric $CO_2$ can be attributed explicitly to the incorporation of an active sea ice cover in the model calculations (Rind et al. 1995).

Because of the importance of sea ice, Goddard has had an active sea ice research

group since the 1970s, and this continues in the EOS era. In fact, the science team members responsible for sea ice algorithm development from the two EOS instruments being used most for sea ice studies, AMSR-E and MODIS, are all from the Earth Sciences Directorate. AMSR-E is on board the EOS Aqua satellite, launched in May 2002, and the two MODIS instruments are onboard Terra, launched in December 1999, and Aqua.

1) AMSR-E

The AMSR-E instrument, provided to the Aqua mission by Japan's National Space Development Agency (NASDA), is being used to extend the satellite multichannel passive microwave record of global sea ice coverage derived for the period since November 1978 from data from the Nimbus 7 Scanning Multichannel Microwave Radiometer (SMMR) and the DMSP Special Sensor Microwave Imager (SSMI). A major advantage of the passive-microwave data for sea ice and other surface observations is the fact that at many microwave wavelengths the surface radiative emissions can go through clouds nearly unaffected, enabling collection of high-quality surface data even in the presence of nonprecipitating clouds. Results of the analysis of the SMMR/SSMI record by the Goddard sea ice group have included a widely publicized overall decreasing sea ice cover in the northern hemisphere since 1978 (Parkinson et al. 1999) and an overall increasing sea ice cover in the southern hemisphere since 1978 (Zwally et al. 2002), both with considerable regional and temporal variability. The Aqua AMSR-E data are allowing extension of those records with a spatial resolution improved by about a factor of 2. To illustrate the resolution, Figure 14 shows an AMSR-E 89 GHz

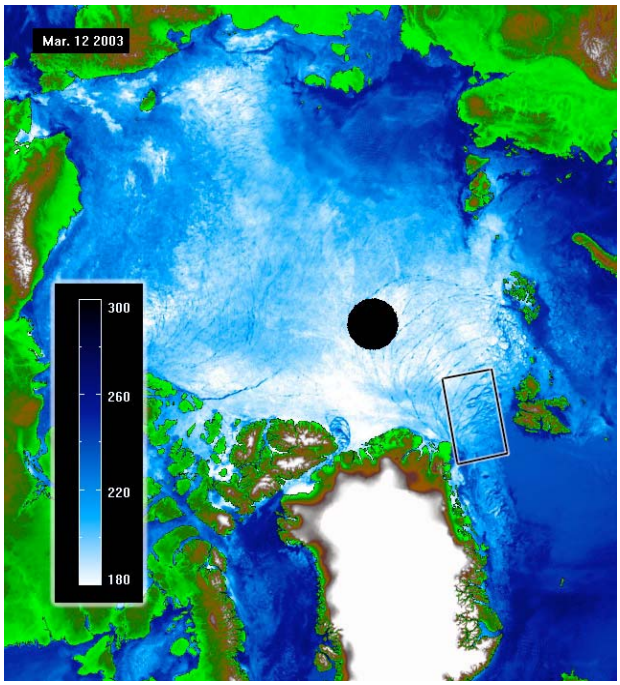


Figure 14. Brightness temperature image of the Arctic on March 12, 2003 from AMSR-E 89 GHz vertically polarized data. This image, at 6.25 km resolution, shows many individual large ice floes and numerous leads (from Hall et al. 2004).

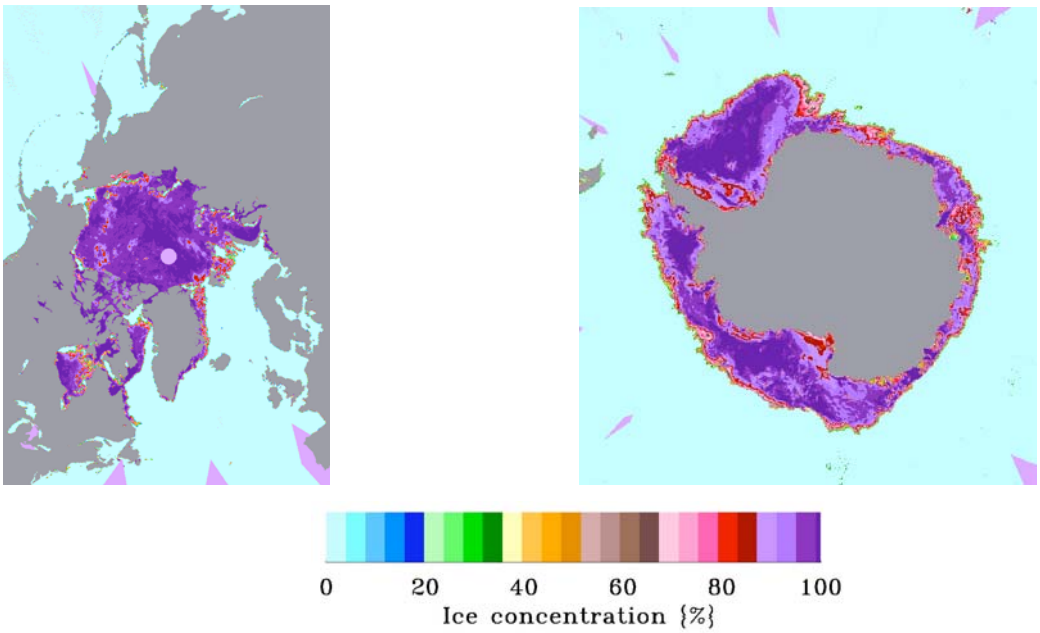


Figure 15. AMSR-E sea ice concentration for the Arctic and Antarctic for a day in June 2002.

image of the Arctic for March 12, 2003. Because of the improved resolution, large individual leads and ice floes can be resolved, something not available from previous satellite passive-microwave radiometers.

The AMSR-E standard sea ice products are sea ice concentrations, sea ice temperatures, and snow cover thickness on sea ice. Each of the algorithms for these products has been developed within the Directorate (Comiso et al. 2003; Markus and Cavalieri 1998, 2000). Figure 15 illustrates the sea ice concentration product for both polar regions, and Figure 16 illustrates the snow depth on sea ice and

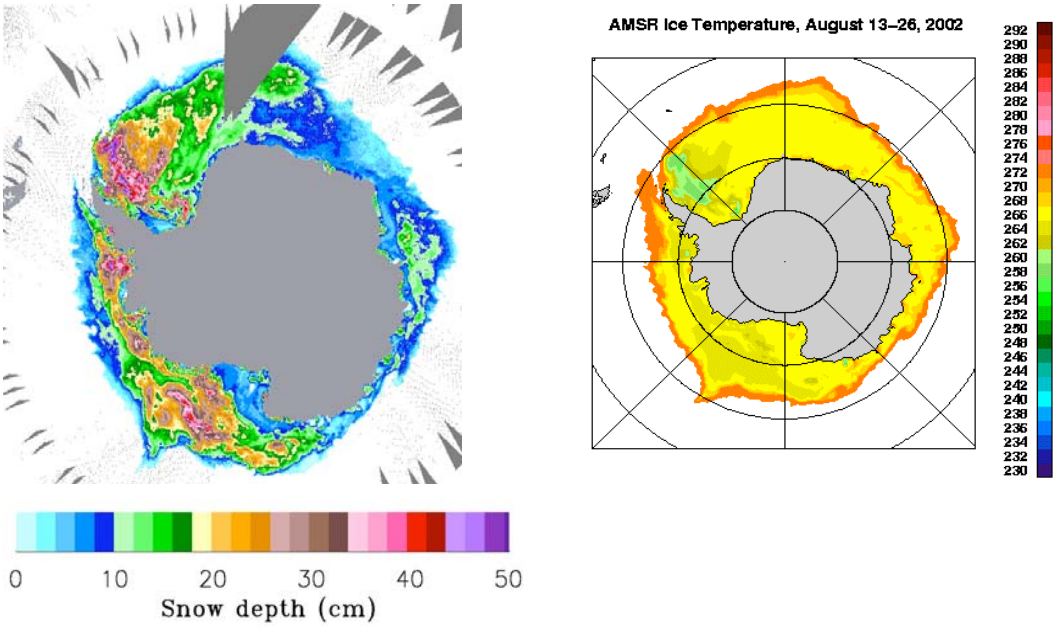


Figure 16. AMSR-E Antarctic snow depth on sea ice (left) and sea ice temperature (right) for late August 2002.

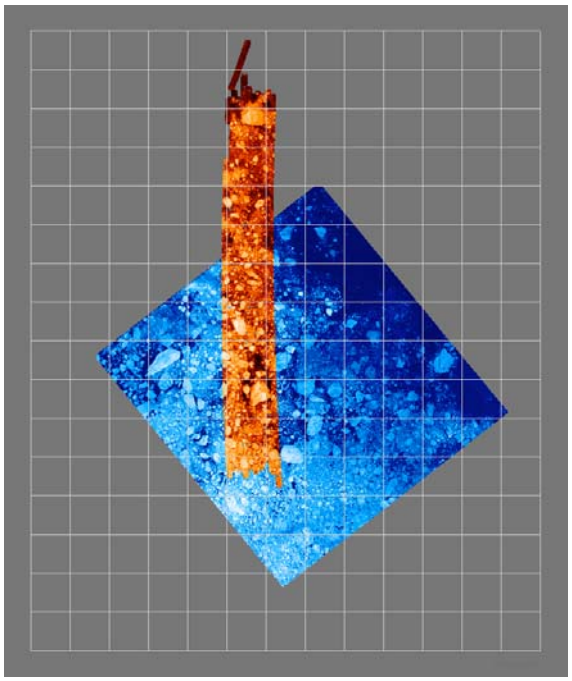

Figure 17. Landsat 7 ETM+ image (in blue) of Baffin Bay with NOAA Environmental Technology Laboratory (ETL) Polarimetric Scanning Radiometer (PSR) brightness temperature (19 GHz, V-polarization) mosaic (in orange) overlain for June 27, 2000. The Landsat and PSR data are gridded at a resolution of 0.5 km. The DMSP SSMI polar stereographic grid (in white) is also shown for comparison (from Cavalieri 2000).

sea ice temperature products. The algorithm developers and others in the Directorate are using these and related products to derive sea ice extents, extend the satellite passive-microwave record, and analyze these data for trends in the sea ice cover (e.g., Cavalieri et al. 2003) and relationships of changes in the sea ice to changes in such other climate variables and phenomena as surface temperatures (Comiso 2000), the North Atlantic Oscillation (Parkinson 2000), atmospheric planetary waves (Cavalieri 2002), and the Antarctic circumpolar current (Gloersen and White 2001). The AMSR-E data are also being used to derive sea ice motions with a wavelet analysis technique applied earlier to SSMI data (Zhao and Liu 2001).

Considerable efforts are being undertaken to validate the accuracy and limitations of the current algorithms for the AMSR-E sea ice products. In 2003, aircraft validation campaigns took place over the Sea of Okhotsk in February and over the Beaufort and Bering seas in March, and a campaign over the Weddell and Bellingshausen seas in the Antarctic is scheduled for August and September. Each of these campaigns has used or will use a heavily instrumented NASA P-3B aircraft and ship-based or ice-based ground observations. Earlier, Meltpond 2000 over flew the ice of Baffin Bay and the Canadian Archipelago, using a U.S. Navy P-3B (Cavalieri 2000). This campaign examined meltpond discrimination from microwave observations. Figure 17 illustrates the aircraft and Landsat 7 satellite coordination during the Meltpond campaign. It is hoped that the validation data, in addition to providing error bars for the sea ice data products, will lead to a determination of which of the two primary EOS algorithms for sea ice concen-

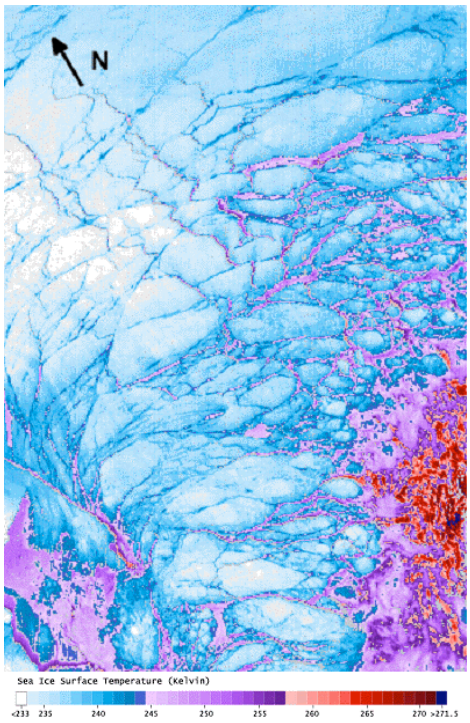


Figure 18. MODIS ice-surface temperature product (MOD29) acquired on March 12, 2003 for the rectangular region to the northeast of Greenland outlined on the AMSR-E image for the same date in Figure 14. The approximate center point of the image is 81.7°N, 1.0°E (from Hall et al. 2004).

tration from AMSR-E is doing a better job, both overall and on the basis of different regions and seasons.

Also, regarding AMSR-E data-product validation, Ed Kim has led the development of an airborne AMSR-E simulator named the Airborne Earth Science Microwave Imaging Radiometer (AESMIR). The AESMIR contains all the channels of the AMSR-E and is compatible with a variety of research aircraft. It underwent three successful test flights on the Wallops C-130 in April and May 2003. It is now ready to be installed on the NASA P-3B and to be used in collecting validation data for sea ice, snow cover, precipitation, soil moisture, ocean winds, and sea surface temperature.

2) MODIS

Sea ice algorithms for the MODIS instrument were developed by Dorothy Hall and George Riggs from the Earth Sciences Directorate and Jeff Key from NOAA/NESDIS. The resulting sea ice products take advantage of the much higher spatial resolution available from the visible and infrared MODIS data, versus the AMSR-E and other satellite passive-microwave data, although they are restricted by not being available under cloudy conditions.

Sea ice extent and ice-surface temperature (IST) at 1 km spatial resolution are produced as MODIS standard products, during daylight and darkness (Riggs et al. 1999; Hall et al. 2004) (cf., Figure 18). The MODIS IST algorithm is based on a

heritage algorithm developed by Key and Haefliger (1992). Climate-modeling grid (CMG) maps at 4-km resolution are also in the development phase, and will provide daily ice extent and IST. The CMG maps should be available by the fall of 2003.

The MODIS sea ice extent and IST products can be used to provide detailed information on the ice edge under clear skies. IST is valuable for modeling efforts in order to gain an improved understanding of ocean-atmosphere energy exchange. ISTs can also provide information on locations of thin or newly-formed ice because the temperature of very thin ice is often higher than that of the surrounding older ice.

Validation efforts show that under clear skies, the MODIS-derived IST is within 1.2 K of the near-surface air temperature as determined from in-situ meteorological station data and drifting buoy data, and that most of the difference is caused by the difference in physical temperature between the surface and the atmosphere at the height of the air temperature measurement (Hall et al. 2004). Field and aircraft data from the AMSR-E sea ice validation campaigns mentioned above will also be used to validate the MODIS ice extent and IST maps.

3) MODELING

EOS funding also supports sea ice modeling efforts within the Directorate. These include studies of sea ice export from the Arctic and the influence of sea ice on ocean overturning (Häkkinen 1999), the role of sea ice in forming decadal sea surface salinity anomalies in the northern North Atlantic (Häkkinen 2002), and the impact of sea ice concentration accuracies on climate model simulations (Parkinson et al. 2001).

*c. Aqua*

1) PRECIPITATION FROM AMSR-E (C. D. Kummerow, R. R. Ferraro, R. F. Adler)

The AMSR rainfall algorithm (Wilheit et al. 2003) has been developed and tested against AMSR-E data using the preliminary calibration curve developed by the AMSR-E team (while waiting for the final calibration to come from NASDA). Figure 19 shows results for the accumulated rainfall for October 2002 compared to the corresponding TRMM TMI product. In general the agreement is good with the main rainfall maxima obvious in both data sets. Some differences are expected due to the preliminary AMSR-E calibration and sampling differences between the two missions. Figure 20 shows a similar comparison for instantaneous rainfall rates for a tropical cyclone interacting with a mid-latitude front. The algorithm development for AMSR-E was the first attempt to implement a parametric algorithm that maintains the physical basis for the retrieval and changes only the sensor specifications from one instrument to the other. Valuable lessons related to strengths and weaknesses of such algorithms will be incorporated into

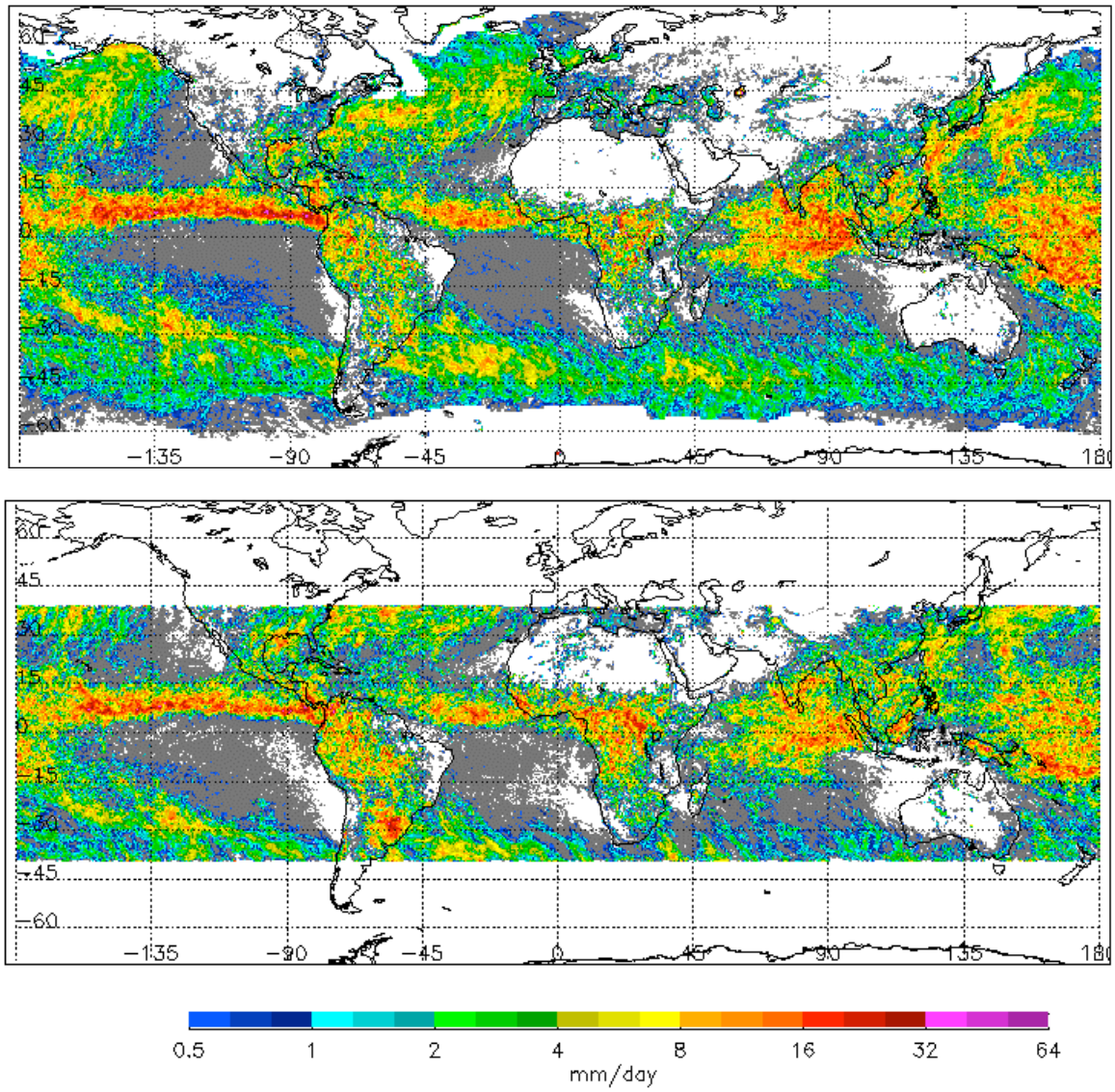


Figure 19. Monthly aggregation of AMSR-E Level-2 algorithm for land and ocean compared to TRMM for October 2002.

the algorithm being developed for the Global Precipitation Measurement (GPM) mission.

AMSR precipitation retrievals will shortly be incorporated into the NASA/TRMM Multi-Precipitation Analysis (MPA) that uses TRMM radar/radiometer information to calibrate or adjust rainfall estimates from other satellites and combines them into real-time rain maps at 3-hr time resolution. These analyses are being used to monitor floods and droughts across the globe. A research (non real-time) version of the MPA will be available for retrospective studies. The AMSR-E precipitation retrievals are the prime component of this analysis outside the latitude bounds of TRMM, and will become the prime satellite instrument at all latitudes if TRMM data are unavailable. Thus TRMM and AMSR-E will become the core satellites/instruments in global precipitation analysis leading up to GPM.

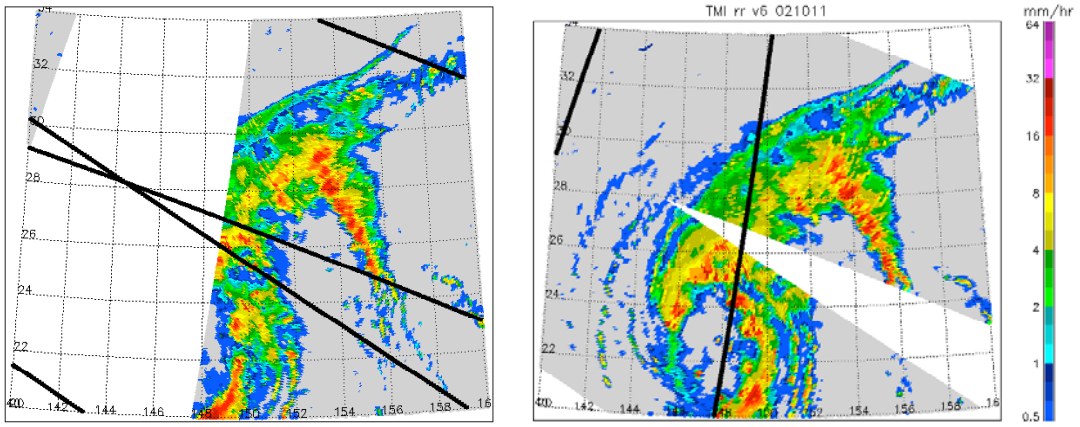


Figure 20. An instantaneous rainfall comparison between (left) AMSR-E and (right) TRMM TMI oceanic rainfall products. The top right portion of each figure corresponds to orbits within 15 minutes of one another.

Validation of AMSR-E rainfall products is underway over both land and oceans. Over land, in collaboration with Ralph Ferraro at NOAA/NESDIS and Witold Krajewski at the University of Iowa, AMSR-E rainfall is being validated against a dense rain gauge network installed in order to assess errors in the satellite algorithm. These dense network comparisons will also help to assess the accuracy of comparisons done against less dense gauge networks. The latter will be critical to assessing the algorithm in a number of regimes that have limited gauge coverage. Initial validation results are shown in Figure 21 and indicate good comparison for the limited data set obtained thus far.

Over oceans, there are not enough validation sites to obtain globally representative statistics. Figure 22 shows highlights of the successfully completed Wakasa Bay experiment. The objective being pursued here is to determine if the current algorithm formulation accurately represents the true problem (i.e., if given actual values for the assumed aspects of the algorithm, does the algorithm produce the

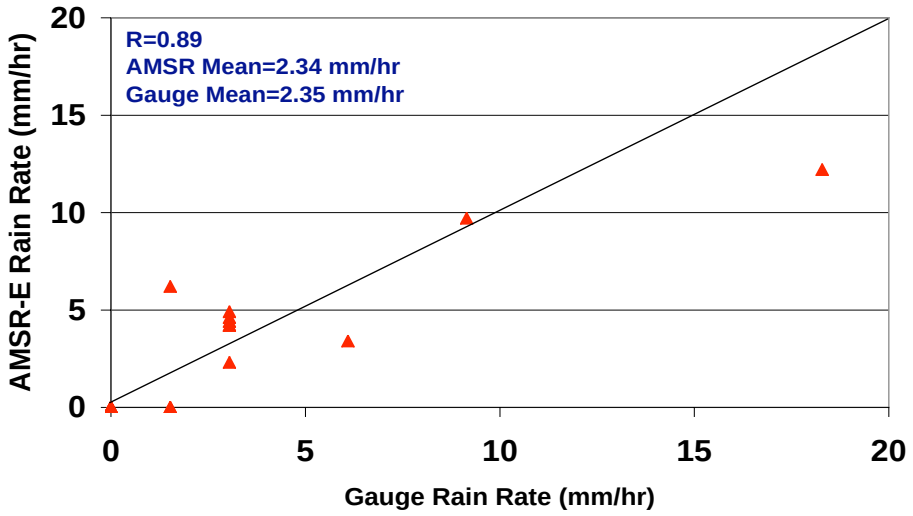


Figure 21. Results from the AMSR-E algorithm over land, compared to the Iowa dense-gauge network.

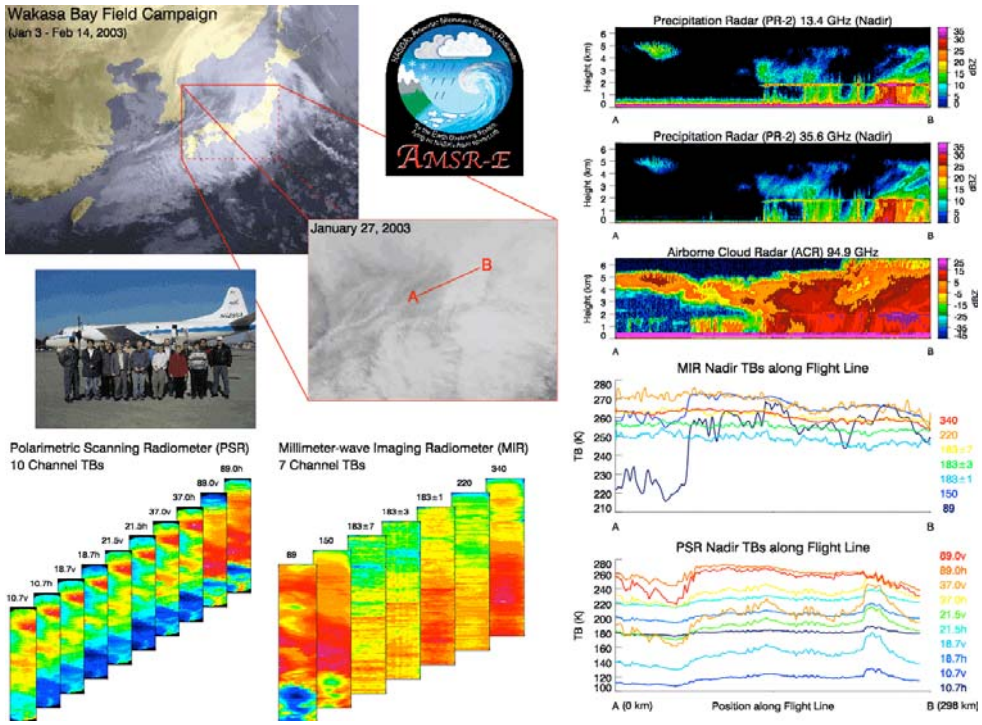


Figure 22. The Wakasa Bay (Japan) Field Experiment.

correct result?). To investigate this, simulations are being carried out to determine the extent to which hydrometeor profiles can be constructed within the algorithm framework to simultaneously match all 3 radar and 17 radiometric channels (shown on the right hand side of Figure 22). Any modifications to the current procedure will be implemented in the operational algorithm to insure that the retrieval is working properly and that an error model can be constructed once the assumptions have been individually characterized. Retrieved hydrometeor profiles from the airborne campaign will be compared with in situ observations from the Japanese Gulfstream II aircraft to verify the conclusions.

*d. GLAS*

GLAS is a space lidar on NASA's ICESat mission that was launched into a 590 km altitude circular polar orbit on January 12, 2003. The Earth Sciences Directorate developed the GLAS instrument as well as algorithms for atmospheric cloud and aerosol properties, vegetation canopy height and structure, and ice sheet topography.

1) GLAS DEVELOPMENT AND MEASUREMENT PERFORMANCE (J. B. Abshire, X. Sun, H. Riris, M. Sirota, J. McGary, S. P. Palm, E. A. Ketchum, R. B. Follas)

The Geoscience Laser Altimeter System is a new space lidar developed for long-term continuous measurements in Earth orbit (Zwally et al. 2003). NASA Goddard's Earth Science Directorate led the instrument and measurement definition, and had key roles in the instrument and laser development and testing. The GLAS design combines an altimeter with 5 cm precision with a laser pointing

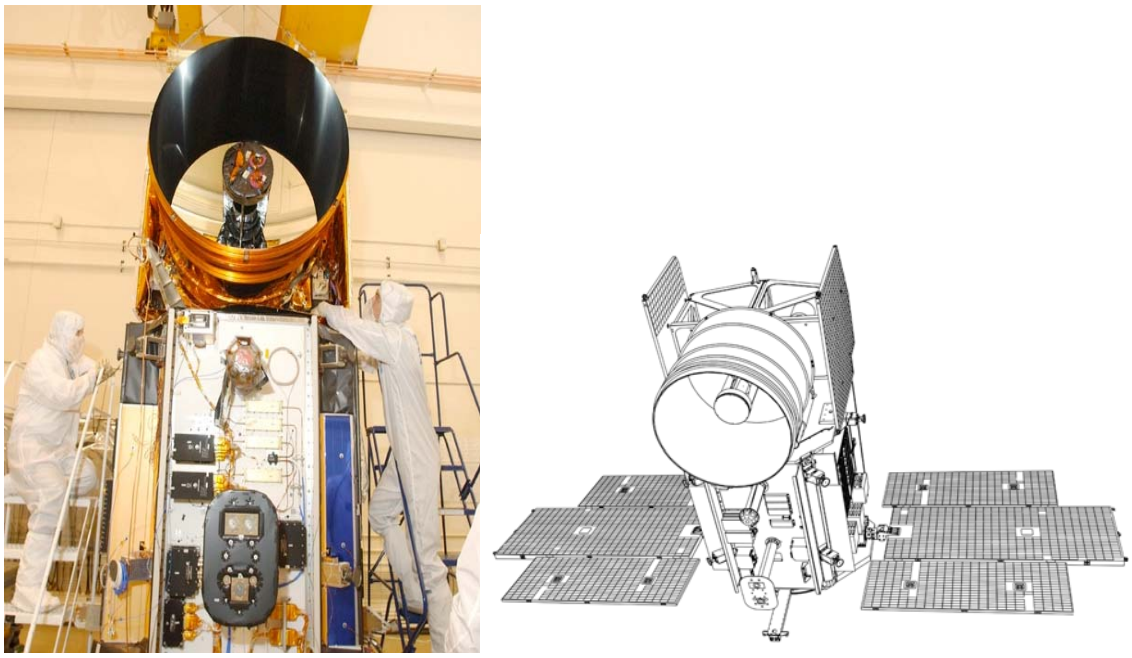

Figure 23. GLAS nadir side during integration.

angle determination system and a dual wavelength cloud and aerosol lidar. GLAS was completed in June 2002, integrated on the ICESat spacecraft, and the integrated observatory launched from Vandenberg AFB on January 12, 2003. GLAS was developed by Goddard Space Flight Center, the ICESat spacecraft by Ball Aerospace, and the GPS receivers used on ICESat and GLAS were developed by JPL to determine orbit altitude, position and time.

GLAS measures the range to the Earth's surface with 1064 nm laser pulses. Each laser pulse produces a precision pointing measurement from the stellar reference system (SRS) and an echo pulse waveform, which permits range determination and waveform spreading analysis. The single shot ranging accuracy is < 10 cm for ice surfaces with slopes < 2°. Changes in regional ice sheet heights will be determined by comparing successive GLAS measurement sets. GLAS will also measure atmospheric backscatter profiles at both 1064 and 532 nm (Spinhirne and Palm 1996). The 1064 nm measurements use an analog Si APD detector and measure the height and profile of backscatter from thicker clouds. The measurements at 532 nm use photon-counting detectors, and will measure the vertical height distributions of optically thin clouds and aerosol layers.

The completed GLAS instrument is shown in Figure 23 and its characteristics are summarized in Table 1. Subassemblies include three Q-switched ND:YAG lasers (Afzal et al. 2002), an SRS that measures the pointing angles of each laser firing (Millar et al. 2003), a 100 cm diameter Beryllium receiver telescope, a 30 pm wide optical filter at 532 nm, and Si APD detectors for 1064 and 532 nm. The subassemblies are mounted on an L-shaped graphite epoxy optical bench. GLAS dissipates heat via radiators, which are shown in Figure 23.

Table 1. GLAS instrument specifications.

| | | | |
|---|---|---|---|
| Laser Type | ND:YAG slab, 3 stage passively Q-switched, di-ode pumped | Mass | 330 kg |
| Number of lasers | 3 each, one on at any time | Power | 300 W average |
| Laser firing rate | 40 pps | Instrument duty cycle | 100% |
| Laser pulse width | 5 nsec | Data rate | ~550 kbps (uncompress) |
| Laser Energy | 75 mJ 1064 nm | Physical size | ~110 x 140 x 110 cm |
| | 32 mJ, 532 nm | | |
| Laser Divergence | 110 $\mu$rad | Thermal control | Radiators & variable conductance heat pipes |
| Telescope diameter | 100 cm | 532 nm detector | Si APD - Geiger (8 each) |
| 1064 nm detector | Si APD - analog (2 each) | | |

The measurement performance of the completed GLAS instrument was evaluated using a lidar test instrument called the Bench Check Equipment (BCE) (Riris et al. 2003). The GLAS BCE was developed in parallel with GLAS and served as an inverse altimeter and lidar. It was used to simulate the range of expected optical inputs to the GLAS receiver by illuminating its telescope with simulated background light as well as laser echoes with known powers, energy levels, widths and delay times. It also allowed monitoring of the laser energy, the angle measurements of the SRS, and the co-alignment of the transmitted laser beam to the receiver line of sight. These measurements were evaluated when GLAS was in air, before and after vibration tests, during and after the thermal vacuum chamber tests, and after delivery to the spacecraft.

After ICESat launch, the ICESat spacecraft was tested and verified. The operation of the 1064 nm function of the GLAS instrument was evaluated incrementally in a series of orbital tests. At the end of these, Laser 1 was first operated on February 20, 2003. The GLAS measurements showed strong echo pulses from ranging to the surface and cloud tops, and a surface height profile. Operation of the 532 nm receiver was delayed to allow sufficient time for detector out-gassing. To date Laser 1 has operated for 38 continuous days on orbit, using the 1064 nm receiver channel. During this time the GLAS measurements have produced nearly continuous height profiles of ice, land and ocean surfaces, cloud tops and aerosol backscatter illuminated by its laser beam. These span the Earth surface in over 4 complete cycles of coverage in the 8-day ICESat repeat orbit.

2) ATMOSPHERIC CLOUD AND AEROSOL PROPERTIES (J. D. Spinhirne)

The launch of the Geoscience Laser Altimeter System (GLAS) in 2003 marks the advent of global space-based laser profiling of the atmosphere. Part of the NASA

Earth Observing System program, the GLAS mission was conceived as a multidisciplinary earth science experiment that applies the unique capabilities of laser remote sensing. For atmospheric science, GLAS cloud and aerosol measurements address critical applications not available from existing satellite observations. For aerosol, the height distribution must be known for transport and radiative heating models, but existing passive satellite measurements provide little information. GLAS provides global measurements of vertical aerosol structure and optical thickness, planetary boundary layer height, artic haze, episodic dust events and enhanced stratospheric aerosol layers for the first time. Global measurements of aerosol distribution will improve climate models by providing better knowledge of the anthropogenic direct aerosol forcing, which must now be estimated from sulfate source models.

For clouds, passive sensors view cloud tops very well, but are limited in their ability to distinguish multi-level cloud formations and to determine the vertical distribution of clouds. Passive remote sensors typically underestimate the fraction of optically thin clouds, while overestimating the percent of broken, optically thick clouds. Sensitivity studies indicate that the largest uncertainty in long wave radiative flux at the surface is caused by the lack of knowledge of the amount of cloud overlap or multiple layering. In polar regions, improved measurements of clouds is especially important for understanding the radiation balance and for improving the atmospheric modeling of precipitation, both of which directly affect the surface ice mass balance. The GLAS lidar measurements provide for the first time a highly accurate detection of cloud heights and cloud overlap from global satellite observations.

The GLAS observations and the data processing algorithms provide several measures of vertical distribution of cloud and aerosol scattering in the atmosphere. Signal linearity, pulse energy, background offset and other corrections are applied to create the normalized relative backscatter (NRB) product for both the 1064 and 532 nm channels of the instrument. When a calibration is applied, based on collaborative ground measurements in the case of the 1064 nm channel and self calibration to molecular cross sections for the 532 nm channel, the attenuated backscatter cross section data product at both wavelengths are obtained. An example of the back scatter cross section at 1064 nm for an orbit track over the equatorial Atlantic region in shown in Figure 24.

A second product of the algorithms developed for processing GLAS data is the direct height levels of cloud and aerosol layers. The algorithms employ a complex threshold analysis to detect layer heights and for overlapped cloud and aerosol layers, up to the level of signal attenuation, both the top and bottom multiple layers are obtained. An example of the cloud and aerosol height level data product is shown in Figure 24 in association with the cross section data. In the complete analysis it is important to distinguish between aerosol and thin cloud layers. This is accomplished by an analysis that makes use of the magnitude of both the cross section profiles and their first derivative, along with an analysis of the spatial inhomogeneity of layers.

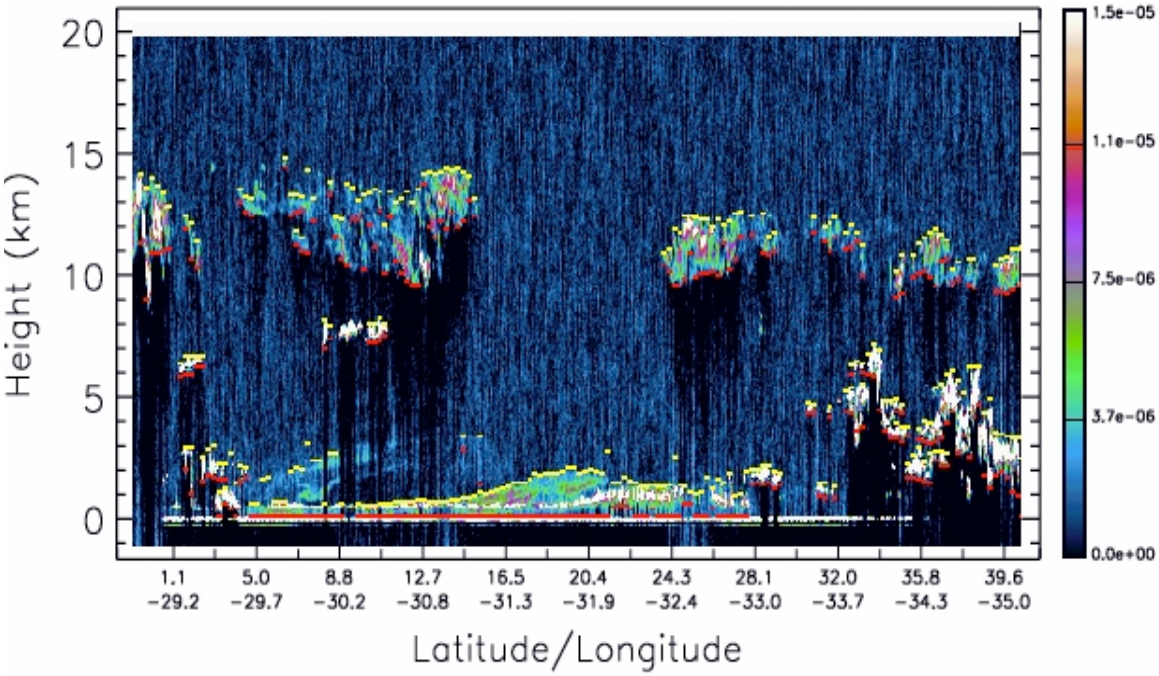


Figure 24. GLAS attenuated backscatter ($m^{-1}$ $sr^{-1}$) at 1064 nm obtained for a 10 minutes of an orbit on March 5, 2003. The cloud layer top (yellow) and bottom (red) are identified for each cloud layer.

In addition giving a direct measurement of heights, the GLAS data and layer detection algorithms give an extremely sensitive and accurate detection of cloud presence for all conditions and densities. Figure 25 shows a result for the detection of Antarctica cloud cover.

The third type of data algorithm developed for GLAS is the calculation of the optical thickness of aerosol and thin cloud layers, and the associated extinction cross section profiles. The algorithm employs, where possible, a direct measure of apparent signal attenuation below layers. Where the low boundary analysis can't be applied, a forward integration based on table values of the integration constant is used. The optical thickness analysis currently requires the 532 nm

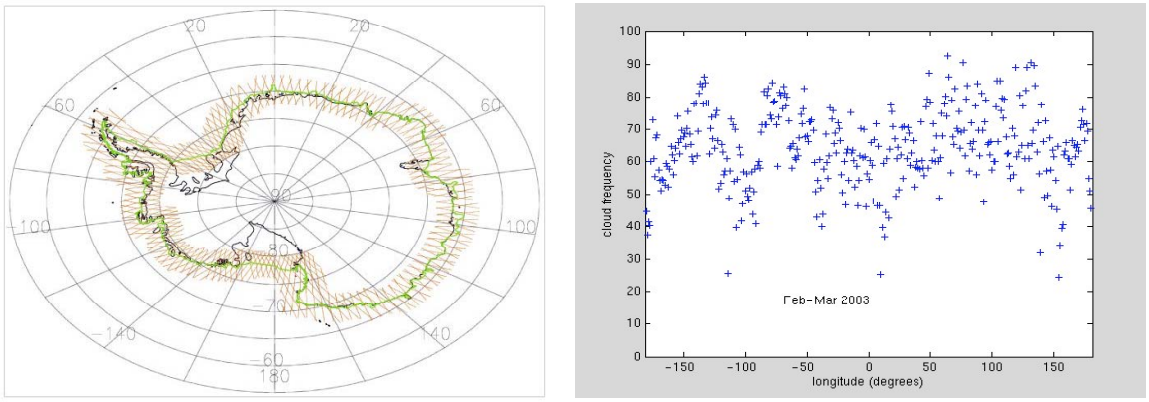


Figure 25. GLAS analysis of Antarctica coastal cloud amount.

data from the instrument and is soon to be realized.

3) VEGETATION CANOPY HEIGHT AND STRUCTURE (D. J. Harding, J. L. Bufton)

Members of the Geodynamics and Space Geodesy Branches in the Laboratory for Terrestrial Physics are contributing to the ICESat mission in a variety of ways, including algorithm development, calibration, validation, and scientific research. Experience applying waveform processing procedures to Shuttle Laser Altimeter (SLA) data, a precursor to ICESat, by David Harding and Claudia Carabajal, contributed significantly to the Gaussian-fitting algorithms used by ICESat to represent complex vertical structure within the GLAS footprints. Harding, working with academic and United States Forest Service colleagues, has established algorithms for converting waveforms to plant-area height distributions and estimations of above ground biomass that will be applied to the ICESat data (Harding et al. 2001; Lefsky et al. 2002).

Methods for establishing on-orbit calibration of the ICESat orbit, pointing, range, and time biases were developed by Scott Luthcke and David Rowlands, using SLA and Mars Observer Laser Altimeter data (Rowlands et al. 2000; Luthcke et al. 2001, 2002). Their Integrated Residual Analysis (IRA) approach using direct altimetry, acquired during ocean scan maneuvers, and dynamic crossovers has been applied to the early cal/val phase data acquired by ICESat (Luthcke et al. 2003). They have confirmed the accuracy of the mission orbit determination, identified and characterized errors in the mission attitude determination, and have produced the pointing, range, and timing biases now used in the operational geolocation processing. Matching of ICESat elevation profiles to digital elevation models (DEMs) by Harding and Carabajal has validated the IRA bias solutions (Carabajal et al. 2003). A more precise validation is being done by matching ICESat waveforms to simulated waveforms derived from very high-resolution DEMs and a model of instrument response. Continuing IRA work is accurately quantifying temporal variations in pointing biases related to changes in illumination and thermal conditions. Jack Bufton is assessing ICESat ocean elevation and pulse spreading statistics in comparison with radar altimeter elevation and significant wave height data, in order to constrain ocean state effects on the IRA and to evaluate potential ICESat contributions to physical oceanography.

When the ICESat geolocation solution is finalized, profile matching to the global Shuttle Radar Topography Mission (SRTM) DEM will be used by Harding and Carabajal to evaluate SRTM accuracy and quantify errors caused by variable microwave penetration through vegetation. The finalized ICESat data will also be used by Harding, working with the NASA Surface Water Working Group, to assess laser altimeter retrieval of time-varying river, lake, and wetland surface elevation (i.e., stage). Jeanne Sauber has worked with the GLAS instrument team, pre- and post-launch, to assess operation of the altimeter gain algorithm in the presence of rapidly varying surface albedo. Sauber and student Darius Mitchell are evaluating the use of the exact repeat capability of ICESat to monitor Alpine and outlet glaciers (Mitchell et al. 2003). They are using Airborne Terrain Map-

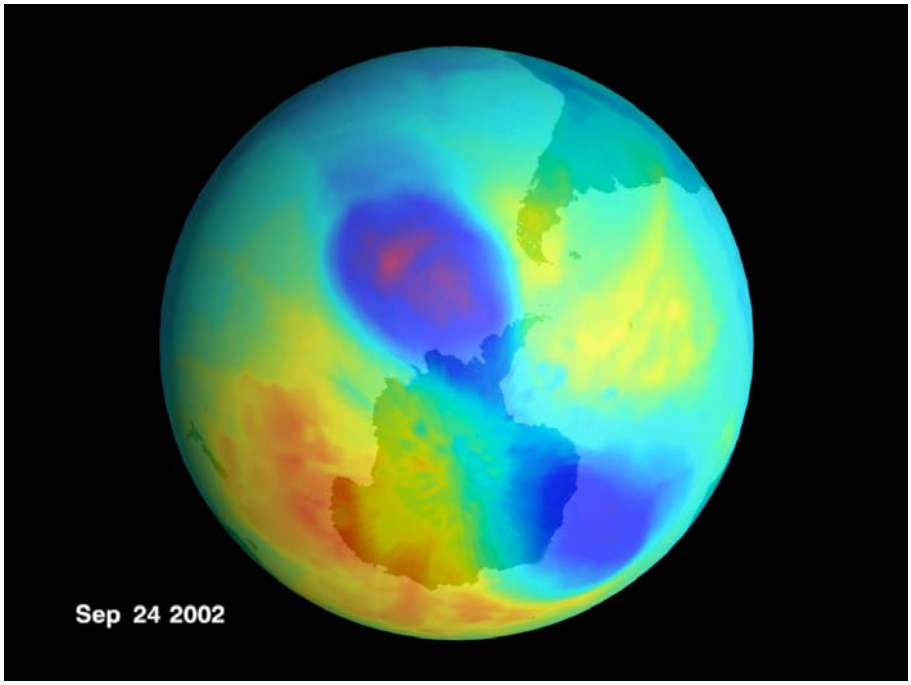


Figure 26. TOMS total ozone content for September 24, 2002 as derived from the Earth Probe TOMS satellite.

per (ATM) laser altimeter data from Greenland to simulate ICESat's potential for retrieval of ice thickness changes on rugged, sloped outlet glaciers. Sauber has worked with University of Alaska colleagues to identify the regions in which ICESat exact repeat capability should be used to monitor ice thickness changes of the large and rapidly thinning southern Alaska glaciers (Sauber et al. 2000).

*e. OMI* (P. K. Bhartia)

Scientists in the Atmospheric Chemistry and Dynamics Branch (Code 916) in the ESD developed the backscattered ultraviolet (BUV) technique in the late 60s to monitor ozone from space. A series of instruments (SBUV and TOMS) based on this principle has flown on NASA and NOAA satellites. This unique data record, developed and maintained by Code 916 scientists, now spans more than 3 decades and plays key role in the assessment of the health of the ozone layer, including careful monitoring of the yearly depletion of ozone in the polar vortex (popularly known as the ozone hole). The behavior of the ozone hole can be highly variable from year-to-year due to complex non-linear influence of the shape, size and temperature of the polar vortex on ozone photochemistry. Figure 26 shows last year's splitting of the ozone hole (shown in blue), as monitored by TOMS, caused by highly unusual vortex dynamics in the South Polar Region. Given the likely influence of global warming on stratospheric temperature and dynamics, there is considerable uncertainty regarding the future evolution of the ozone layer requiring continued long-term monitoring of this important atmospheric constituent.

The Ozone Monitoring Instrument (OMI) is an advanced UV-VIS (270-500 nm)

hyperspectral instrument developed by the Netherlands for the EOS Aura satellite, scheduled to be launched in Jan 2004. Though the primary goal of OMI is to continue the climate-quality data record of total column ozone produced by the SBUV and TOMS instruments, it is also designed to produce a suite of important products relevant to photochemistry, with better accuracy and precision compared to those currently being produced using TOMS and GOME data (GOME is an ESA instrument currently flying on the ERS-2 satellite). These products include extinction and absorption optical depths of aerosols in the UV, and tropospheric column amounts of $O_3$, $NO_2$, HCHO and $SO_2$. In addition, OMI will measure cloud height using the recently developed $O_2$-$O_2$ absorption and rotational Raman scattering (ring effect) techniques.

Four years ago, NASA selected the OMI US Science team to develop several key OMI algorithms as well as to build the data system to process the OMI data in the US. This team is led by Dr. Pawan K. Bhartia/916 and includes several scientists from Goddard ESD. The team works closely with the Dutch science team led by Dr. Pieternel Levelt/KNMI. In addition to the total $O_3$ algorithm, which has been carefully designed to maintain continuity with SBUV and TOMS record, Goddard ESD scientists are responsible for developing aerosol, $NO_2$ and cloud algorithms for OMI.

*f. Data Assimilation Office* (M. M. Rienecker, R. M. Atlas, R. B. Rood)

1) GEOS DATA PRODUCTION FOR EOS INSTRUMENT TEAMS

The near real-time GEOS data production system, developed and operated by the DAO, produces 8 first-look (FL) and 13 late-look (LL) assimilated data products daily for EOS instrument teams and other DAO data users. The GEOS system has been in operation since January 2000, in time to support the EOS Terra instrument teams. All the GEOS data products are sent to the GSFC DAAC for long-term archive and distribution to EOS instrument teams. All the GEOS data products were initially produced at 1° x 1° horizontal resolution and on 36 pressure levels. The horizontal resolution later changed to 1.25° x 1°.

All the FL data are produced and delivered within a day after the data date while the late-look data are produced about 2 weeks behind the FL. The GEOS data products are used by the EOS instrument teams as ancillary input data for their instrument data processing. FL data are used by instrument teams primarily for near real-time satellite data products that follow more stringent delivery timelines.

*Major achievements and deliveries:*

- The DAO successfully implemented the operational GEOS data production system late in 1999 in time for the EOS Terra instrument team support. The GEOS data production operation started with the GEOS-3 system, which was subsequently replaced by the GEOS-4 system in October 2002. The GEOS-4 system was implemented with the DAO next generation assimilation system

called the finite-volume data assimilation system (fvDAS).

- The DAO provided technical collaboration to ESDIS in successfully completing the interface control document (ICD) between ECS and Data Assimilation System (DAS). The DAO continued to provide technical support for the maintenance of the ICD.

- All the GEOS data, 8 FL and 13 LL assimilated daily data products, have been produced since January 2000 without any gap or serious operational anomaly. The data products have been archived at the GSFC DAAC, which distributed the data products to the EOS instrument teams.

- The GEOS-3 system underwent 3 system upgrades to improve the data product quality. The DAO maintained close communications with ESDIS, the GSFC DAAC, and EOS instrument teams to share the GEOS system upgrade plan and to develop a joint schedule for the system changes. The DAO provided all the necessary technical support to the instrument teams to ensure successful system changes at the instrument team facilities as well as at the ground systems facilities. The DAO also worked closely with ESDIS and the GSFC DAAC to implement changes to the system interface, such as for a secure network connection.

- Per request by the MODIS team for MODIS consistent year data processing in 2001, the DAO successfully reprocessed the GEOS-3 data for October 2000 through December 2000 and provided the data to MODIS on time.

- DAO LL products are used by the MODIS Oceans and Land team algorithms to generate their net primary productivity products.

- The DAO developed and maintained the File Specification for GEOS-DAS Gridded Output. The File Specification captures all the EOS HDF data format and metadata standards to which GEOS data product files adhere. Changes to the file specification have been made only after full consultation with ESDIS and EOS instrument teams to minimize the impact of the changes to the GEOS data users.

- The DAO developed and maintained the GEOS system operations status Web page. The status Web page provides up-to-date system information as well as daily status of the GEOS data production. EOS instrument teams can also access the GEOS system documentation, such as the File Specification, on the Web page.

- The DAO continues to provide technical assistance to the EOS instrument teams on future EOS satellites, such as Aura, to facilitate their development of science algorithms that use GEOS data products. For example, the DAO produced and provided GEOS-4 data to the Aura/MLS team in 2002 for use in testing MLS data processing software.

- The DAO provided real-time support about twice a year on the average to EOS-related field experiments, such as the SOLVE mission and the TRACE-P experiment. The DAO provided forecast data as well as the assimilated data products and met tighter timeliness requirements for these missions.

## 2. Interdisciplinary Science Investigations

*a. Atmospheric Transport of Trace Gases and Aerosols: Evaluating Models and Observations* (M. R. Schoeberl, R. S. Stolarski, A. R. Douglass, P. A. Newman, A. M. Thompson, S. Pawson)

This IDS focuses on stratospheric processes, atmospheric chemical change, and stratosphere-troposphere exchange. A key component of the effort is to use satellite, aircraft, ground-based data along with the assimilation and modeling products of the Goddard DAO (now GMAO) to characterize both the observations and develop improved products. A brief summary of these activities is given below.

### 1) Polar Ozone Loss

Members of the IDS participated in the SOLVE (1999-2000) and SOLVE II (2003) missions. The PI was Co-Mission Scientist for the DC-8 and a Co-I (Newman) was Co-Mission scientist for the ER-2 for SOLVE I, both were Co-PI's for SOLVE II which only involved the DC-8. The SOLVE mission is discussed in Newman et al. (2002). During the SOLVE mission a new method to estimate ozone loss was developed. This method takes advantage of all measurements made during SOLVE by satellite, ozonesondes, and aircraft by starting a trajectory whenever a measurement is made. These trajectories are carried forward diabatically until the end of the measurement period (December – mid-March). Comparison of recent and early mission observations for local parcels gives ozone loss. This analysis method is reported in Schoeberl et al. (2002). The authors also showed in this work that biases in the analysis made by POAM can develop because POAM preferentially samples the edge of the vortex. The POAM loss rate estimates were thus higher in January than loss rates over the entire vortex. We also made PV/$\theta$ coordinate transformation estimates of ozone loss during SOLVE (Lait et al., 2002) that agreed well with the trajectory method (Newman et al., 2002).

### 2) Stratosphere-troposphere Exchange

Within this investigation, a new method was developed to quantify the mid-latitude ozone transport to the troposphere using total ozone observations and analyzed potential vorticity (PV) (Olsen et al., 2002). We use the observation that PV is lost in irreversible mass transport to the troposphere. Advantages of this method include the use of global observed or modeled ozone, and the location as well as the magnitude of the ozone flux is calculated. Results for each hemisphere in the year 2000 are shown in Figure 27. A distinct seasonal variability is

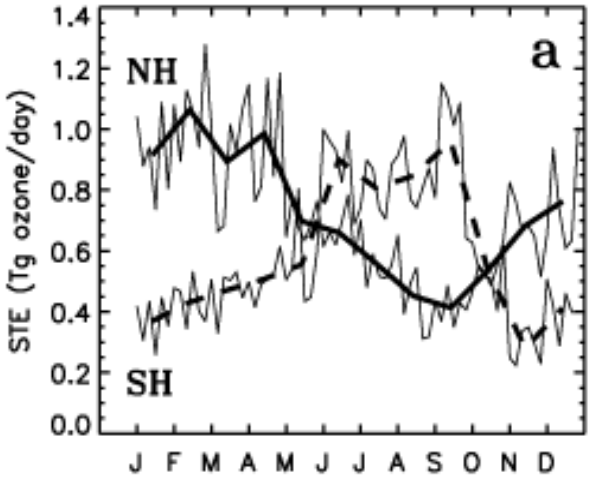


Figure 27. Year 2000 downward cross-tropopause ozone mass flux in units of Tg day$^{-1}$. Bold lines are the monthly averages based upon 6 days per month for the NH (solid) and SH (dashed) mid-latitudes. Thin lines are the flux for the 6 days of each month.

seen and shorter time scale variability is greater during the winter/spring months when the total ozone flux is enhanced. The locations of ozone flux for a single day are shown in Figure 28.

### 3) Analysis of Assimilation Models and Chemical Simulations

Our IDS had a strong link to the GMAO and the analysis of their meteorological products. Two important papers have been produced by this IDS relating to the transport characteristics of the FVDAS compared to the UKMO DAS and the FVGCM. In the first publication, Schoeberl et al. (2003) a series of back trajectory analyses showed that the tropics are excessively ventilated in the assimilation analysis. This ventilation produces flattened constituent and age-of-air gradients (Douglass et al. 2003). Schoeberl et al. (op. cit.) go on to show that for non-

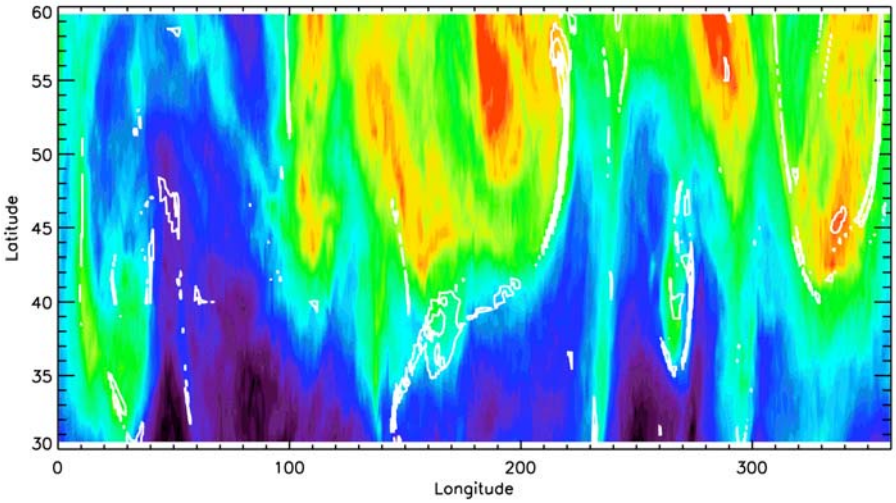


Figure 28. EP/TOMS total column ozone (color shading) and downward cross-tropopause ozone flux (white contours) for April 20, 2000. Total column ozone ranges from 270 DU to 458 DU with warmer colors indicating greater values. Ozone flux contour interval is 5 DU beginning at 10 DU.

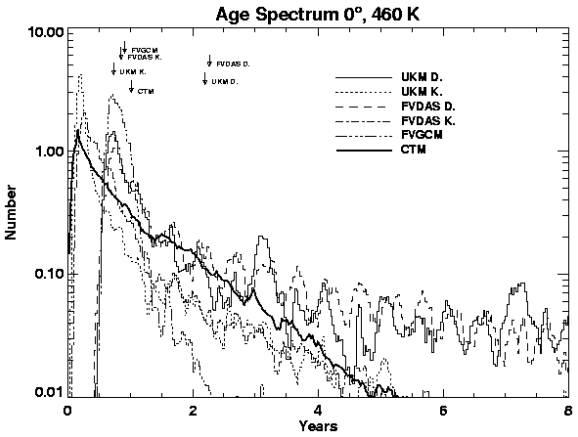


Figure 29. The age spectra computed using the trajectory models for UKMO, FVDAS and FVGCM. Both diabatic (D) and kinematic (K) trajectories were run. The age spectrum using UKMO data and the chemical transport model is also shown. Note the lack of age offset in the kinematic results, and the stretched out spectra in the diabatic cases. These biases lead to a year difference in the mean ages.

isentropic transport, the vertical dispersion associated with the DAS motion fields offsets the bias created by the excessive tropical ventilation, producing reasonable tropical mean ages. These results show that the long-term constituent transport by the DAS fields (including the UKMO) will produce trace gas biases. Figure 29 shows the tropical age spectra computed using trajectories. Figure 29 shows a comparison of constituent gradients observed by aircraft and computed by the DAS driven chemical transport model (CTM).

In contrast to the DAS, the FVGCM shows good tropical isolation compared with observations. Both Douglass et al. and Schoeberl et al. suggest that this significant problem with tropical meteorological fields arises from the failure of the GCM to simulate tropical phenomenon such as the QBO and the MJO.

4) VOLCANIC IMPACTS

Using the interactive 2D model, the effects of future volcanic eruptions on the recovery of the ozone layer were studied. Simulations to the year 2050 were completed. In these simulations, volcanic eruptions having the characteristics of the Mount Pinatubo volcano took place in the model at ten-year intervals starting in the year 2010. These eruptions resulted in transient reductions of globally averaged column ozone of 2-3% relative to background aerosol conditions. These transient losses revert to the nonvolcanic situation within about five years after the eruption, suggesting that the long-term recovery of stratospheric ozone would not be strongly affected by infrequent volcanic eruptions the magnitude of Mount Pinatubo. A sensitivity test was carried out in which a 10% per year increase in the background aerosol loading was imposed. This was found to have a large effect, leading to a slowing of the ozone recovery by more than ten years. These results have been submitted for publication.

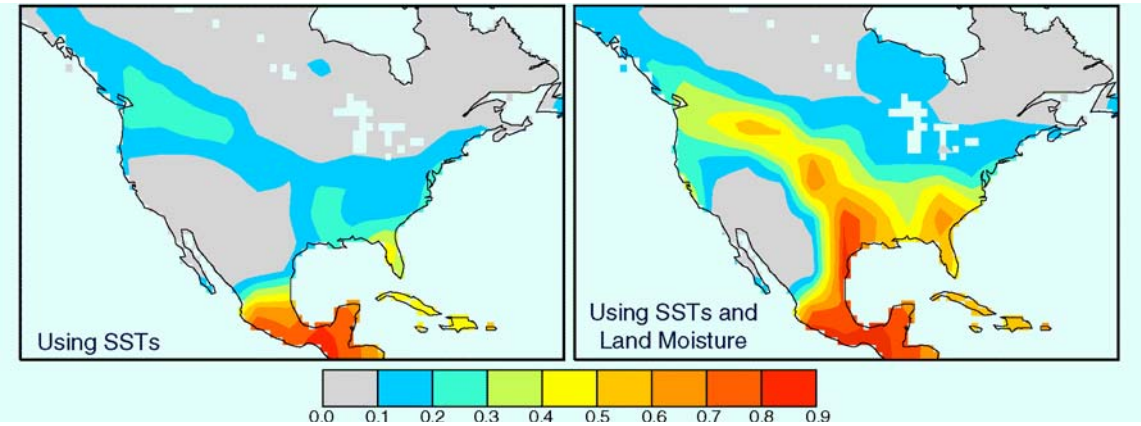


Figure 30. Degree to which precipitation is predictable if sea surface temperatures are perfectly predictable (left) and if both SSTs and land moisture conditions are perfectly predictable (right). The index plotted varies from 0 to 1, with 1 representing perfect predictability (adapted from Koster et al. 2000a).

5) CURRENT STATUS

This IDS was re-proposed in November 2002. The re-proposed work includes an assessment of the tropospheric transport of pollutants and the evaluation of the STE mass flux. As of this writing, we have not heard whether the proposal has been funded. Over the last three years, this IDS has produced 31 publications.

*b. Land Surface Hydrological Processes: Their Representation in Global Climate Models and Their Impacts on Precipitation Predictability* (R. D. Koster, M. J. Suarez, G. J. Collatz, P. Kumar)

The NASA Seasonal-to-Interannual Prediction Project (NSIPP), now incorporated into the Global Modeling and Assimilation Office (GMAO), aims to demonstrate the usefulness of satellite data for seasonal prediction. The basic idea is that the assimilation of satellite-derived data into a forecast model should lead to improved initial conditions for forecasts, which should in turn lead to greater forecast skill. A reliable test for such improvement, however, requires a logical strategy—once the coupled modeling system is set up, we must (1) quantify predictability in the system and establish initialization procedures, (2) perform and evaluate forecasts without a full data assimilation system, to see how well we can do without it, and (3) repeat the forecasts with such a system in place and thereby quantify any increases in skill. On the land surface side, we are applying this strategy to determine the value of remotely sensed measurements of soil moisture and snow for prediction. Our ongoing EOS-IDS project has been the main vehicle for seeing the strategy through.

The predictability analyses (step 1 above) are essentially complete. We have quantified, for example, the degree to which precipitation responds to prescribed, "perfectly forecasted" soil moisture conditions. For the NSIPP system, this response is not global in extent, being limited instead to the transition zones between dry and wet climates (Figure 30) (Koster et al. 2000a). We have also

comprehensively examined soil moisture memory in the model (Koster and Suarez 2001 and the influences on climate of varying vegetation structure (Guillevic et al. 2002. The baseline forecasts (step 2 above) are well underway (Koster and Suarez 2003). Parallel GMAO efforts in soil moisture data assimilation are on the verge of being incorporated into our system.

In parallel to the predictability analysis, our EOS-IDS project has focused on the development of a non-traditional land surface model (LSM) for use with AGCMs: the NSIPP-Catchment LSM (Koster et al. 2000b). Underlying this LSM is the assumption that spatial variability in soil moisture controls in large part the fluxes of moisture and heat from the land surface. This spatial variability (the fact, for example, that hilltops tend to be drier than valley bottoms), which is ignored in traditional LSMs, is treated explicitly in the NSIPP-Catchment LSM through the manipulation of global topography measurements. The resulting improvements in evaporation and runoff generation are expected to increase the realism of simulated seasonal soil moisture storage, which is critical for optimal seasonal prediction. In addition, the structure of the LSM has proven amenable to the assimilation of satellite-derived data (Reichle et al. 2002).

c. *Quantifying the Uncertainty in Passive Microwave Snow Water Equivalent Observations* (J. L. Foster, C. Sun, J. P. Walker, R. E. J. Kelly, A. T. C. Chang)

Snow plays an important role in governing the global energy and water budgets, as a result of its high albedo and thermal and water storage properties. Snow is also the largest varying landscape feature of the Earth's surface. For example, in North America, the snow cover extent may vary from greater than 50% to less than 5% in the course of six months (Hall et al. 2002b). Thus, knowledge of snow extent and snow water equivalent (SWE) are important for climate change studies and SWE applications such as flood forecasting.

Despite its importance, the successful forecasting of snowmelt using atmospheric and hydrologic models is challenging. This is due to imperfect knowledge of physics used in models, model simplifications and errors in the model forcing data. Furthermore, the natural spatial and temporal variability of snow cover is characterized at space and time scales below those represented by the model, meaning that significant scale–related bias or error is often present. Therefore, snow initialization based on model spin-up will be affected by these errors. However, passive microwave observations of brightness temperature from remote sensing satellites may be used to estimate the snow water equivalent (or snow depth with knowledge of the snow density), and hence snow cover extent. By assimilating snow observation products into models such as the Land Surface Models (LSMs), the effects of model error may be reduced. A critical requirement for successful assimilation of snow observations into models is an accurate knowledge of the observation errors. In order for the remotely sensed SWE observations to be useful for climate modeling, for water resource managers and for flood forecasters, it is necessary to have a quantitative, rather than qualitative, estimate of the uncertainty. In data assimilation, error statistics of the observa-

tional data are required so that the correct weighting between observations and model estimates may be applied.

For most passive microwave algorithms, the effects of snow grain size, density and the effects of forest cover are the main source of error in estimating SWE. Of lesser concern are the effects of topography and atmospheric conditions.

The main assumptions made in passive microwave algorithms are that snow density and snow crystal size remain constant throughout the snow season everywhere on the globe; in reality, they vary considerably over time and space. The passive microwave algorithms are found to be very sensitive to snow crystal size. Another major assumption is that vegetation cover does not affect the SWE estimates. In fact, forest cover can have a significant impact on the accuracy of SWE estimates in the densely forested areas, such as the boreal forest of Canada, the underestimation of SWE can be as high as 50% of the estimated values from retrieval algorithms.

Thus, there are both systematic (bias) and random errors associated with the passive microwave measurements. These errors are well known but have thus far not been adequately quantified. Understanding the retrieval errors in remotely sensed snow water equivalent is important for correct interpretation and successful assimilation of such observations into numerical models. This study uses a novel approach to quantify these errors and to formulate a bias-free algorithm that can estimate SWE more reliably. The uncertainty analysis is based on error estimation theory, combined with detailed knowledge of various factors that impact passive microwave response. Among these factors are vegetation cover, snow morphology and topography, calibration errors from a radiative transfer are also considered. This methodology is applied to twenty-two years of daily Scanning Multichannel Microwave Radiometer (SMMR) and Special Sensor Microwave/Imager (SSM/I) passive microwave measurements in order to produce an unbiased SWE dataset and to derive monthly SWE error maps for North America.

*d. Hydrological and Nutrient Controls on the Structure and Function of Southern African Savannas: A Multi-scale Approach* (H. H. Shugart, J. Albertson, J. L. Privette. R. J. Swap, S. A. Macko)

This IDS project analyzes the importance of feedbacks between the atmosphere and land surface in southern African savanna ecosystems. To achieve its goals, the project has strongly leveraged the NASA-supported Southern African Regional Science Initiative (SAFARI 2000) and associated EOS validation resources.

In 2000, the IDS team developed an intensive research campaign on the IGBP Kalahari Transect (KT; See Figure 31). The KT follows a north-south decline in mean annual rainfall from ~1000 mm/yr to ~250 mm/yr on homogenous sandy soils deposited during the Pleistocene (Kalahari Sands). Vegetation type ranges from partially closed woodlands in the north to open shrub land in the south, however the mixed life-form composition characteristic of savanna communities


Figure 31. Distribution of Kalahari sands and major rivers in southern Africa. Locations of existing Kalahari transect sites to be used in this study are also provided.

is maintained throughout.

By driving their savanna models with these data, team demonstrated that the spatial pattern and temporal dynamics of soil moisture and nutrients are strongly coupled to the regional-scale climatic gradient (mean annual rainfall and nutrient availability) and patch-scale distribution of vegetation structure (e.g., as determined by competitive relationships between plant individuals). This conclusion has significant implications for (i) understanding how changes in global climate affect savanna ecosystems, and vice-versa, and (ii) monitoring vegetation at different resolutions in time and space, a central issue in the interpretation of remotely sensed data collection.

1) RESULTS SUMMARY

Through extensive field work, the IDS team found that canopy structural differences, coupled with the regional rainfall gradient, lead to changes in the relative contribution of trees and grasses to vegetation productivity across the transect (Dowty et al. 2000, 2003; Scholes et al. 2002; Caylor et al. 2003; Privette et al. 2003). The team also addressed the functional consequences of structural variability in vegetation through a model-based characterization of productivity distribution (Caylor et al. 2003). Spatial information provided by a large eddy simulation model (Scanlon and Albertson 2003) indicates that the spatial distribution of the vegetation fluxes can be strongly tied to the distribution of the canopy sublayer air properties, indicating scaling complexity for heterogeneous vegetation associated with highly water-limited conditions.

The team's analysis of water's role in controlling structure indicates strong shifts in water stress under and between tree canopies, depending on annual rainfall. In an analysis of multi-temporal AVHRR-NDVI data in the context of water availability, Scanlon et al. (2002) found a strong relationship between fractional

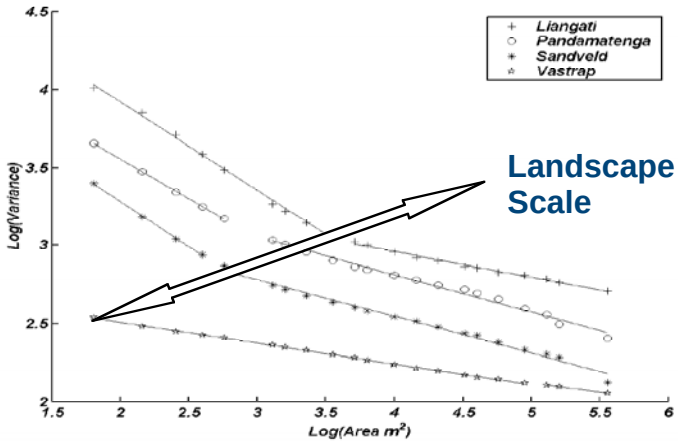


Figure 32. Realization of the multi-scale nature of savanna ecosystems, depicting the variance of the NDVI field as a function of the area over which the field is averaged (from Caylor et al. 2003).

tree cover and mean wet season precipitation. Potential grass cover peaked at approximately 450 mm of mean wet season precipitation. Above this value, the tree cover controlled the potential grass area. Below 450 mm, the potential grass area appeared to be limited by the available rainfall.

Scanlon and Albertson (2003) found that, in the northern portion of the KT, a large portion of the water balance may be accounted for by leakage through the bottom of the root zone in sandy soils, and vegetation may be limited by nutrient availability. In the southern portion of the KT, however, the tree fractional cover is governed by the long-term mean rainfall. These results suggest that the vegetation composition in water-limited portion areas, over interannual to multi-decadal timescales, can be modeled largely as a function of the mechanistic constraints imposed by the water cycle. A scaling analysis with fine-scale NDVI data showed a change in scaling regime between the patch and the landscape scales (See Figure 32). The breakpoint appears to be a consequence of plant canopy processes controlling pattern at small scales and other landscape processes then controlling pattern at larger scales.

2) PRODUCTION

In the last three years, this IDS has produced approximately 25 peer-reviewed publications. The work associated with our this project has been synthesized as special issues in the *Journal of Arid Environments* [Vol 54, Number 2, June 2003] (for initial model documentation), *Global Change Biology* [*Special Issue*, 2003] (for the synthetic products from the field campaign), and *International Journal of Remote Sensing* [Special Issue, 2004] (remote sensing analyses and EOS validation).

3) CURRENT STATUS

This IDS was re-proposed in April 2003. Using EOS data and models, we proposed to determine the impact of global climate change scenarios on savanna

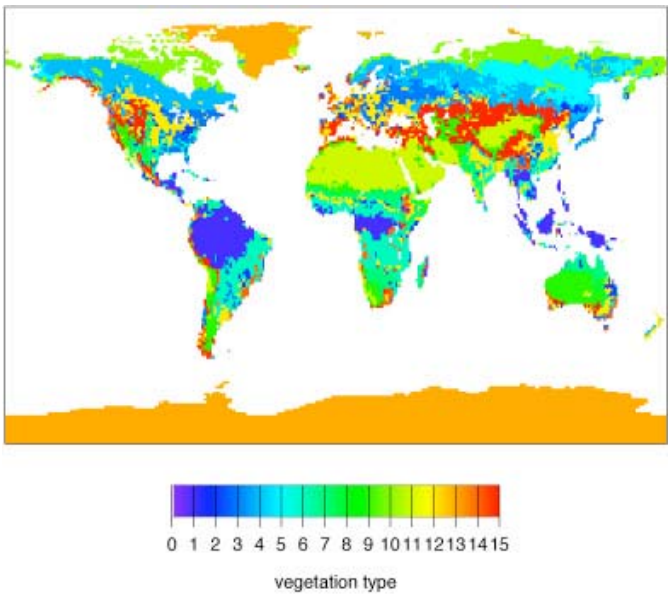


Figure 33. Vegetation classification based on temporal dynamics of satellite derived vegetation index. Data released as part of ISLSCP I Project.

structural and functional evolution. A funding decision was not announced at the time of this writing.

*e. Biosphere – Atmosphere Interactions* (P. J. Sellers, D. A. Randall, I. Y. Fung, C. J. Tucker, G. J. Collatz)

This IDS project focused on the interactions between the land surface carbon cycle and the climate. The project was funded by EOS-IDS program from 1991-2000 based on periodic highly favorable reviews by the science community and NASA HQ. The team was headed by Piers Sellers of GSFC and Harold Mooney of Stanford University (and in later years by David Randall, CSU and then Inez Fung, currently at UC Berkeley). Besides the number of significant accomplishments listed below, the project also participated in the training of 31 students and post-docs, several of whom have since risen to leadership roles in the science community.

*Major achievements and deliveries:*

- Global distributions of land surface properties have been for the first time derived from satellite observations for use in GCM studies of energy and water exchange (Figures 33 & 34) (Los et al. 1994; Defries and Townshend 1994; Sellers et al. 1994, 1996c). These data sets have been extensively used by the team in accomplishing the results listed below and have also been released to the science community including ISLSCP Initiatives I and II (see Sellers et al. 1996d).

- Members of the team produced a global 20-year time series of NDVI by merging and inter-calibrating observations across different instruments on different polar orbiters (Los et al. 1994, 2000). Through the significant reduction in er-

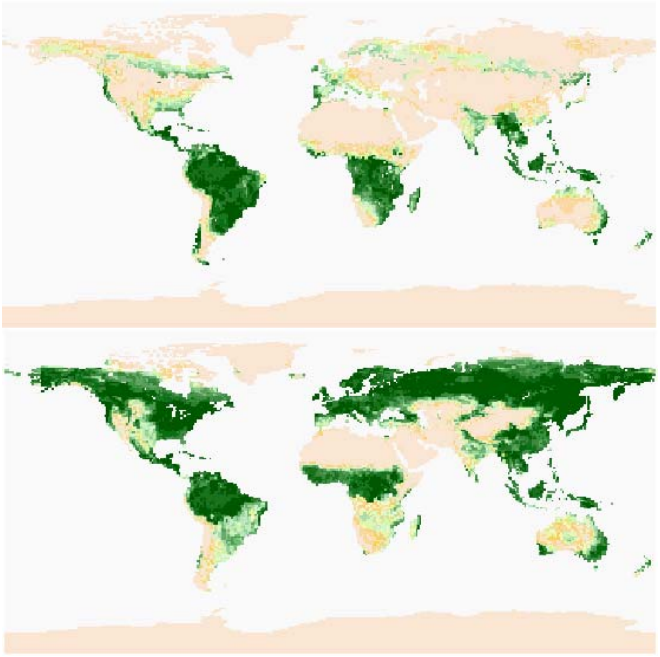

Figure 34. The seasonal distribution of vegetation activity derived from specially processed satellite vegetation index (FASIR) from AVHRR instrument and used to derive vegetation parameters for models (e.g. FPAR, LAI, vegetation classification. Top: January vegetation index. Bottom: July vegetation index.

rors in the NDVI, the time series can be used to assess interannual variations in vegetation at the global scale (Myneni et al. 1996, 1997; Nicholson et al. 1998; Los et al. 2001).

- The project developed a new generation of Land Model (Sellers et al. 1997), SiB2, for implementation in atmospheric GCMs (Randall et al. 1996; Sellers et al. 1996a, 1996b; Denning et al., 1996). SiB2 incorporates realistic biophysics and mechanistic links between the transpiration of water and the assimilation of carbon (Figure 35). A unique feature of this approach is the *a priori* incorpo-

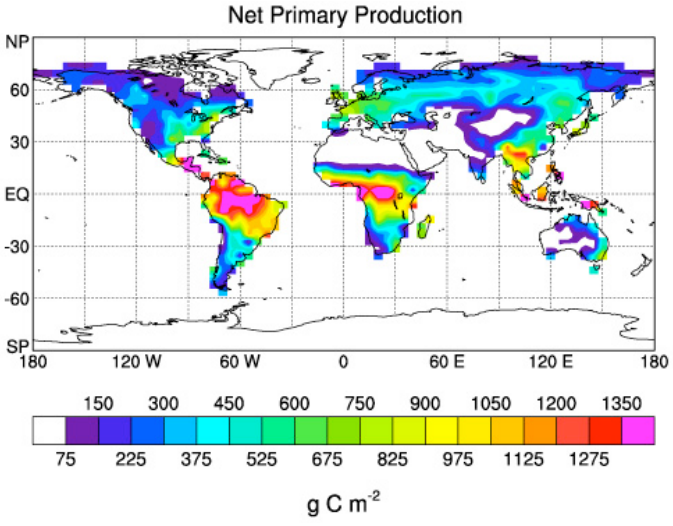


Figure 35. Coupled SiB2-GCM simulation of the yearly carbon uptake by Earth's vegetation.

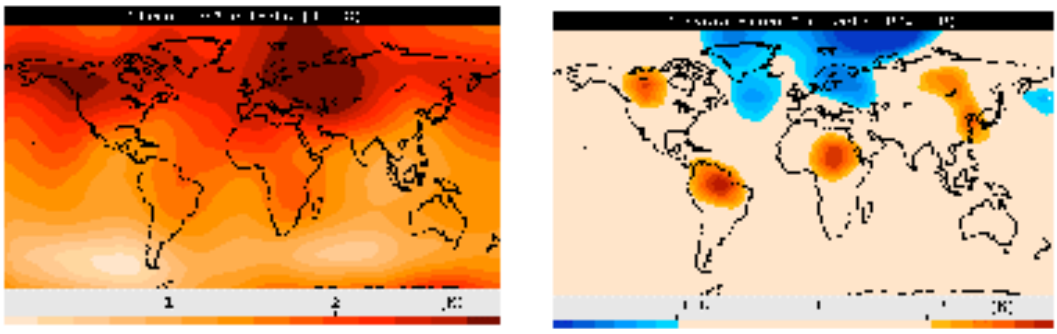

Figure 36. Increases in surface air temperature (K) in a 2x$CO_2$ atmosphere: (left): due to radiative effects alone; (right) due to plant physiology feedbacks.

ration of satellite information into the model formulation and data stream. Satellite-derived vegetation classification maps and biophysical models were expanded to include classifications based on C4 physiological mechanism characteristic of certain vegetation and climate types (Collatz et al. 1992, 1998).

- The project led to the development of a new global biogeochemical model CASA that is forced by, *inter alia*, satellite observations of photosynthetically active radiation and employs distribution of FPAR from NDVI (Potter et al. 1993; Field et al. 1995).

- Using the NDVI time series and an inverse model, we showed that an early growing season at high latitudes is directly observed by the NDVI (Myneni et al. 1997) and is corroborated by analysis, via tracer transport modeling, of the changing seasonal cycle of atmospheric $CO_2$ in the Northern Hemisphere (Randerson, et al. 1999).

- Using SiB2-GCM, we showed that vegetation variability (based on 1982-1990 NDVI) may contribute to the variability in the physical climate (Bounoua et al. 2000; Collatz et al. 2000).

- Using the SiB2-GCM, we showed, for the first time, that direct effects of increased $CO_2$ on vegetation physiology will lead to a relative reduction in evapotranspiration over the continents, with associated regional warming and drying over that predicted for conventional greenhouse warming effects, particularly in the tropics (Figure 36) (Sellers et al. 1996a; Bounoua et al. 1999).

- Using the SiB2-GCM, we showed that co-variation of seasonally varying $CO_2$ fluxes and the height of the planetary boundary layer contributes to a positive $CO_2$ concentration in the PBL in the annual mean, even when fluxes cancel in the annual mean (the rectifier effect) (Denning et al. 1995). This finding has significant implications for the magnitudes of $CO_2$ sources and sinks inferred from atmospheric $CO_2$ measurements in the planetary boundary layer.

- Using CASA, we have produced the first global model of $C^{13}$ exchange with the biosphere and first calculation of the isotopic disequilibrium due to the long residence time of carbon in the biosphere (Fung et al. 1997). The long

residence time suggests that C4 vegetation takes up a non-trivial fraction anthropogenic $CO_2$ (Fung et al. 1997) and that $CO_2$ fertilization is not the only mechanism responsible for the uptake (Randerson et al. 1999).

- With the end of the funding for large scale- long duration IDS projects the members of this projects splintered into several smaller projects that were successful in obtaining funding from the new IDS Program. These groups continue to collaborate with one another and hold meetings twice a year. One such project is investigating the role of global fires in determining the $CO_2$, CO and $CH_4$ composition of the atmosphere. Using fire detection data from satellites and a biogeochemical processes model we are able to estimate the contributions of different regions and different time periods to the emissions of carbon from fires for the globe (van der Werf et al. 2003). Results thus far show that much of the observed variability in the $CO_2$ growth rate in the atmosphere is controlled by variability in forest fires both in tropical and boreal regions.

*f. A Carbon Balance Approach to Measuring Human Impacts on Biodiversity and Carrying Capacity of Ecosystems* (M. L. Imhoff, L. Bounoua)

Originally initiated as an EOS Interdisciplinary Science Investigation entitled, "Assessing the Impact of Expanding Urban Land Use on Agricultural Productivity…" this work was continued in its present form under the Land Use Land Cover Change and Carbon Cycle Science Programs. The goals of this investigation were to investigate the consequences of urbanization and human consumption patterns on net primary production (NPP) and biological diversity. A brief summary of results is given below.

*Consequences of Urbanization on NPP*

Our breakthrough in mapping urbanization (Figure 37) enabled some first ever assessments of the consequences of urbanization on important biological functions and climate. By integrating the urbanization data with AVHRR observations of NDVI and a terrestrial carbon model we were able to quantify the impact of urbanization on the carbon cycle and food production in the U.S. as a result of reduced net primary productivity (NPP) (Imhoff et al. 2003). Our results showed that urbanization has a disproportionately large overall negative impact on NPP compared to other forms of land cover change. Urban land transformation in the US has reduced the amount of carbon fixed through photosynthesis by 0.04 Pg per year or 1.6% of the pre-urban input. The reduction is enough to offset the 1.8% gain made by the conversion of land to agricultural use, even though urbanization covers an area less than 3% of the land surface in the US and agricultural lands approach 29% of the total land area (Defries et al. 1999). This work also demonstrated satellite evidence of urban heating through the NPP signal (Imhoff et al. 2000). At local and regional scales, urbanization increases NPP in resource-limited regions, and through localized warming "urban heat" contributes to the extension of the growing season in cold regions (Figure 38).

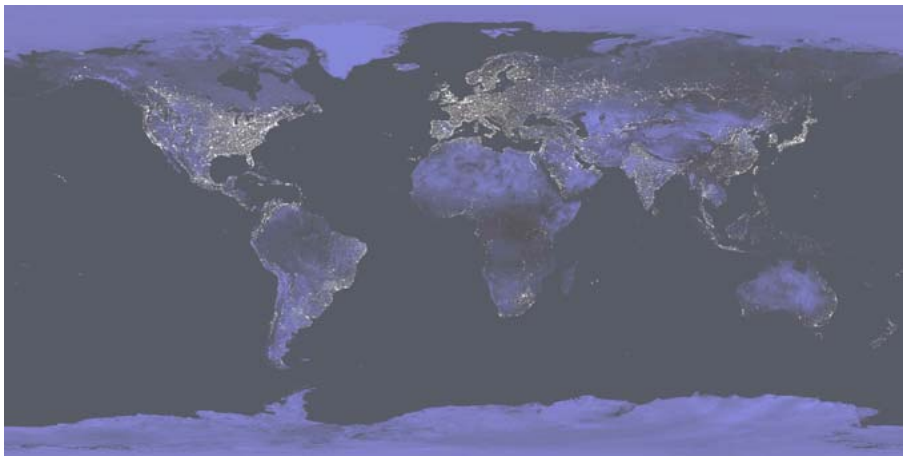

Figure 37. Global view of Earth's urban areas compiled from over 200 VIS-NIR (0.5 to 0.9 micrometers) nighttime images acquired by the Defense Meteorological Satellite Program's Operational Linescan System (DMSP/OLS). The images used to make this compilation were acquired between 20:30 and 21:30 local time and are timed with waning phases of the moon so that the world's city lights are among the brightest objects on the Earth's surface.

We subsequently worked with the Goddard Institute for Space Studies to help in the detection and elimination of a consistent urban heating bias in the temperature record for the US (Hansen et al. 2001). As part of this work, we also quantified the consequences of urbanization on biologically available energy and food production. We estimated the annual reduction of energy input to the U.S. biological system due to urbanization at $3.9 \times 10^{14}$ kilocalories. Loss from agricultural lands alone is $1.4308 \times 10^{13}$ kilocalories, equivalent to the caloric requirement of 16.5 million people, or about 6% of the US population.

*Consequences of Human Consumption Patterns on NPP*

An important measure of humanity's cumulative impact on the biosphere is the fraction of the planet's total net primary production (NPP) humans appropriate for their own use (Vitousek et al. 1986; Rojstaczer et al. 2001). As part of this IDS research we used satellite observations, data on human consumption, biophysical models, and population data to compare the rate of NPP demand to the rate of supply. Terrestrial NPP (i.e., "supply") was estimated using a carbon model, global fields of satellite derived vegetation index averaged over the 1982-1998 period, and climate drivers obtained from surface climatology (Potter et al., 1993). We estimate Earth's current total annual NPP as 56.8 Pg of carbon.

NPP "demand" was estimated using statistical data from the United Nations Food and Agriculture Program and biological models. The average annual global NPP demand was estimated to be 11.5 Pg or about 20% of total terrestrial NPP supply. A global map of NPP demand was created by applying the country level values to a global map of human population. We then used the supply and demand maps to quantify the differences in NPP supply and demand across the landscape (Figure 39).

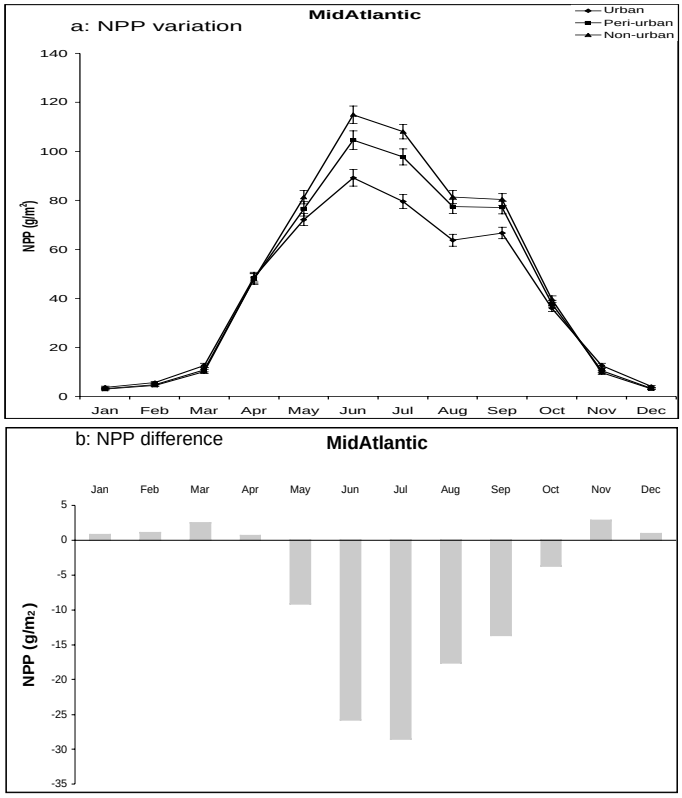


Figure 38. Seasonal dynamics of the impact of urbanization on NPP for the Mid-Atlantic Region of the United States showing evidence of urban heating. (a) Monthly mean NPP rates for urban (diamonds), peri-urban (squares), and non-urban (triangles) areas, (b) NPP difference showing the loss (negative) or gain (positive) in NPP rates ($gm^{-2}$) resulting from urbanization (urban – non-urban). Note the increase in wintertime photosynthetic activity in the urbanized area as compared to non-urban areas.

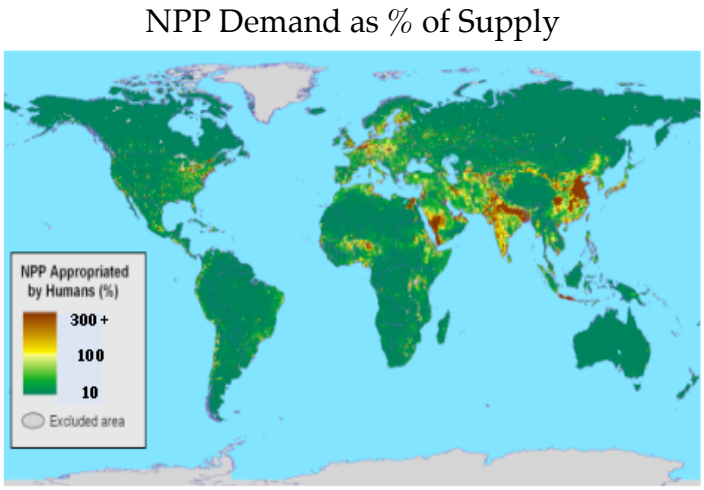


Figure 39. Amount of NPP consumed by humans annually (demand) as a % of NPP supply. Even in areas with relatively low *per capita* consumption, demand can exceed supply at sub-regional and regional scales due to diminished local productivity, large populations, and inefficient harvest and processing methodologies. At the individual grid cell level, demand in heavily urbanized areas can greatly exceed the local NPP supply.

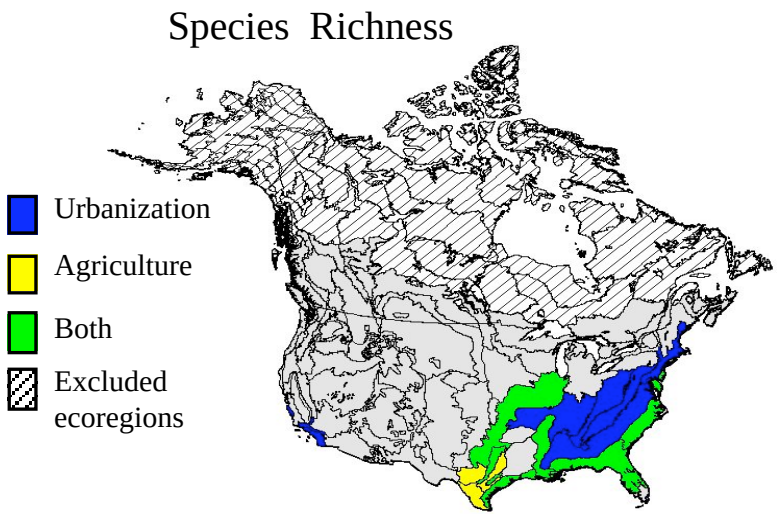


Figure 40. Map of ecoregions in the top 66% quantile of biodiversity and land use indices. Shown is species richness versus urbanization, agriculture, or both.

*Consequences of Land Use Land Cover Change on Biodiversity*

Urbanization and agriculture are two of the most important threats to biodiversity worldwide. Team members of this IDS combined distributional data for eight major plant and animal *taxa* (comprising over 20,000 species) with remotely sensed measures of urbanization and agriculture to assess conservation priorities among 76 terrestrial ecoregions in North America (Ricketts and Imhoff 2003). The analyses yielded four "priority sets" of 6-16 ecoregions (8-21% of the total number) where high levels of biodiversity and human land use coincide (Figure 40). Across all 76 ecoregions, urbanization is positively correlated to both species richness and endemism, emphasizing that human activities and biodiversity are on a collision course. Conservation efforts in densely populated areas are therefore equally important (if not more so) as preserving remote parks in relatively pristine regions.

*g. Climate Forcings and Response on Satellite and Century Time Scales* (J. E. Hansen, A. D. Del Genio, A. A. Lacis, M. I. Mishchenko, D. H. Rind, W. B. Rossow, B. E. Carlson)

This EOS IDS investigation has produced more than 200 publications over the past 12 years. Summaries of these publications are included in the annual GISS Research Publications document.

The subject of this investigation evolved over the 12 years, as indicated by its successive titles, first "Interannual variability of the global carbon, energy and water cycles", next "Climate forcings and response on interannual and decadal time scales", and now "Climate forcings and response on satellite and century time scales". The topic of the investigation was initially unfocused, as indicated by its unofficial title "global modeling of everything," but over the past several

years it became focused on climate forcings and climate change in the industrial era with emphasis on the satellite era.

The approach of the investigation has been to provide partial support for a number of scientists working on a coordinated investigation of this topic, including support or partial support for post-doctoral researchers. Current co-investigators are Susanne Bauer, Tomothy Hall, Yongyun Hu, Dorothy Koch, Surabi Menon, Ronald Miller, Larissa Nazarenko, Judith Perlwitz, David Rind, Gary Russell, Makiko Sato, Gavin Schmidt, Drew Shindell, Shan Sun and George Tselioudis.

The principal products of the investigation are the publications and the implications of these for research and observational strategies, and, even further, the information that the investigation provides decision-makers relevant to the question of how to deal with global climate change. Two current documents that epitomize these ultimate products are: (1) "Long-Term Climate Change: Research Plan" a strategic plan for Goddard Earth Sciences research in climate change, written at the request of Franco Einaudi, and (2) "Can we defuse the global warming time bomb," a presentation by J. Hansen to the Council on Environmental Quality available at:
ftp://169.154.204.80/outgoing/HansenPresentation/hansenpresentation.11aug2003v1.doc

## 3. Calibration Facilities

The GSFC calibration facilities include the Radiance Calibration Facility (RCF) and Diffuser Calibration Facility (DCaF) both residing in Code 920.1 and the Radiometric Calibration Development Facility (RCDF) residing in Code 916. These facilities play an important role in maintaining GSFC's Earth Sciences Directorate as NASA's center of expertise in instrument calibration and characterization and in calibrating and characterizing Earth Observing System (EOS) satellite and validation instrumentation.

### *a. Radiance Calibration Facility* (P. Abel)

The Radiance Calibration Facility maintains instruments and National Institute of Standards and Technology (NIST)-traceable calibrated sources to calibrate, monitor, and assess the performance of satellite, aircraft, and ground-based remote sensing instrumentation. RCF instruments and sources span the spectrum from the ultraviolet through the visible and into the shortwave infrared wavelength regions. RCF instruments, sources, and expertise are available to US Government agencies, the international remote sensing community, and academic institutions.

The RCF offers extended uniform sources of spectral radiance in the wavelength range 0.4 to 2.4 $\mu$m with a range of spectral radiance levels (cf. Figure 41). Source aperture diameters of 40 cm and less are available, with radiance uniformity

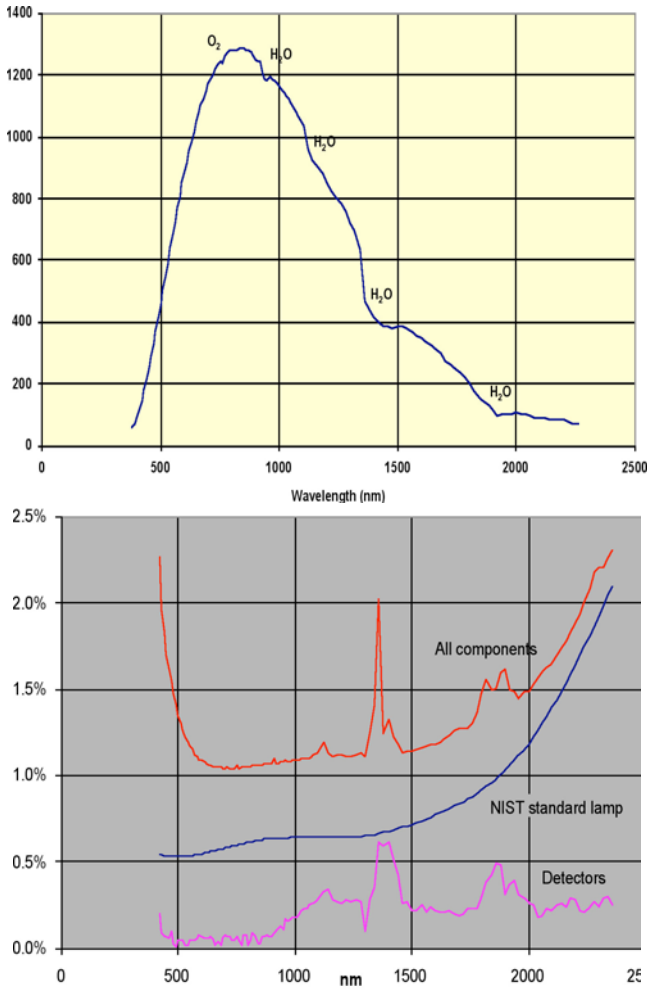


Figure 41. The maximum spectral radiance levels available from the RCF 1.8 m diameter integrating sphere (top) and the anticipated standard deviation of its absolute radiance measurement uncertainty.

much better than ±1%.

1) RADIANCE MEASUREMENTS IN SUPPORT OF EOS

The AERosol Robotic NETwork (AERONET) is the dominant customer of the RCF. All 225 Cimel sun photometers in the world-wide network are calibrated for radiance responsivity approximately once a year in the facility.

The South African Regional Science Initiative (SAFARI), the Asian pacific regional aerosol Characterization Experiment (ACE-Asia), and the Large scale Biosphere-atmosphere experiment in Amazonia (LBA) projects have calibrated some of their ground-based spectrometers within the RCF, as has the Clouds and the Earth's Radiant Energy System (CERES) project at NASA's Langley Research Center (LaRC). Miscellaneous radiometers have been calibrated for *ad hoc* studies (e.g., chlorophyll-a surface truth for MODIS). Sources used in support of the MODIS Airborne Simulator (MAS) and MODIS/ASTER Airborne Simulator (MASTER) programs are re-calibrated at NASA's Ames Research Center (ARC)

by RCF personnel on an approximately annual basis.

RCF sources form part of an internationally recognized network of secondary EOS radiance standards. Teams from government, university, and industry laboratories regularly compare network sources to ensure that they are on the same radiometric scale. Spectroradiometers from the RCF have participated in a number of EOS radiance measurement comparisons. In addition, the RCF has hosted an EOS radiometric measurement comparison campaign in April 2001 and a SIMBIOS Radiometric Intercomparison (cf. Table 2).

*b. Diffuser Calibration Facility* (J. J. Butler)

The DCaF has operated within Code 920.1 since May 1993. The facility is a class 10,000 clean room containing a unique, state-of-the-art, out-of-plane optical scatterometer capable of measuring the bidirectional scatter distribution function (BSDF)* of transmissive or reflective, specular or diffuse optical elements and surfaces in addition to granular, powdered, or liquid samples (Schiff et al. 1993). The current operating wavelength range of the out-of-plane scatterometer is 230 nm to 900 nm employing a lamp/monochromator source and a variety of laser sources. The parallel development of an in-plane BSDF measurement capability in the shortwave infrared from 1000 nm to 2500 nm has recently been completed using independent hardware. The out-of-plane scatterometer is capable of performing polarized and unpolarized scatter measurements on samples up to 12 inches on a side and 10 pounds weight. Samples can also be rastered to measure reflectance and transmittance uniformity. In addition, the DCaF has fully implemented a capability to measure the 8 degree/directional hemispherical scatter of reflective samples. This measurement complements and validates the facility's established approach of integrating BRDF over the complete scattering hemisphere of a sample to determine hemispherical scatter. The facility is a secondary standards calibration facility, the primary standard facility being the Spectral Tri-function Automated Reflection Radiometer (STARR) facility located at the National Institute of Standards and Technology (NIST) in Gaithersburg, Maryland (Proctor and Barnes 1996). The measurement uncertainty of DCaF BSDF measurements is 0.7% (k = 1), and agreement between absolute BSDF measurements made by the DCaF and by NIST on identical samples is 1% or better over the complete wavelength operating range of the scatterometer. The current measurement uncertainty of DCaF directional hemispherical measurements is 1% (k = 1) over the complete operating wavelength range.

1) SCATTER MEASUREMENTS IN SUPPORT OF EOS

Since 1993, the DCaF has performed a number of scatter measurements on a variety flight and non-flight hardware in support of satellite and validation programs in NASA's EOS.

* Bi-directional scatter distribution function (BSDF) is a term which includes the more specific terms of bi-directional reflectance function and bi-directional transmittance function (i.e. BRDF and BTDF).

Table 2. RCF participation in EOS radiometric measurement comparisons.

| Date | Host Institution | Radiance Source Measured | EOS Instrument(s) Supported | Reference |
|---|---|---|---|---|
| Feb. 1995 | NEC, Japan | 2 m $BaSO_4$ sphere | ASTER | 1,2,3 |
| | | 1 m $BaSO_4$ sphere | | |
| Aug. 1996 | Raytheon Santa Barbara Remote Sensing | 1 m $BaSO_4$ sphere | MODIS, ETM+ | 1,2,4 |
| | | 1.22 m $BaSO_4$ sphere | MODIS | |
| Aug. 1996 | Jet Propulsion Lab | 1.6 m $BaSO_4$ sphere | MISR | 1,2,4 |
| Nov. 1996 | NEC, Japan | 1 m $BaSO_4$ sphere | ASTER | 1,2,5 |
| | MELCO, Japan | 1 m $BaSO_4$ sphere | | |
| Nov. 1997 | NASA's GSFC | 1.07 m $BaSO_4$ sphere | SeaWiFS, Validation Instruments | 1 |
| Aug. 1999 | NASA's Ames Research Center | 0.76 m $BaSO_4$ sphere | MAS, MASTER | 1,6 |
| | | Lamp + panel | | |
| | | 0.3 m $BaSO_4$ sphere | EOS calibration | |
| Apr. 2001 | NASA's GSFC | 1.8 m $BaSO_4$ sphere | Validation Instruments | 1,7,8 |
| | | 0.5 m $BaSO_4$ sphere | SOLSE, LORE, TOMS, SBUV/2 | |
| | | 0.3 m $BaSO_4$ sphere | EOS calibration | |

*BSDF Measurements in Support of the Long-term Monitoring of Ozone*

The DCaF has made BSDF measurements for NASA's and NOAA's uv albedo measuring satellite programs since June 1993. Facility customers from 1993 to 2000 included the Solar Backscatter Ultraviolet-2 (SBUV-2) and the Total Ozone Mapping Spectrometer (TOMS) flight programs. The DCaF has acquired and maintained the long-term historical BRDF database for the SBUV-2 and TOMS pre-flight calibration diffusers. In addition, the DCaF measured thousands of BRDF data points on the roughened aluminum flight diffusers of the Meteor, Earth Probe, and QuikTOMS instruments. In 1999, the DCaF participated in an international BRDF measurement comparison with TPD/TNO using the TOMS pre-flight calibration diffusers (Butler et al. 2002). TPD/TNO is the Netherlands-based calibration facility responsible for the pre-flight calibration of the Ozone Monitoring Instrument (OMI) on EOS Aura. The DCaF has recently acquired diffuser BRDF measurements in support of the pre-launch calibration of the Ozone Monitoring Instrument (OMI) on the EOS Aura platform (cf. Figure 42). The succession of ozone instrument customers was recently extended to the NPP/NPOESS era with the addition of the Ozone Mapping and Profiler Suite (OMPS) project as a facility customer.

In support of the calibration of instrumentation used in the validation of satellite

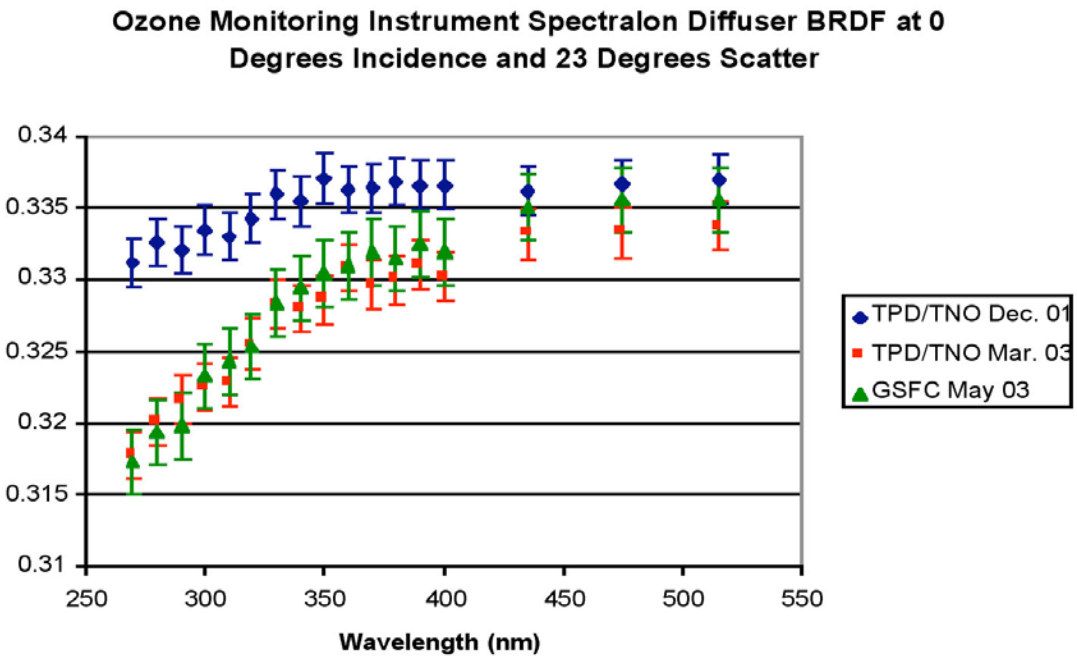


Figure 42. Bidirectional reflectance distribution function (BRDF) measurements on the Spectralon diffuser used in the pre-launch calibration of the EOS Ozone Monitoring Instrument (OMI) on EOS Aura. The DCaF recently validated the unexpected decrease in the BRDF of this diffuser shown in this figure.

ozone measurements, the DCaF measured BRDF data on the diffusers used to calibrate the Shuttle Solar Backscatter Ultraviolet (SSBUV) from 1993 to 1997 and on the diffusers used to calibrate the Shuttle Ozone Limb Sounding Experiment/Limb Ozone Retrieval Experiment (SOLSE/LORE). The DCaF has also measured the BRDF of the diffuser used in the calibration of the Research Scientific Instruments (RSI) Calibration Transfer Standard Radiometer (CTSR). The CTSR was employed in the pre-launch calibration of the OMI instrument.

In support of the calibration of instrumentation used in the validation of satellite ozone measurements, the DCaF measured BRDF data on the diffusers used to calibrate the Shuttle Solar Backscatter Ultraviolet (SSBUV) from 1993 to 1997 and on the diffusers used to calibrate the Shuttle Ozone Limb Sounding Experiment/Limb Ozone Retrieval Experiment (SOLSE/LORE). The DCaF has also measured the BRDF of the diffuser used in the calibration of the Research Scientific Instruments (RSI) Calibration Transfer Standard Radiometer (CTSR). The CTSR was employed in the pre-launch calibration of the OMI instrument.

*BSDF Measurements in Support of the Landsat ETM+ and EO-1 ALI Instruments*

The DCaF was uniquely able to acquire BRDF data on the Landsat Enhanced Thematic Mapper Plus (ETM+) flight and flight spare diffusers in addition to 12 witness samples coated with different formulations and uv exposure times of white YB-71 thermal control paint (cf. Figure 43). The measurement versatility of the DCaF scatterometer enable the measurement of the two 20 inch hexagonal flight and flight spare diffusers down to the twelve one inch diameter witness

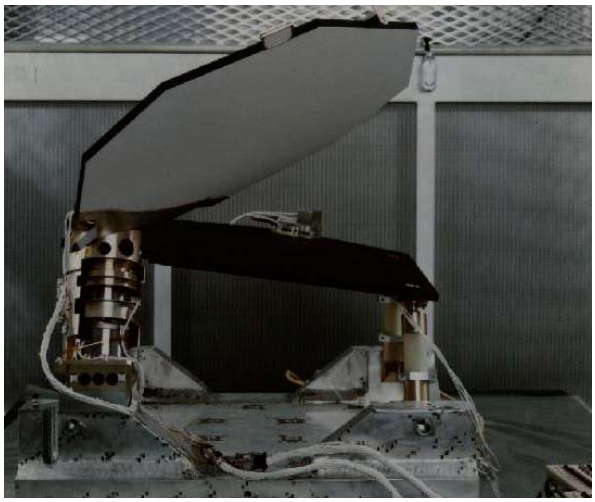

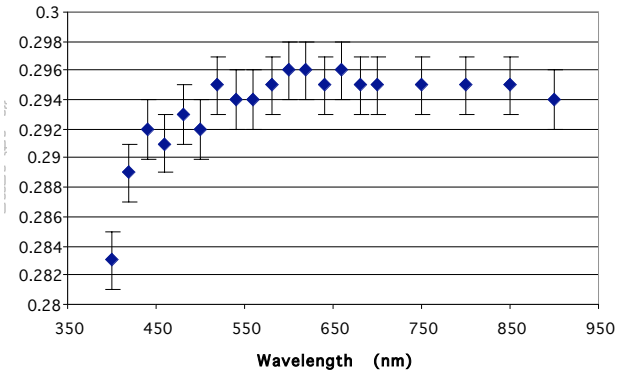


Figure 43. The Landsat ETM+ flight diffuser and deployment assembly (top) and associated DCaF BRDF measurements at the ETM+ deployment geometries of 71° elevation incidence, 150° azimuthal scatter, and 23.5° elevation scatter (bottom).

samples.

At the request of MIT/Lincoln Laboratories, the DCaF measured the BRDF of Spectralon witness samples for the Advanced Land Imager instrument on EO-1.

*BSDF Measurements in Support of TRMM, TES, GLAS, and SORCE*

The ability of the DCaF scatterometer to measure optical scatter at any incident and scatter geometry over a range of BRDF values from $10^{+5}$ to $10^{-7}sr^{-1}$ has led to measurement requests by a number of EOS instrument projects on a variety of materials and surfaces. In 1995, the DCaF measured the BRDF of a number of candidate earth shade materials for the Tropical Rainfall Measurement Mission (TRMM) project. Between 1999 and 2001, BRDF measurements were also acquired on earth shade materials for the Tropospheric Emission Spectrometer (TES) and the Geoscience Laser Altimeter System (GLAS). The DCaF measured BRDF data on aluminum samples coated with black nickel and underplated with electroless nickel that were subsequently provided to the University of Colo-

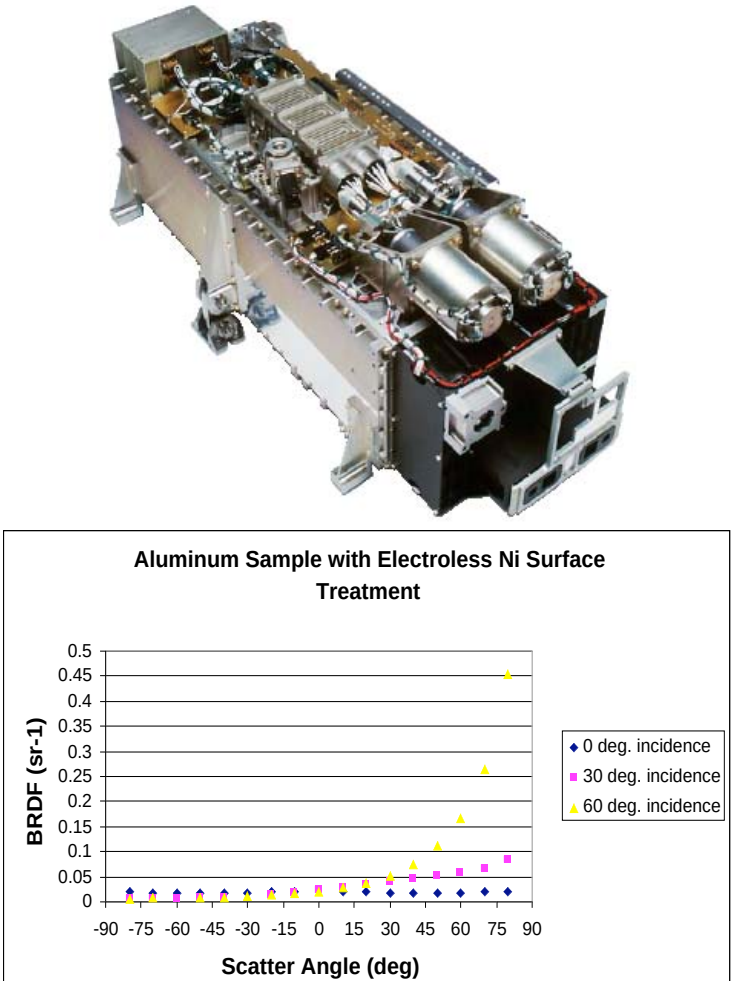


Figure 44. The EOS SORCE Spectral Irradiance Monitor (SIM) instrument (top) and the 400 nm BRDF of the electroless Ni surface measured by the DCaF and used inside the SIM instrument for stray light suppression.

rado's Laboratory of Atmospheric and Space Physics (LASP) (cf. Figure 44). Those data were used in LASP's decision to employ that material inside the EOS Solar Radiation and Climate Experiment (SORCE) Spectral Irradiance Monitor (SIM) instrument for stray light suppression.

*BRDF Round-robin in Support of the Calibration of Terra's Solar Reflective Instruments*

Laboratory measurements of the BRDF of diffusers were required to support the calibration of the Moderate Resolution Imaging Spectroradiometer (MODIS) and the Multi-angle Imaging SpectroRadiometer (MISR) on EOS Terra. In 1997, a BRDF round-robin was coordinated by the EOS Project Science office and NIST to assess the ability of EOS instrument calibration laboratories to perform accurate BRDF measurements (Barnes et al. 1998; Early et al. 2000). In addition to the DCaF and NIST, round-robin participating institutions included the University of Arizona (UA), Raytheon Santa Barbara Remote Sensing (SBRS), and the Jet Propulsion Laboratory (JPL). The UA is an established EOS validation labora-

tory; and SBRS and JPL built and calibrated the MODIS and MISR instruments, respectively. The round-robin included Spectralon, pressed halon, and roughened aluminum samples. BRDF measurements were made by each institution at an ensemble of MODIS and MISR operating wavelengths and at incident and scatter angles experience by MODIS and MISR during on-orbit operation. The participating laboratories were able to measure the BRDF of the comparison samples to within 2% of the values measured by NIST, indicating an excellent level of agreement.

*c. Radiometric Calibration Development Facility* (E. Hilsenrath and S. J. Janz)

The Code 916 Radiometric Calibration and Development Facility (RCDF) supports several NASA EOS and international Earth observing missions for calibrations and instrument characterizations. Both satellite and ground based instruments benefit from RCDF resources. In addition to this support, the facility also provides a laboratory resource for development of test instruments and payloads that fly on the Space Shuttle and for advanced instrument development such as Instrument Incubator. The RCDF compliments the RCF and the DCaF in that it focuses on the ultraviolet and visible with some capability in the near-infrared. The facility is supported under the EOS Calibration line item at Goddard Space Flight Center, the TOMS Program, and various NASA Research and Analysis (R&A) programs selected via NRA's.

The facility provided a test and maintenance and pre- and post-flight calibration for the eight successful SSBUV flights. The facility continues to maintain "flight hardware" handling capability to support ongoing flight missions. Because of its excellent record, the facility has become world renown for ultraviolet calibrations and has provided calibration services to every ozone mission using backscatter ultraviolet techniques. This includes TOMS and SBUV (USA), GOME and SCIAMACHY (ESA), and OSIRIS (Canada). These services are expected to continue with GOME-2 (Eumetsat) and OMI (Aura) and will be available for OMPS on NPP and possibly NPOESS. In addition, the facility has provided resources for and supported development of several other NASA and cooperative space flight missions. These include the Shuttle SOLSE/LORE mission for the IPO and MEIDEX, an Israeli initiative to study aerosols from the Space Shuttle. Services have also been provided for the AERONET and MODIS Airborne Simulator.

1) PRE-LAUNCH CALIBRATION

The RCDF maintains a suite of calibration standards and fixtures for radiometric characterization of Earth observing instruments. This capability originally focused on ozone instruments working primarily in the ultraviolet. More recently capabilities have extended to the visible and near-infrared, a wavelength range for new instruments observing atmospheric chemistry using reflected and backscattered sunlight.

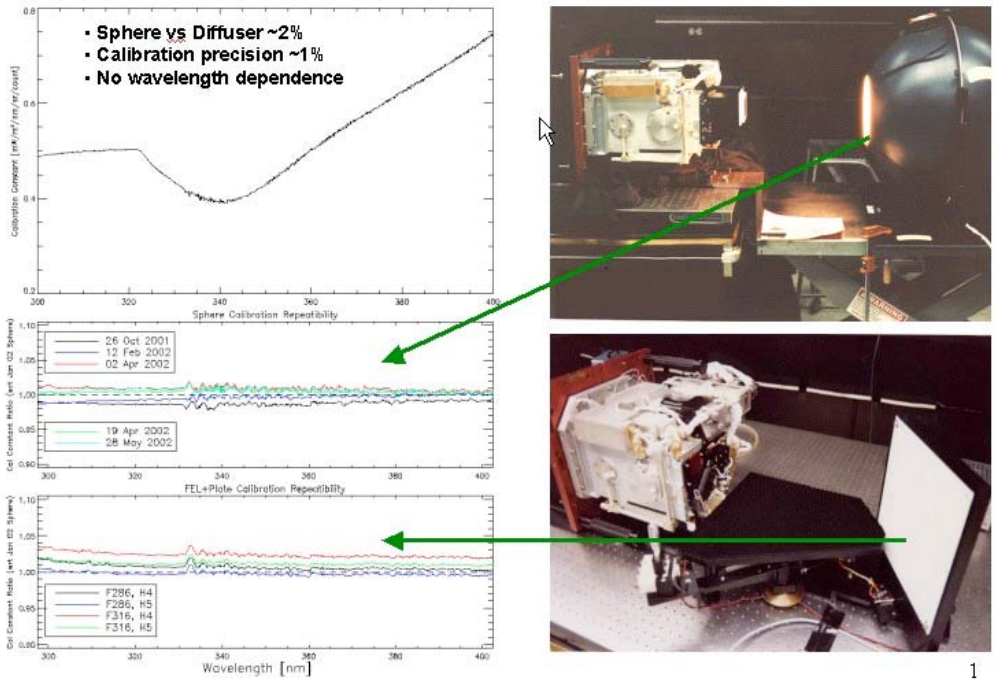


Figure 45. Illustration of radiance calibrations compared using sphere (upper right) with flat plate diffuser (lower right). Calibration constant for the instrument under test is shown in the upper left. Repeatability of sphere comparisons is less than 1% (middle left) and comparability with sphere calibration is about 2%, within NIST uncertainties. Wavelength dependence is nearly zero from 300 to 400 nm.

Instrument radiance calibration methods employ both scatter plates (whose BRDF were measured in the DCaF) and integrating spheres. For the various instruments either one or both are used for radiance calibrations in order to accommodate unique viewing requirements or for redundancy. It has been a long term objective to make these two calibration techniques result in nearly identical calibration. This has been achieved through extensive tests and analysis. The results comparing the two methods appear in Figure 45. The SSBUV instrument (SBUV/2 engineering model used for eight Shuttle missions) is used as a transfer standard for these tests.

Repeatable and accurate calibrations for successive instruments are needed for deriving long-term climate data records. All planned ozone instruments using reflected and backscatter solar observations, with their new capability for measuring other atmospheric parameters, e.g., trace gases and aerosol characteristics, will rely on the techniques developed in the RCDF.

### 2) Post-launch Validation

A long-term measurements program also requires a rigorous validation program. Traditional validation of ozone instruments employ the operational ozone ground networks (Dobson, Brewer, etc). Studies of long term ozone data sets show that in order to further improve the data record, validation measurements

themselves need improvement. Therefore the RCDF is now using its resources to better calibrate ground-based spectrometers used for validation. Improvements have already been made by more accurate knowledge of instrument bandpass, slit function, polarization sensitivity, and radiometric response.

Capabilities developed in the RCDF are being deployed to other agency networks such as EPA, DoE and the USDA, which monitor trace gases, aerosols and surface UV irradiances. These instruments, which will be used for continued validation of TOMS, SBUV/2, GOME and SCIAMACHY that are currently in orbit, plus upcoming missions that will carry OMI, OMPS, and GOME-2, will now be traceable to a common standards. Finally the SSBUV (used as transfer calibration standard) is being tested for ground validation of Level 1 radiances from BUV instruments by taking zenith sky observations coincident with satellite overpasses. To close the loop the spaceborne instruments will all be traceable to RCDF standards as well. Overall accuracy will be traceable to NIST through on going collaborations, including the Round Robins, via support from EOS Project Science office.

3) ADVANCED INSTRUMENT CHARACTERIZATION

Atmospheric chemistry instruments have evolved from a single observed pixel to an imaging and hyperspectral capability. These instruments employ array detectors with one and two dimensions. These enhanced capabilities put further demands on calibration and instrument characterizations techniques and associated ground support equipment. RCDF now has the capability to measure end-to-end performance of these advanced instruments. In addition to the conventional wavelength and radiometric calibrations, the capability exists to measure IFOV, FOV, goniometry, focus, aberrations, instrument response functions (PSF/MTF), spectral and spatial stray light, detector flat field, signal noise, linearity, offsets and gains.

These capabilities have been employed for in-laboratory calibration and testing of SOLSE and LORE flown twice on the Shuttle, and MEIDEX, an Israeli dust experiment. Resources were also used for Aura/OMI and Envisat/SCIAMACHY in their own facilities.

4) INSTRUMENT DEVELOPMENT

The RCDF has supported the development of the RSAS pointing technique. This technique employs the natural Rayleigh scattering with altitude to determine instrument pointing. The first instrument was built in RCDF and test flown successfully on the Shuttle. The technique has been used to determine pointing for ODIN/OSIRIS and for Envisat/SCIAMACHY. The technique will also be employed for OMPS on NPP and NPOESS. The facility supported the development of SOLSE-1 and –2 missions, the first spaceborne instrument to employ hyperspectral measurements for Earth science observations. The mission was partially supported by the Integrated Program Office NPOESS/OMPS risk mitigation. The facility also supported ChyMERA funded by the Instrument Incubator Pro-

gram. CHyMERA is a wide field hyperspectral radiometer employing a CCD array overlaid with a mosaic of filters responsive in the wavelengths sensitive to ozone, sulfur dioxide, nitrogen dioxide, and aerosols, all EPA criteria pollutants.

5) UPCOMING ACTIVITIES

The laboratory is now supporting a new Instrument Incubator Program called GeoSpec, which is an advanced hyperspectral imager for geostationary operation. GeoSpec is being designed to measure pollutant and their precursors in the lower troposphere, ocean color, and vegetation indices with high spatial resolution over selected geographical regions of the Earth. A breadboard will be built with a possible instrument to be operated in the field.

The next expected development; pending an announcement of an NRA, will be the development of a multiangle spectrometer employing fiber optics and CCD detectors for collecting atmospheric chemistry data in the troposphere for pollution monitoring and Aura validation. This is a joint effort with Washington State University.

## 4. Validation Activities (D. O'C. Starr)

The EOS Validation Program was established in 1995 and since that time has organized and coordinated a project-wide validation program based on a set of guidelines, policies, and milestones. To facilitate effective communications and stimulate collaborative activities, timely workshops and scientific meetings have been conducted. The Validation Scientist has coordinated with other NASA and non-NASA programs, conducted community reviews of team validation plans, and provided supplemental support for team validation tasks. Examples of supporting activities include support for development of airborne simulators, participation in field experiments, acquisition of correlative measurements including measurement networks, and enhancement of databases such as HITRAN. Two major NASA Research Announcements have been issued and approximately 70 research tasks have been funded for supporting or enhancing activities to the EOS Terra and Aqua team validation studies. In each case workshops were held to define the science requirements to be included in the research announcements.

### *a. Terra and Aqua NASA Research Announcement Investigations*

1) ATLANTIC MERIDIONAL TRANSECT MEASUREMENTS FOR MODIS CALIBRATION AND VALIDATION (S. B. Hooker)

The SeaWiFS Field Team has combined the collection of ground-truth observations with specific experiments to investigate the sources of uncertainties in upper ocean apparent optical property (AOP) measurements. Many of the experiments and data collection opportunities took place during several Atlantic Meridional Transect (AMT) cruises onboard the Royal Research Ship James Clark Ross (JCR) between England and the Falkland Islands. The majority of the AMT

dataset was from Case-1 conditions and took place from September 1995 to June 1999. Additional experiments and data collection activities have been executed to extend the AMT predominantly in-water data set to other open ocean areas and above-water methods. These include (i) the Productivité des Systemes Oceaniques Pelagiques (PROSOPE) cruise, that took place between 4 September and 4 October 1999; (ii) a cruise into the Mid-Atlantic Bight, that took place between 24 April and 3 May 2000, and (iii) February and 1 March 2000 as well as 22 February and 1 March 2001.

2) VALIDATION OF CLOUD OPTICAL DEPTHS RETRIEVED FROM MODIS DATA (A. Marshak, T. Várnai, A. J. Davis, R. F. Cahalan, W. J. Wiscombe)

This project has made major contributions to the validation of operational MODIS cloud optical thickness retrievals by estimating the errors that horizontal cloud variability introduces into the retrievals. A technique was developed that can give information on retrieval accuracy even at locations where no ground-based or in-situ measurements are available. Prior to the launch of MODIS on Terra, radiative transfer simulations were used to study the effects of cloud variability and to develop simple parameterizations of the uncertainties they introduce into cloud property retrievals. After MODIS data became available in 2000, a statistical analysis of MODIS observations was conducted, both to improve the methods that estimate retrieval uncertainties and to establish the magnitude of the uncertainties that cloud variability causes in the real atmosphere. The main achievements of the project are:

- Development of the first algorithms that estimate retrieval uncertainties caused by cloud heterogeneity effects;
- New knowledge on the importance of cloud variability in the real atmosphere; and
- New insights into the radiative effects of cloud variability, which can help improve future cloud retrieval algorithms.

Results from the project were published in 12 journal articles, were discussed in 14 conference presentations, and were informally reported to MODIS team members who used them to improve the current operational algorithms.

3) UNCERTAINTIES FOR MODIS CLOUD RETRIEVALS OF OPTICAL THICKNESS AND EFFECTIVE RADIUS (S. Platnick, R. Pincus)

This project used model calculations, along with analysis of MODIS and MODIS Airborne Simulator (MAS) data, to assess the accuracy of the MODIS cloud product retrievals of liquid water cloud optical thickness and effective radius. The investigation included determination of:

- Errors in the computation of reflectance and emission libraries used in the retrieval algorithm, including effect of wavelength integration, cloud droplet size distribution assumptions, complex index of refraction of water, etc.;
- Uncertainty produced by imperfect knowledge of the retrieval environ-

ment, including instrument performance and above-cloud atmospheric effects;
- Effect of vertical stratification in droplet size on retrieved optical properties, especially discrepancies between retrieved effective radii made from reflection measurements in different near-IR bands; and
- Uncertainties and biases due to horizontal inhomogeneity in cloud optical properties, and development of a theoretical framework for using image spatial variability to estimate pixel level uncertainty.

Results have provided quantitative guidance for the assessment of quality assurance parameters for the MODIS cloud retrieval algorithm.

4) SOUTHERN AFRICA VALIDATION OF EOS (SAVE) (J. L. Privette, R. J. Swap, A. M. Thompson)

The SAVE project has made major contributions to validation of multiple land and atmospheric products from EOS satellites over southern Africa. Observations included monthly field measurements to validate products over full vegetation phenological cycles and through different EOS sensor and algorithm configurations. The studies included targeted multiple field sites spanning the IGBP Kalahari Transect, a ~1000 km north-south precipitation gradient, for evaluation of products over varying vegetation structure. Atmospheric products were validated by comparisons with data collected during an intensive aircraft field campaign in August-September, 2000. Finally, this project, along with other SAFARI 2000 projects, established an enduring regional capacity for satellite product validation beyond EOS Terra (i.e., into the EOS Aqua and NPP/NPOESS eras). All SAVE data are either available through the ORNL Mercury system or in the SAFARI 2000 Data CDROM series.

SAVE directly validated six EOS products, including:

- Leaf Area Index (MOD15A2)
- Fraction of Photosynthetic Radiation Absorbed by vegetation (FPAR; MOD15A2)
- Vegetation Index (NDVI; MOD13)
- Surface Albedo and BRDF (MOD43B3)
- Land Surface Temperature (MOD14A2)
- Tropospheric Ozone (TOMS)

SAVE supported validation efforts of five EOS products, including:

- Fire and burn scars
- Aerosol Optical Depth (AOT)
- Water Vapor
- Net Primary Production
- Vegetation overstory fractional cover (MODIS Continuous Fields)

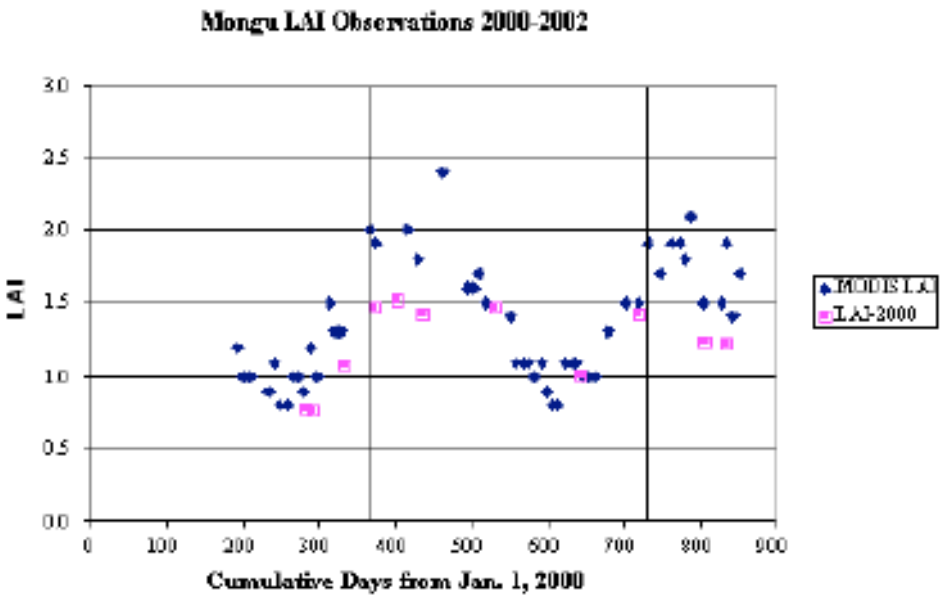


Figure 46. Multidata comparisons of MODIS and field-measured LAI values indicate that the MODIS LAI responds correctly to woodland phenological changes.

Figure 46 shows the Leaf Area Index derived from MODIS (blue) and field measured LAI derived from the Plant Area Index, which is the sum of Leaf Area Index and Stem Area Index (i.e., it includes wood area and leaf area). Since MODIS LAI estimates green leaf area, and the ground instruments measure any plant material obscuring the sun, we have subtracted the estimated wood area to compare field data against MODIS data.

During March 2000, we participated in the Kalahari transect from the Western Province of Zambia to southern Botswana (cf. Figure 31). Figure 47 shows an image of the MODIS-derived LAI for March 17, 2000, and the derived LAI from MODIS and that derived from the ground-based measurements (after correcting the plant area index for the stem area index) shows good validation of this product.

5) ERROR ESTIMATES FOR AMSR-E RAINFALL DATA (T. L. Bell)

The main objectives of this project were to:

- Produce estimates of the sampling error in the monthly area-averaged rain rate on a global 5° x 5° grid as measured by AMSR-E. This error arises from the intermittent and often incomplete observation of a grid box on the earth by the satellite. It is determined by the rain statistics and the total area sampled by the satellite in the course of a month. The rms error gives the 95% confidence interval for the satellite retrieval error.

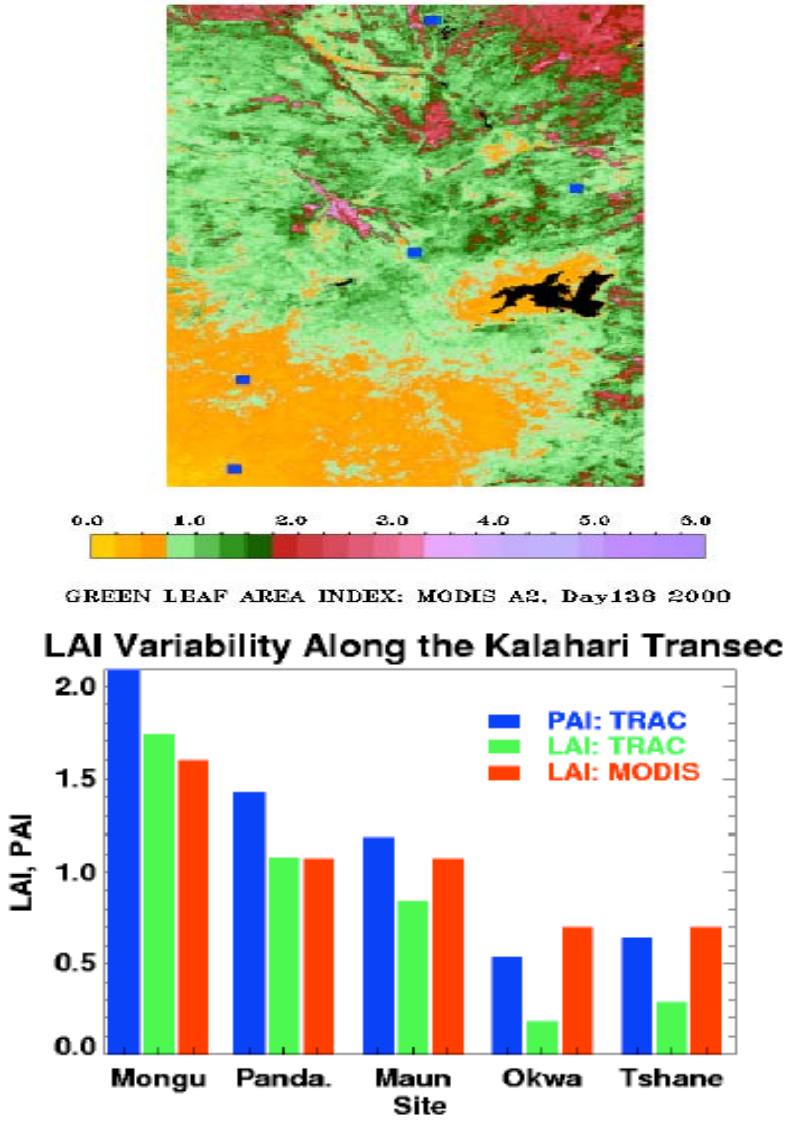


Figure 47. (upper) The Green Leaf Area Index image derived from MODIS data on March 17, 2000 along the Kalahari Transect characterized five sites (blue rectangles) in Zambia and Botswana. (lower) Measurements revealed that the MODIS LAI product is accurate to < 0.5 units over varying vegetation structural conditions ranging from woodland to shrubland.

- Carry out a comparative study of the rain statistics derived from collocated satellite and ground-based radar images at Kwajalein and other ground validation sites.

The error estimates are themselves essential for utilizing the data in scientific investigations, such as comparison with other data sets and numerical climate model predictions. Extracting modulating signals like the diurnal cycle and other longer-term trends also requires knowledge of the error distribution. Intercomparison of ground radar and satellite-derived rain statistics can reveal systematic differences. These differences are indicative of the presence of retrieval errors and can lead to improvement of the rain retrieval algorithms.

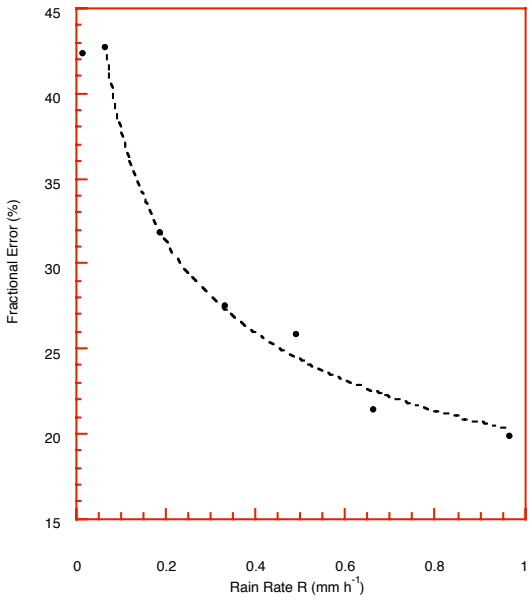


Figure 48. TRMM Microwave Imager (TMI) sampling error over the tropical pacific (January 1998 as a function of rain rate $R$ (mm $h^{-1}$).

While awaiting the accumulation of a substantial amount of level 2 rainfall data from AMSR-E, we examined a number of aspects of rain statistics from the TRMM Microwave Imager (TMI) version 5 data over the Equatorial Pacific between 10□N - 10□S and 150□E - 90□W taken during 1998. Figure 48 illustrates the dependence of the fractional error $\sigma_E/R$ as a function of the monthly mean rain rate $R$ computed for January 1998.

6) AIRS VALIDATION EFFORT FROM WALLOPS FLIGHT FACILITY (F. J. Schmidlin)

Following the insertion of Aqua and the turn-on of the AIRS instrument, in situ validation measurements were scheduled from Wallops Island, (38°N), Andenes, Norway (69°N), and Andros Island, The Bahamas (24°N), Natal, Brazil (6°S), and Ascension Island (8°S). Why the Andoya Rocket Range in Andenes, Norway was included is because of the planned MaCWAVE Campaign. Dr. R. A. Goldberg (690) and F. J. Schmidlin (972) were investigators in a Code S mission to obtain rocket measurements for the purpose of studying wave activity in Scandinavia. The campaign, name MaCWAVE, or Mountain and Convective Waves Ascending Vertically Experiment presented UAIRP the opportunity to leverage the cost of the personnel needed in Norway. MaCWAVE was a two-part campaign; part 1 took place in Norway in July 2002 and, part 2 took place in Norway and in Sweden in January 2003. Regular radiosonde types were flown as well as chilled mirror profiles in Norway. Because of the high latitude involved, sufficient overpasses of AIRS occurred each day enabling a balloon release close to the most desirable orbit. Four standard radiosonde profiles and five SNOW (chilled mirror) profiles were delivered to the JPL AIRS archive files. The MaCWAVE rocket observations launched for MaCWAVE also coincided with AIRS ephem-

eredes and eight Falling Sphere temperature profiles will soon be delivered to the JPL archive.

7) WATER VAPOR AND CLOUD DETECTION VALIDATION FOR AQUA USING RAMAN LIDARS AND AERI (D. N. Whiteman)

This investigation involves the use of Raman lidar, AERI, and radiosonde measurements of water vapor, temperature, pressure and clouds to study and validate Aqua retrievals of water vapor and to develop cloud particle size retrieval techniques. According to the needs of the Aqua activity the first 18 months of this activity have focused on combined ground-based measurements during nighttime overpasses of the Aqua satellite in order to validate Aqua water vapor and temperature profiles.

Two measurement campaigns have thus far been completed. The first of these occurred at NASA/GSFC in Greenbelt, Maryland and spanned September 5 – November 3, 2002 with 26 nighttime overpasses (nominally between 2 and 3 am local) being covered. For each of these overpasses, the NASA/GSFC Scanning Raman Lidar (SRL) was used to acquire profiles of water vapor and clouds. These measurements were supported by launches of Sippican Mark-II radiosondes, which provided measurements of temperature and pressure, and SuomiNet GPS measurements of total precipitable water, which were used as the calibration source for the Raman lidar.

The second of these campaigns occurred at the University of Maryland Baltimore County and spanned January 8 – January 27, 2003. In addition to the previously mentioned instrumentation, the ground-based BBAERI (Baltimore Bomem AERI), the ALEX Raman Lidar and the ELF backscatter lidar made measurements during the overpasses. The results from this second campaign are still being processed. Therefore this report will focus on the results from the first campaign at NASA/GSFC and related efforts including a statistical analysis of cirrus cloud data from earlier SRL deployments, study of GOES, MODIS and AERONET precipitable water measurements using GPS and preliminary comparisons of particle size retrievals from ground-based AERI and Raman lidar.

Figure 49 shows a comparison of 5 Aqua retrieval schemes with the reference temperature profiles provided by radiosonde. The measurements have been separated into clear and cloudy conditions for the water vapor comparisons. The results indicate that for much of the troposphere between ~250 and 900 hPa all retrievals agree with the reference profile within ±1.5 K. Deviations exceed 1.5 K both above 200 hPa and below 900 hPa with all retrievals showing the same general features.

8) GLOBAL VALIDATION OF EOS-AQUA LAND SURFACE DYNAMICS USING DATA ASSIMILATION (P. R. Houser)

The primary goal is to develop data assimilation technology to validate the land products generated from the AMSR-E instrument onboard the EOS Aqua satel-

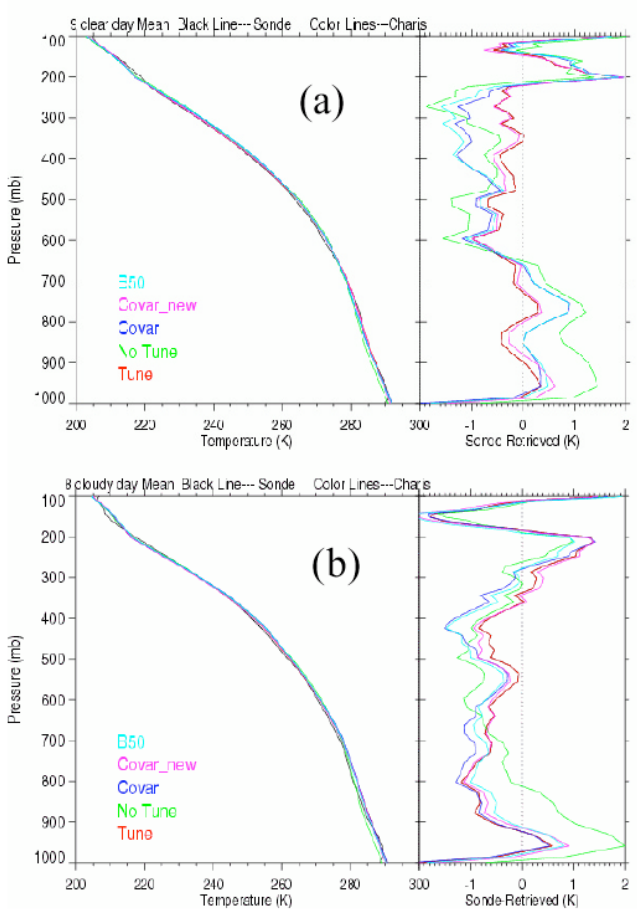


Figure 49. Comparison between 5 Aqua temperature profiles and radiosondes, showing general agreement within ±1.5 K for the bulk of the troposphere.

lite. These land products include: surface soil moisture, brightness temperatures, surface temperature, and vegetation water content. An Extended Kalman Filter (EKF) data assimilation algorithm has been implemented in NASA's Land Data Assimilation System (LDAS) using the MOSAIC land surface model. Before real and reliable AMSR-E land surface soil moisture data become available, the EKF-LDAS was successfully tested with data derived from the Tropical Rainfall Measurement Mission (TRMM) Microwave Imager (TMI) (cf. Figure 50). As a team effort, the SMEX02 field experiment was carried out in central Iowa for more than three weeks. We have participated in the field data collection and analysis. These field data sets together with new field data sets to be collected in Okalahoma in the summer of 2003 will be used to cross validate the AMSR-E soil moisture products.

9) GEOPHYSICAL VALIDATION ACTIVITIES IN SUPPORT OF AIRS (R. M. Atlas, J. Joiner, I. Stajner)

This research involves a detailed geophysical validation of AIRS data products, with the goal of improving the impact of AIRS data on both weather prediction and scientific investigations. Specific objectives include: (i) determining the accuracy and error characteristics of AIRS level 1B radiances, temperature and hu-

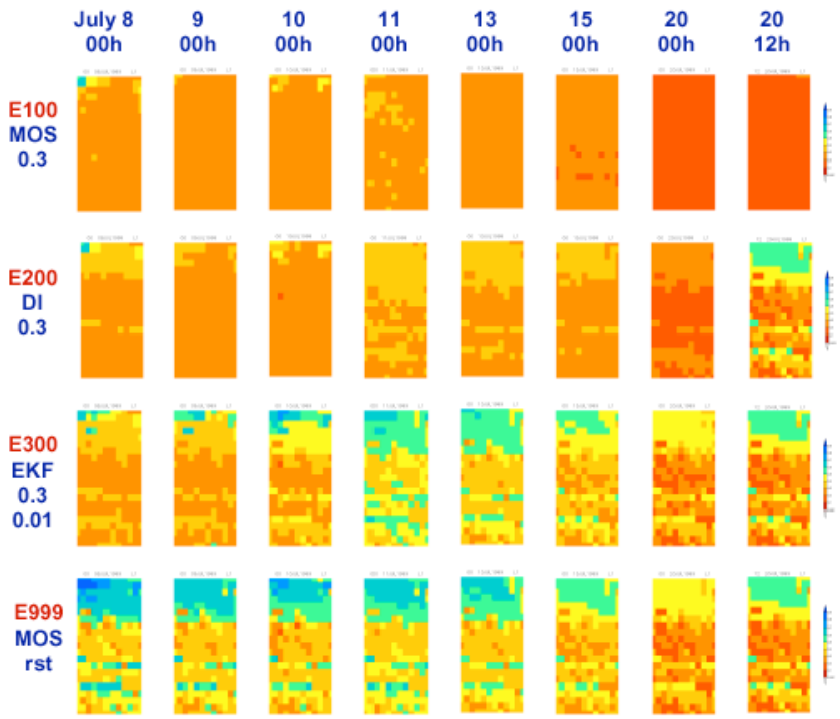


Figure 50. Results of the numerical experiments with EKF-LDAS: Comparison between Extended Kalman Filter (EKF) and Direct Insertion (DI) data assimilation methods. EKF is shown to be superior to DI in term of data assimilation efficiency.

midity retrievals, clouds and ozone, (ii) determining the meteorological characteristics associated with reduced accuracy in AIRS data, (iii) assessing the initial impact of AIRS data on atmospheric analyses and numerical weather prediction, (iv) providing feedback to the AIRS Science Team to improve the AIRS data products, and (v) developing methodology to improve the utilization of AIRS data in atmospheric models.

Figure 51 shows one of the highest peaking channels in the 15 $\mu$m band (668.64 $cm^{-1}$). Several interesting features can be seen. Some of the orbits exhibit positive observed minus forecast (O-F) values (red), while other negative (orange). We believe that this is an artifact of treating the satellite data as if it were taken at a single synoptic time. The DAO model produces realistic stratospheric tides. However, the forecast and analysis fields are produced only once per 6 hours. All data are treated as if they were taken at this time. For fields with significant temporal variability on hourly time scales (such as temperature in the upper stratosphere), this can create an orbital signature in O-F. We have noted such a signature previously from the NOAA Stratospheric Sounding Unit (SSU).

*b. Validation Field Campaigns*

1) CRYSTAL-FACE (D. O'C. Starr, P. A. Newman, M. D. King, S. Platnick, S. C. Tsay, E. J. Welton, J. C. Gerlach, M. J. McGill, G. M. Heymsfield, J. R. Wang)

Members of the Laboratory for Atmospheres played key roles in the Cirrus Re-

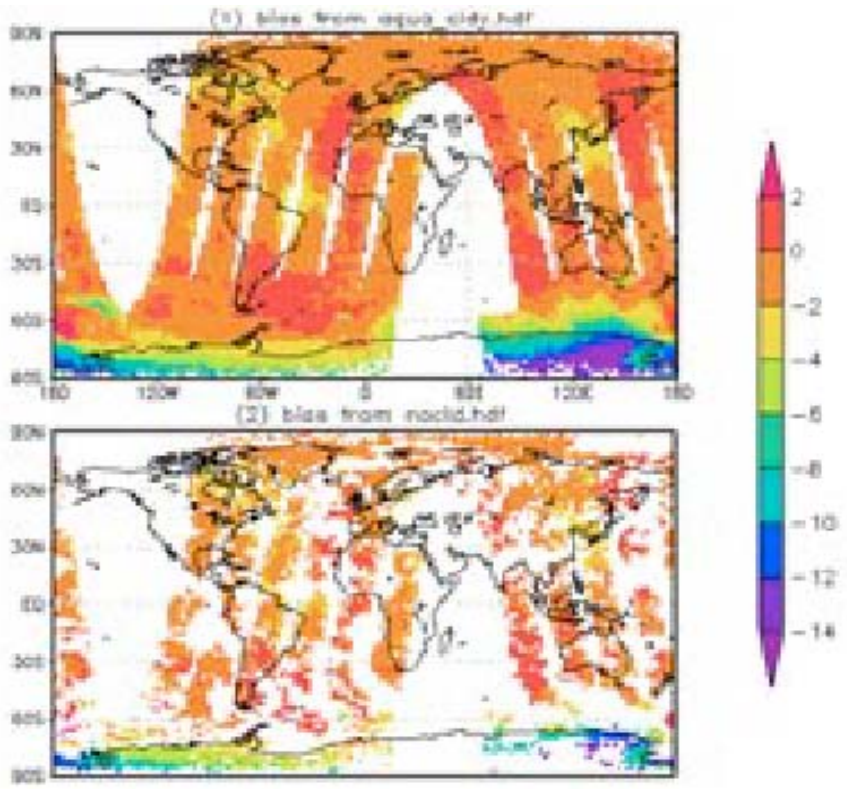


Figure 51. Observed minus forecast values of outgoing longwave radiation at 668.64 $cm^{-1}$ as derived from AIRS. Red indicate observed greater than forecast while orange and red denote negative values of the observed-forecast.

gional Study of Tropical Anvils and Layers – Florida Area Cirrus Experiment (CRYSTAL-FACE), a major NASA field experiment conducted in South Florida in July 2002. The experiment sought to:

- Improve understanding of cirrus anvil properties in relationship to the properties and strength of deep convection (e.g., does stronger convection imply a larger longer-lived anvil? ...more anvil ice mass? ...larger ice crystals? ...more complex ice crystals?).
- Provide a direct basis for improvement of large-scale models used for numerical weather prediction and climate studies by quantitatively linking anvil properties to convective mass flux, a parameter predicted in such models.
- Improve understanding of the physical factors that control lifetime and area coverage of cirrus anvils and tropical cirrus layers (e.g., what is role of microphysical, radiative and dynamical processes in cirrus cloud development and lifecycle and what is the effect of environmental factors such humidity and stability?).
- Improve understanding of how deep convection affects tropical upper tropospheric and lower stratospheric humidity, a key climate-radiation variable, and also a key factor in stratospheric chemistry.

These objectives both support the evaluation and improvement of state-of-the-art, high-resolution, cloud system models that account for the full range of cloud physical processes and provide another path for improvement of global circulation models (GCMs).

An additional important objective was the validation of ground-based and satellite remote sensing observations of cloud properties including observations from Terra (MODIS, MISR, CERES), Aqua (MODIS, AIRS, CERES), GOES, POES, and TRMM (Precipitation Radar) as well as to provide data sets supporting algorithm development for future measurements from space such as lidar (CALIPSO) and millimeter wavelength radar (CloudSat) – key elements of NASA's "A-Train" that will be in-place in 2004.

CRYSTAL-FACE (C-F) was principally sponsored by NASA under the Code Y Radiation Sciences Program, the Upper Atmosphere Research Program, the EOS Validation Program, and the Atmospheric Chemistry Modeling and Analysis Program. Additionally, C-F was also sponsored by the National Science Foundation, the Department of Energy Atmospheric Radiation Measurement Program (ARM), the Office of Naval Research, and the NASA-NOAA-DoD Integrated Program Office. The National Weather Service (NOAA) was a cooperating agency.

There were six aircraft participating in CRYSTAL-FACE: NASA's ER-2 and WB-57, the Proteus (contracted by IPO), the University of North Dakota Citation, Naval Research Laboratory's P-3, and CIRPAS Twin Otter. The aircraft were based at Key West Naval Air Facility where the science team of over 200 members was assembled. There were two cloud-observing ground sites, located at Tamiami Airport, near Miami, and at Everglade City on the west coast of southern Florida. Goddard provided and staffed the Surface Measurements for Atmospheric Radiative Transfer system (SMART, Tsay/913) at the eastern site that included a Micropulse Lidar (MPL, Welton/912) and a suite of radiometers. In addition, a sophisticated polarimetric precipitation radar (Goddard's NPOL radar from Wallops Flight Facility, Gerlach/972) was operated at Ochopee, 5 km east of Everglades City. In-flight aircraft operations were directed from this location. Multi-aircraft science missions were conducted on 12 days with the ER-2 flying 11 missions. Underflights of Terra (3) and Aqua (5) were performed and good coordination was often achieved with the ground sites. On many occasions, all six aircraft flew simultaneous coordinated patterns.

Goddard investigators played key roles in the successful execution of the mission, serving as ER-2 Platform Scientist (Platnick/913, King/900, Newman/916) and as the co-Mission Scientist responsible for real-time direction of in-flight aircraft operations (Starr/912). In addition, daily regional forecasts of convective activity and chemical transport were generated to support mission planning using MM5 (Wang/JCET/912 and Pickering/ESIC/916). Other 910 scientists supported the daily mission planning cycle in various ways.

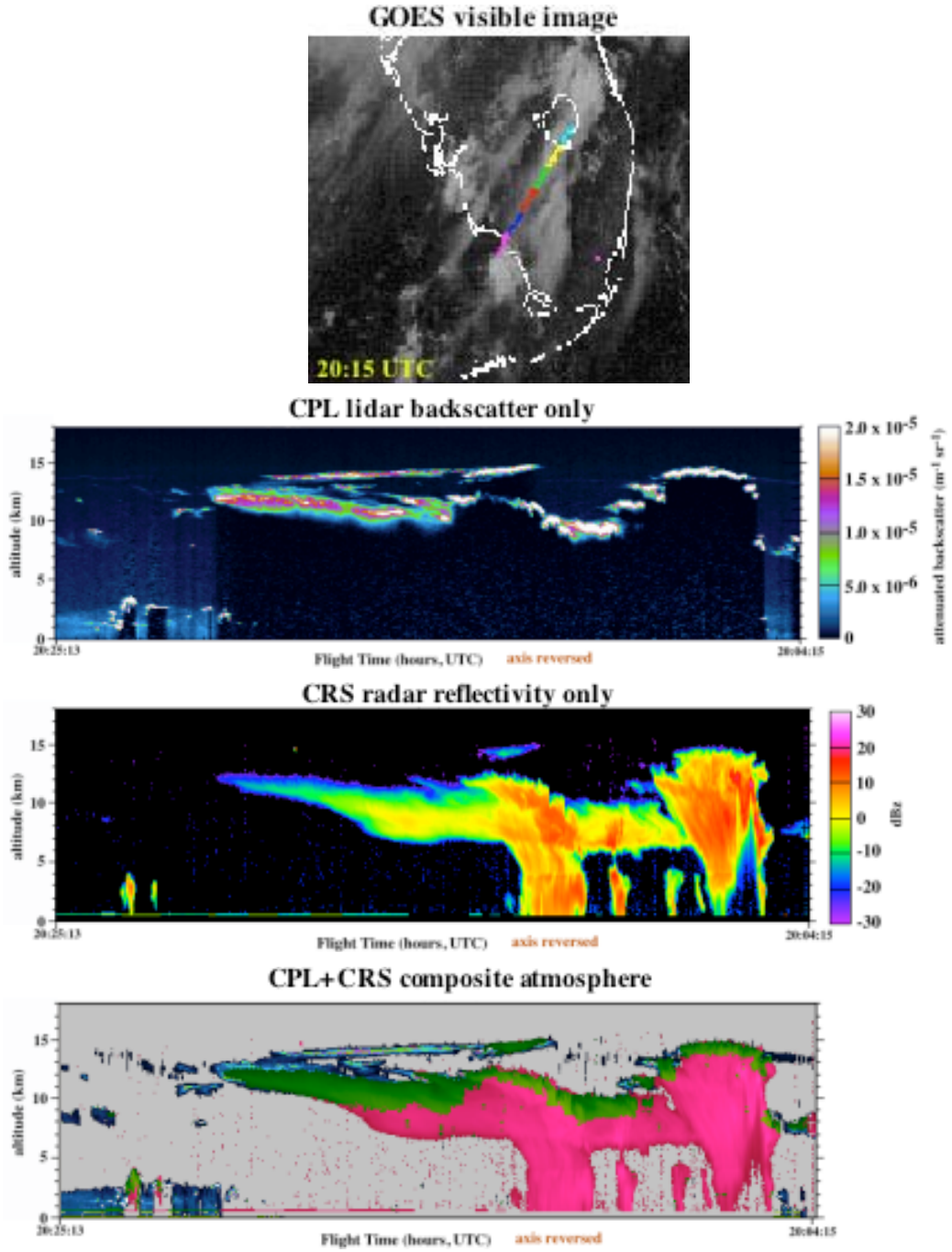


Figure 52. GOES image shows generating convective system on July 23, 2002, near Lake Okeechobee with cirrus anvil streaming to the southwest and overlaid by 15-minute aircraft tracks at about this time. Shown are concurrent CPL and CRS profile images of cloud properties along the ER-2 flight track, as well as combined image.

Goddard instruments constituted the core of the sensors carried on the ER-2, including the MODIS Airborne Simulator (MAS, Platnick/913 and King/900), the Cloud Physics Lidar (CPL, McGill/912), the 95 GHz (3 millimeter) Cloud Radar System (CRS, Heymsfield/912), the 3-cm wavelength (precipitation) ER-2 Doppler radar (EDOP, Heymsfield/912) system and Conical Scanning Sub-mm wave

Imaging Radiometer (COSSIR, Wang/975) a microwave sensor for detection of ice and precipitation. MAS, CPL and CRS provided an effective simulation of key elements of NASA's planned A-Train satellite constellation, especially as regards sensing of upper tropospheric clouds, i.e., Aqua/MODIS, CALIPSO and CloudSat. Coincident data from the instruments are shown in Figure 52, where the complementary nature of the observations is readily apparent. Cirrus clouds are a particularly difficult remote sensing target due to their lack of optical opacity and great variability. Combination of multi-wavelength observations from active and passive sensors holds the greatest promise of enabling detailed and accurate retrievals of cirrus cloud properties. This was the first CRS mission and the first time coincident MAS, CPL and CRS data were obtained.

Special radiosonde observing support (3-hourly soundings on operational days) by the National Weather Service Forecast Offices at Tampa, Miami and Key West was arranged and coordinated by Goddard (Starr/912). Special arrangements were also made to acquire a very complete NWS NEXRAD data set for the experiment from the these same sites, as well as from the NWS Melbourne site, using a new system to enable real-time data transmission to GSFC (Rickenbach/JCET/912).

A new ER-2 dropsonde system (Halverson/JCET/912), developed and operated by NCAR in collaboration with NASA, was used to obtain profiles of atmospheric state when the aircraft was far from operational sites (missions were flown to the deep tropics southeast of the Yucatan Peninsula, Figure 53) and to characterize the offshore pre-convective and anvil environments. A mobile radiosonde system (Halversion/JCET/912) was also operated in the interior of southern Florida by staff from the University of Central Florida, and sondes were provided for the western Everglades City remote sensing site manned by scientists from PNNL (DoE).

2) SAFARI 2000 (M. D. King, S. Platnick, M. J. McGill, S. C. Tsay, J. L. Privette, E. J. Welton, C. Gatebe)

The Southern African Regional Science Initiative (SAFARI 2000) was a regional project investigating emissions, transport, transformation and deposition of trace gases and aerosols over southern Africa. SAFARI 2000 involved coordinated satellite, aircraft and ground-based observations in a series of intensive field campaigns and longer term continuous monitoring at core ground sites, with ~200 scientists from eighteen countries participating.

The SAFARI 2000 drew on a number of ongoing science projects including the South African Lead Project on sulfur and nitrogen cycling, the Southern African Validation of EOS (SAVE, Privette/923) project for land data products, and validation of all remote sensing instruments on the Terra satellite platform. SAFARI 2000 was accomplished through a series of intensive field campaigns.

The SAFARI 2000 August-September 2000 Dry season campaign was a major surface, airborne and space-borne field campaign, that addressed a broad range

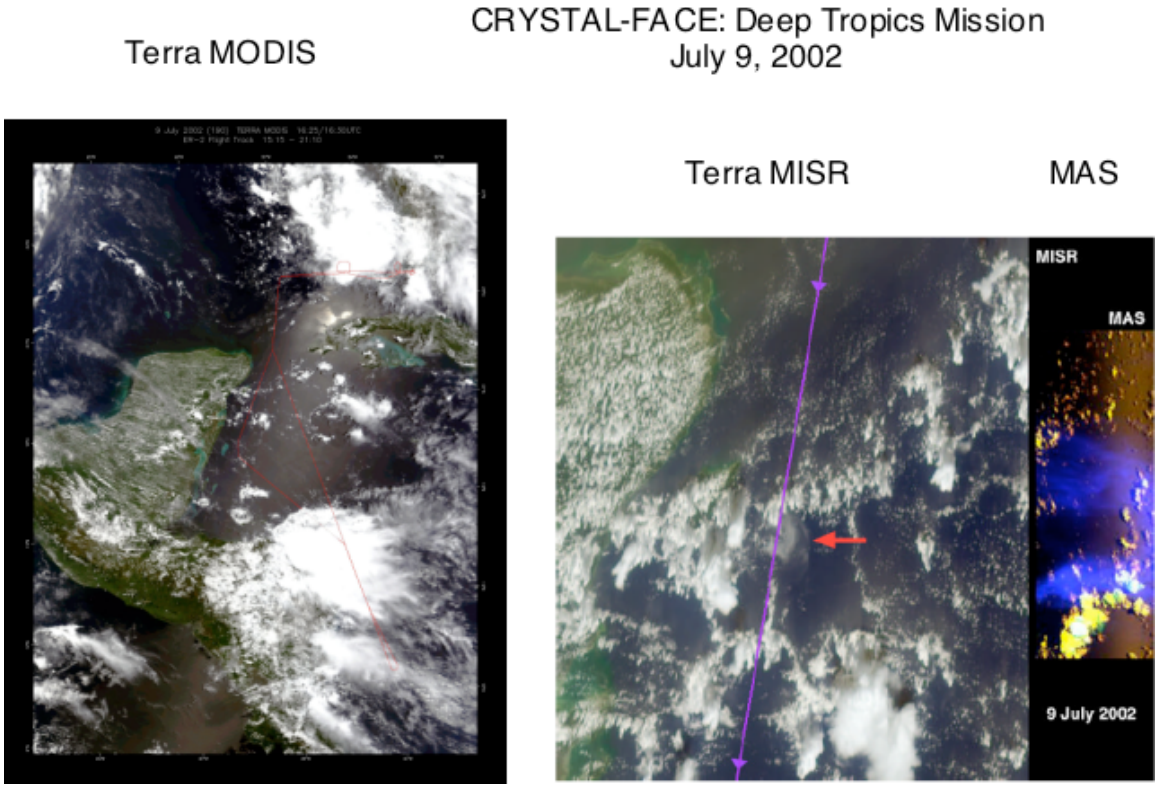


Figure 53. MODIS, MISR and MAS imagery during a deep tropics mission to study tropical tropopause transition layer. MISR image courtesy of Ralph Kahn/JPL.

of phenomena, related to land-atmosphere interactions and the biogeochemical functioning of the southern African system. Research aircraft used included: the NASA ER-2, University of Washington CV-580, two South African Weather Service Aerocommander 690As, and the U.K. Met Office C-130. Ground-based components included GSFC contributions from MPL (Welton/912) and SMART (Tsay/913). McGill/912 was instrument PI for the CPL on the ER-2 and Gatebe served as instrument scientist for the GSFC/CAR instrument on the CV-580.

The NASA ER-2 aircraft carried a sophisticated array of instruments including MAS, AirMISR, MOPITT-A, upward and downward spectral flux radiometers, and two metric mapping cameras (King et al. 2003b). King/900 and Platnick/913 served as ER-2 aircraft Lead Scientists during the campaign. The primary purpose of the ER-2 observations was to obtain independent observations of smoke, clouds, and land surfaces that could be used to check the validity of various remote-sensing measurements derived by Earth-orbiting satellites. These include such things as the accuracy of the Moderate Resolution Imaging Spectroradiometer (MODIS) cloud mask for distinguishing clouds and heavy aerosol from land and ocean surfaces and Terra analyses of cloud optical and microphysical properties, aerosol properties, leaf area index, vegetation index, fire occurrence, carbon monoxide, and surface radiation budget. In addition to coordination with Terra and Landsat 7 satellites, numerous flights were conducted over surface AERONET sites, flux towers in South Africa, Botswana, and Zambia, and in situ aircraft from the University of Washington, South Africa, and the United King-

Table 3. SAFARI 2000 intensive field campaigns.

| Period/Campaign | Season | Primary Goals |
|---|---|---|
| August-September 1999<br><br>Ground based & Airborne | Dry | Identify and quantify major dry-season sources of emissions including those from biomass burning, land use, and industry, prototype ground-based and airborne measurement techniques, characterize incoming radiation, boundary layer profiling, determine spectral characteristics of vegetation |
| February-March 2000<br><br>Ground based | Wet | Identify and quantify major wet season sources of emissions, examine ecosystem structure, functioning and processes at peak biomass, collect data to calibrate and initialize ecosystem models at point, local and regional scales, determine spectral characteristics of vegetation |
| August-September 2000<br><br>Airborne & Ground based | Dry | Track the movement, transformations, and deposition of dry-season emissions from biomass burning and other sources, quantify burnt area<br><br>Terra satellite validation |
| March 2001<br><br>Ground based | Wet | Quantify wet season fluxes of VOCs, $CO_2$ and $H_2O$ at core sites Maun and Skukuza, ground and tower measurements. |

dom. As a result of this experiment, the MODIS cloud mask was shown to distinguish clouds, cloud shadows, and fires over land ecosystems of southern Africa with a high degree of accuracy. In addition, data acquired from the ER-2 show the vertical distribution and stratification of aerosol layers over the subcontinent and make the first observations of a ''blue spike'' spectral emission signature associated with air heated by fire advecting over a cooler land surface (cf. Figure 54).

SAFARI 2000, as an integrating theme, has been able to give significant new insights into the regional scale biogeochemical cycling of southern Africa, and contributed in important ways to the validation of remote sensing instruments on board the NASA Terra spacecraft.

3) AMSR-E FIELD CAMPAIGNS (D. J. Cavalieri, J. C. Comiso, J. R. Wang, W. B. Krabill, R. F. Cahalan)

A number of AMSR-E data product validation campaigns occurred during 2003:

- Jan 3 – Feb 14 Precipitation Wakasa Bay, Japan
- Feb 4 and 11 Sea Ice Sea of Okhotsk, Japan
- Feb 19 – 27 Snow CLPX, Colorado (IOP3)
- Mar 6 – 23 Sea Ice Fairbanks, Alaska

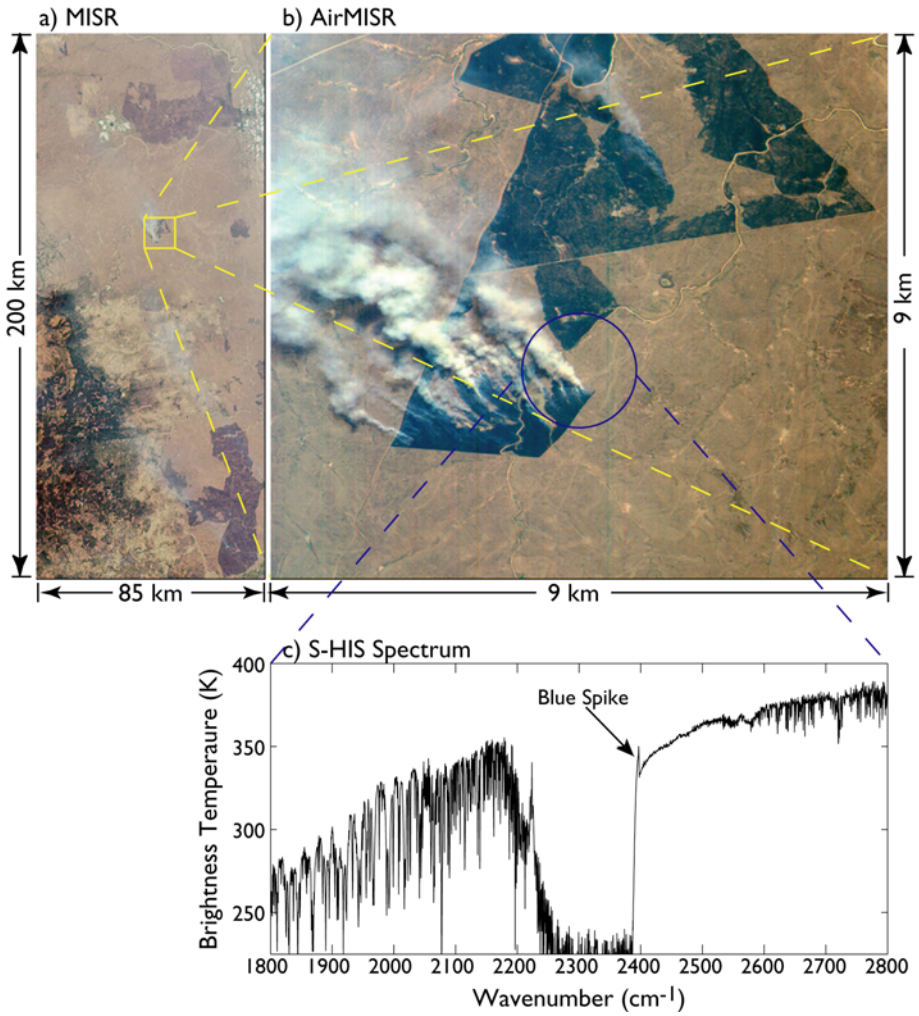


Figure 54. These images of northeastern South Africa were acquired on 7 September 2000 at 0825 UTC by (a) MISR and (b) AirMISR. Figure a is an 85 x 200 km swath of MISR's aft-viewing 45° camera, and Figure b an AirMISR 9 x 9 km nadir-viewing image of the prescribed fire in the Timbavati Private Game Reserve. These scenes were observed nearly simultaneously by the ER-2 and the Terra spacecraft. (c) The brightness temperature as a function of wavenumber obtained by the S-HIS over a 2 km pixel near the center of Timbavati fire. The "blue spike" is a spectral feature associated with the hot fire near 2400 $cm^{-1}$ (4.166 $\mu$m) (from King et al. 2003b).

| | | |
|---|---|---|
| • Mar 25 – Apr 2 | Snow | CLPX, Colorado(IOP3) |
| • Jun 23 – Jul 18 | SMEX 03 | Alabama, Georgia, Oklahoma |
| • Aug 23 – Sep 15 | Sea Ice | Punta Arenas, Chile |
| • Sep 16 – 26 | SMEX 03 | Brazil |

AMSR- E Sea Ice products are being validated through observations in both the arctic and Antarctic regions. GSFC investigators are making key contributions to these missions. Cavalieri was the PI and led the Arctic campaigns and participated in the ground component. Comiso is PI for the Antarctic Sea Ice based in Punte Arenas, Chile. Krabill/WFF was an instrument PI (ATM2) for both the Arctic Sea Ice and Antarctic Sea Ice campaigns. Cahalan is the PI for lidar meas-

urements (THOR) to determine snow and ice thickness as part of the Antarctic Sea Ice campaign.

In the Arctic, validation involved field observations and modeling components with coordinated P- 3 flights and in-situ measurements (Barrow, AK area. Pilot effort – April 2002; Full campaign - Feb. - March 2003). Observations included snow depth and properties on sea ice; sea ice and snowpack temperature; and ice type, thickness, roughness and microphysical properties.

Successfully completed seven aircraft flights with the NASA P-3 to validate the AMSR-E standard sea ice products:

- Sea ice concentration
- Sea ice temperature
- Snow depth on sea ice

P-3 flights were coordinated with (i) measurements at Barrow, AK and at a Beaufort Sea ice camp, and (ii) satellite overpasses: AMSR-E, Landsat 7, MODIS, Radarsat, ICESat.

P-3 instrumentation included: (i) NOAA ETL Polarimetric Scanning Radiometers (PSR-A and PSR-CX), (ii) NASA Wallops Airborne Topographic Mapper (ATM), (iii) NASA Langley Turbulent Air Motion Measurement System (TAMMS), and (iv) NASA Wallops and NOAA ETL digital & video cameras and IR radiometers.

Antarctic AMSR-E sea ice validation will be conducted by P-3 aircraft flights during August 23-September 15, 2003. The aircraft will be based in Punta Arenas, Chile and will overfly (i) Weddell Sea consolidated ice area (near 45°W), (ii) Bellingshausen Sea consolidated ice area (near 90°W), (iii) coastal/polynya regions, and (iv) ice edge/MIZ regions.

In addition to the P-3 airborne sensors, that include the THOR lidar (Cahalan/913) for detecting snow and ice thickness, the Antarctic AMSR-E sea ice validation also includes in situ and high-resolution observations as follows.

Ship Based In Situ Measurements:

- Passive microwave radiometer observations of surface and ice types
- Snow profiles of temperature, granularity, salinity and liquid content
- Ice thickness, salinity, and conductivity
- Radiosonde, surface air temperature & wind velocity

High Resolution Satellite Sensors:

- MODIS (Terra & Aqua) – visible and infrared retrievals of ice concentration and ice temperature
- Landsat 7 – visible for ice concentration
- Envisat and Radarsat SAR for ice type & concentration

AMSR-E oceanic precipitation physical validation was accomplished through the Wakasa Bay Experiment conducted during January/February 2003. The NASA P-3 aircraft was used to make observations for under flight comparisons. The aircraft payload was:

- PSR AMSR Simulator
- MIR 183/220 GHz radiometer
- AMMR 21/37 GHz upward viewing radiometer
- APR 2 frequency precipitation radar
- ACR Cloud radar
- TAMMS Thermodynamic measurements
- IR radiometer, digital camera

Jim Wang/975 was the PI for AMMR and MIR.

4) THORPEX (M. J. McGill)

THe Observing-system Research and predictability experiment (THORpex), a Global Atmospheric Research Programme, is an international research programme to accelerate improvements in the accuracy of 1 to 14-dayweather forecasts for the benefit of society and the economy. The programme builds upon ongoing advances within the research and operational-forecasting communities. It will make progress by enhancing international collaboration between these communities and with users of forecast products.

The North-Pacific THORpex Observing-System Test (TOST/2003: NorPac) was conducted from February 18 to March 10, 2003, including objectives for MODIS and AIRS Level 1 and Level 2 product validation and GLAS validation. A total of 3 GLAS underflights were achived, and the strategy and one example of these intercomparisons of ER-2 CPL measurements with ICESat/GLAS observations are shown in Figure 55.

5) AIRBORNE INSTRUMENTS AND REGIONAL AIRBORNE CAMPAIGNS (M. D. King, M. J. McGill, L. A. Remer, S. C. Tsay, D. K. Hall)

The EOS Project Science Office has supported the development of EOS airborne simulators and other scientific instruments for use in validation campaigns. Instruments developed for the ER-2 aircraft include the MODIS Airborne Simulator (MAS), AirMISR, MASTER, and the Cloud Physics Lidar (CPL). These instruments have been widely used in a large number of EOS validation campaigns and other scientific (Research & Analysis) experiments.

In addition to major field campaigns such as SAFARI 2000, CRYSTAL-FACE, and the recent AMSR-E campaigns, the EOS Validation Program has supported targeted regional and more limited airborne campaigns each year. Support has been provided for missions on a variety of aircraft including the NASA ER-2, DC-8, and P-3B; DoE King Air and Citation; and contracted aircraft like the University of Washington's Convair 580. Some example airborne missions are:

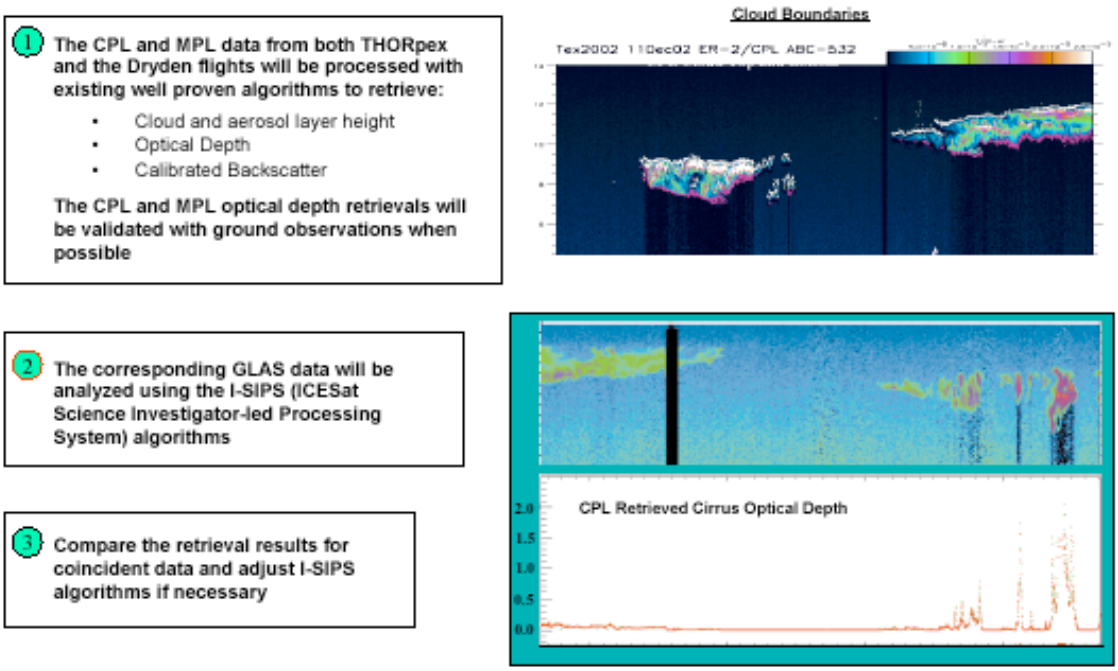


Figure 55. GLAS validation methods during THORpex.

- *CLAMS* – Chesapeake Lighthouse & Aircraft Measurements for Satellites (July 10 – Aug. 3, 2001) to improve the understanding of ocean surface reflectance and atmospheric aerosols (MAS, CPL).

- *TX-2000* – Terra-aqua eXperiment 2002 (November–December 2002) designed in part to assess MODIS and AIRS Level 1B thermal infrared band calibration and science products (MAS, CPL).

6) VALIDATION OF MODIS CHLOROPHYLL FLUORESCENCE LINE HEIGHT (F. E. Hoge, W. E. Esaias)

The MODIS sensor aboard the Terra and Aqua spacecraft contains spectral bands that allow retrieval of solar-induced phytoplankton chlorophyll fluorescence emission radiance. Concurrent airborne laser-induced (and water-Raman normalized) phytoplankton chlorophyll fluorescence data were used to successfully validate the MODIS chlorophyll fluorescence line height (FLH) retrievals within Gulf Stream, continental slope, shelf, and coastal waters of the Middle Atlantic Bight portion of the western North Atlantic Ocean for March 11, 2002. Over the entire ~480 km flight line a correlation coefficient of $r^2 = 0.85$ results from regression of the airborne laser data against the MODIS FLH. Hoge et al. (2003) showed that the MODIS FLH product is not influenced by blue-absorbing chromophoric dissolved organic matter absorption. These regional results strongly suggest that the FLH methodology is equally valid within similar oceanic provinces of the global oceans.

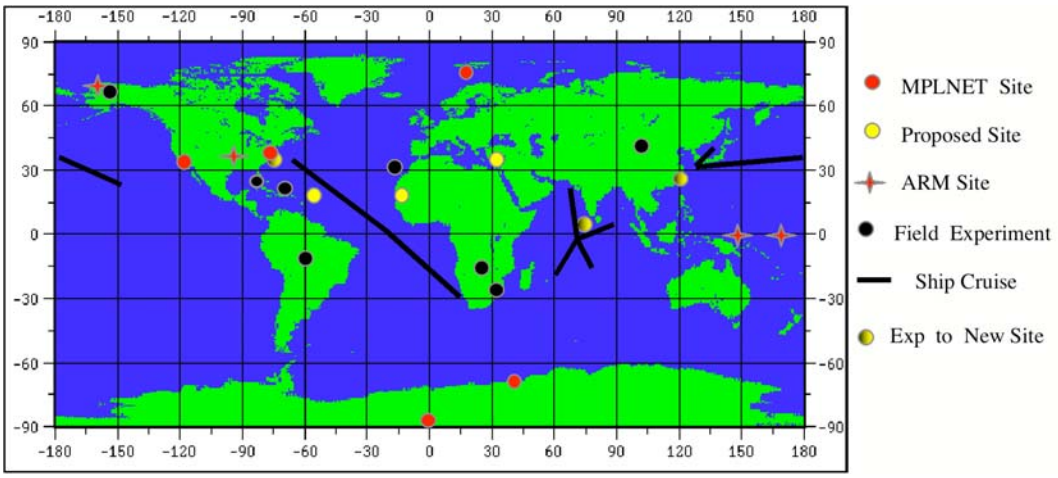


Figure 56. MPLNET sites, field experiments, cruises, and new proposed sites.

*c. Networks*

1) MICRO-PULSE LIDAR NETWORK (MPLNET) (E. J. Welton, J. D. Spinhirne, B. N. Holben, S. C. Tsay)

In the early 1990s, the first small, eye-safe, and autonomous lidar system was developed, the Micro-pulse Lidar (MPL). The MPL has proven to be an instrument capable of determining the vertical profile and optical properties of aerosol and cloud layers, and has done so in many areas not accessible to more conventional lidar systems. In 1999, the Micro-pulse Lidar Network (MPLNET) was proposed to the NASA Radiation Sciences Program as a project that would place MPL systems at strategically located sunphotometer sites in the Aerosol Robotic Network (AERONET; Holben et al. 1998). The combination of both an MPL and an AERONET sunphotometer at the same location creates a super-site that collects data on aerosol and cloud vertical structure, optical depth, particle size, and sky radiance. The MPLNET project (mplnet.gsfc.nasa.gov) started in 2000 with funding provided by EOS. There have been over 6600 visitors to the MPLNET website and over 120 registered users of our database. Figure 56 shows locations where MPLNET has collected data (16 separate data sets). Some of the sites were setup for temporary field experiments and are no longer active. Current MPLNET sites (long-term sites) include: GSFC, Monterey CA, South Pole, Norway, and along the coast of Antarctica. In the past, only 2000-2002 data from the ARM Oklahoma site was included in our network. Instrument upgrades are required for the ARM MPL systems, and selected sites will join MPLNET after this work is accomplished. New long-term sites in Barbados, Senegal, Taiwan, the Maldives, Israel, and off the coast of Virginia will become active over the next 1-2 years.

Since the beginning of MPLNET, data processing algorithms have been constructed, instrument maintenance protocols have been established, and a wide variety of data sets have been collected from different geographic regions of the world. The results have contributed to several scientific investigations of aerosol

properties. In addition, polar snow and cloud heights have been studied, and MPLNET results have been used to aid algorithm development for satellite-based lidar systems such as the Geoscience Laser Altimeter System (GLAS). MPLNET is currently participating in the ground-based calibration/validation for GLAS. Highlights of key MPLNET accomplishments are given below.

*Highlights:* Several papers were recently published containing descriptions of the MPLNET project and our data processing techniques. Welton et al. (2001) present an overview of the MPLNET project and describe the basis of our operational structure, data products, and focus. Campbell et al. (2002) discuss the methodology of our level 1 processing algorithm (daily signal images). Welton and Campbell (2002) present calculations of MPL signal uncertainties associated with our level 1 data products.

In addition to the above papers, several articles associated with our work in the Indian Ocean Experiment (INDOEX) were published during the 1999-2002 time period. INDOEX precedes the beginning of MPLNET, however analysis of those results occurred during the period when MPLNET was just beginning. Many of the algorithms developed to process INDOEX data formed the basis of what are now operational MPLNET algorithms and these papers are significant to this project. The work presented in Welton et al. (2002) contains descriptions of the basis of our level 1.5a algorithms (aerosol extinction profiles), and shows validations of the data based on comparisons to results from co-located instrumentation. In addition, Ackerman et al. (2000) present a study of the role of soot aerosols in tropical cloud production, MPL results were used to show how clouds become embedded within aerosol layers. This work demonstrates the usefulness of MPL data for the study of aerosol-cloud interactions. Finally, Collins et al. (2000) assimilated the MPL data into the NCAR Model of Atmospheric Transport and Chemistry (MATCH) in order to study the utility of using spaceborne lidar data to improve aerosol transport models.

During 2000, an MPL was operated in support of the Puerto Rico Dust Experiment (PRIDE). MPLNET, AERONET, and airborne sensors, were used to determine the vertical profile of Saharan dust properties over the tropical Atlantic Ocean (Livingston et al., 2003; Reid et al. 2003). In addition, MPLNET data were used to study the transport processes involved in the advection of Saharan dust across the Atlantic Ocean, with a particular emphasis on the role of deposition (Colarco et al., 2003). At the conclusion of PRIDE, two MPL systems were deployed in Southern Africa during SAFARI 2000 to study the effects of smoke and pollution on the regional climate (Campbell et al., 2003). MPLNET results from SAFARI have been used in aerosol closure studies between ground-based, airborne, and space-based sensors by Schmid et al. (2003a) and McGill et al. (2003).

In 2001, MPL systems were deployed to China and onboard a research vessel off the coast of Asia during the Aerosol Characterization Experiment - Asia (ACE-Asia) to discover the role Asian dust and pollution play in altering the local climate. Schmid et al. (2003b) have used MPLNET data together with other sensors

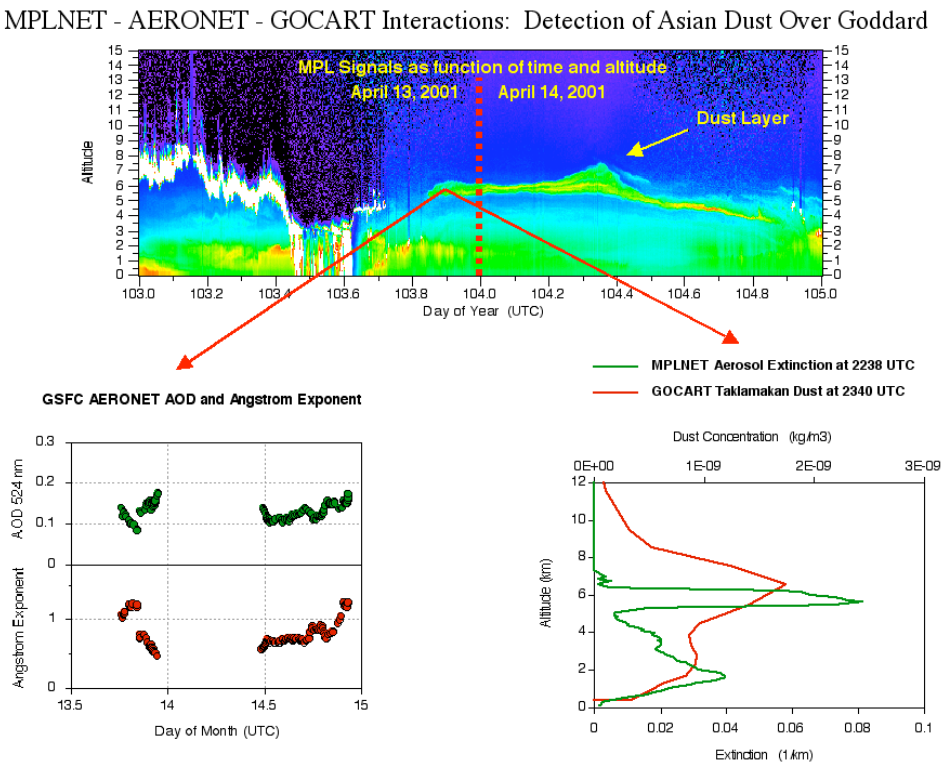


Figure 57. The top plate shows MPLNET data from GSFC on April 13-14, 2001. A layer of Asian dust is visible in the image at an altitude of approximately 6km. The bottom left and right plates show corresponding AERONET data and GOCART results, respectively.

to study aerosol column closure in the region. Markowicz et al. (2003) present analysis of aerosol infrared radiative forcing and use MPLNET results to identify the altitude of aerosol layers. Three other papers have recently been submitted or are in preparation. These include a study of the spatial and temporal homogeneity of aerosol properties across the region using combined space-based sensors, airborne measurements, and ground-based instrumentation (including MPLNET).

*Highlights:* MPLNET data will be used in the future to study aerosol-cloud interactions using data acquired at two new sites, Barbados and Senegal. Through operations at these two sites we will participate in the African Monsoon Multidisciplinary Analyses (AMMA) project. Aerosol transport processes will also be studied using MPLNET and AERONET data, satellite imagery, and results from the GOCART aerosol transport model. Figure 57 shows such a comparison between MPLNET, AERONET, and GOCART results over GSFC on April 13–14, 2001. During this time Asian dust was transported to the Eastern US. The dust layer is visible in the MPLNET data (top plate), and by the sudden change in AERONET AOD and Angstrom exponent (bottom left plate). The GOCART results show correlation with dust transport from the Taklamakan desert in China.

2) EOS Land Validation Coordination of International Global Land Product Validation (J. T. Morisette)

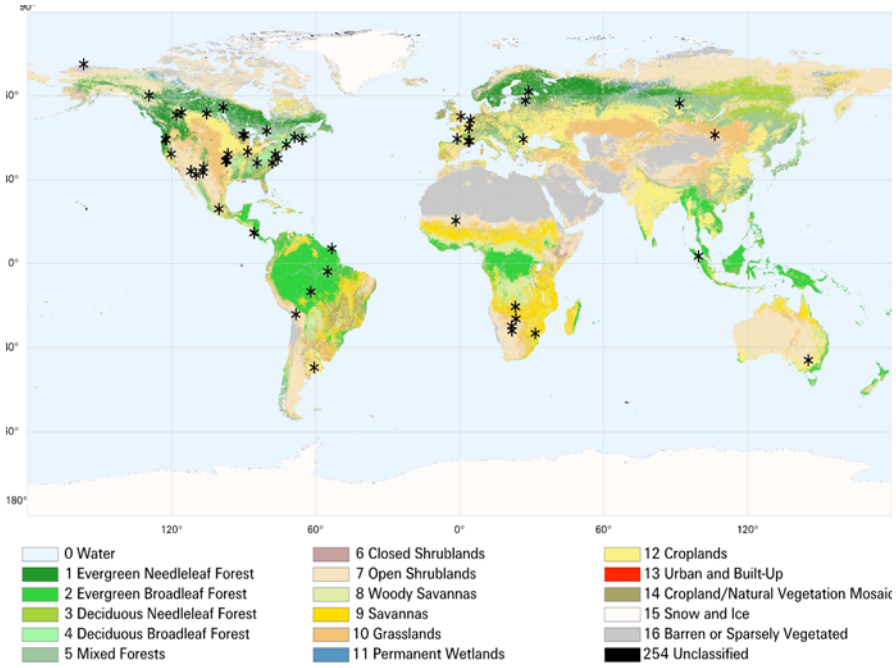


Figure 58. CEOS Land Validation Core Sites, shown on the MODIS land cover product (image provided courtesy of Boston University).

Product validation has been an integral component of the EOS system. In an attempt to leverage off the infrastructure and experience from the EOS validation program and MODIS land validation activities, researchers at GSFC have helped established the Committee on Earth Observing Satellites (CEOS) "Land Product Validation" (LPV) subgroup. Since the LPV subgroup's inception in late 2000, Goddard Scientists have chaired the subgroup. The mission of the subgroup is to foster quantitative validation of higher-level global land products derived from remote sensing data and relay results so they are relevant to users. This mission is being achieved through a series of topical workshops, international product intercomparison activities, and a transition from the EOS to CEOS Land Validation Core Sites. The product-specific workshops are co-chaired by community experts and focus on specific land product validation issues. The workshops are used to (i) establish the core reference data required for the validation of a particular product, (ii) determine sites where this reference data is (or could be) collected, (iii) present case studies from existing validation work, and (iv) formulate international intercomparison efforts. Within each workshop, MODIS land product validation activities have served as a primary example for global land product validation.

The EOS land validation core site system was initiated by the MODIS land team to efficiently support the validation of EOS land products. Now, LPV is leading a joint activity to transition from EOS to CEOS land validation core sites (see Figure 58). The results will be similar to the EOS core site infrastructure but will provide access beyond NASA's EOS satellite data sets to include global land products produced by other CEOS members. The "Core Sites" approach, which

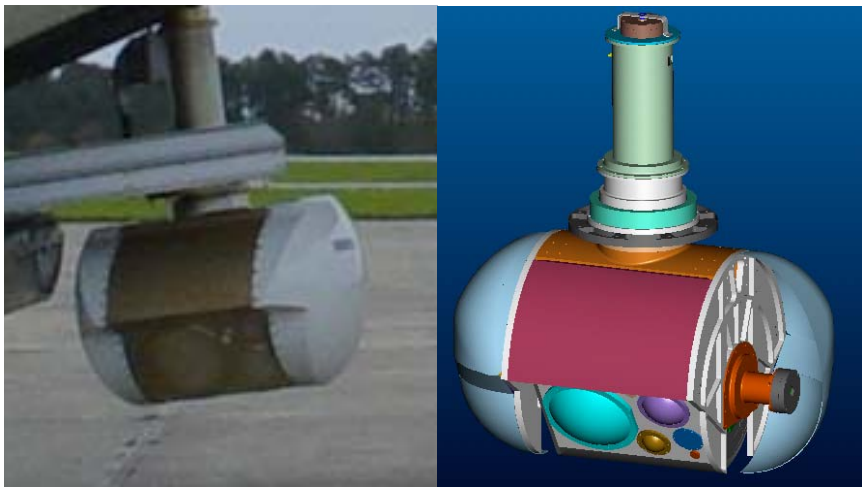

Figure 59. AESMIR integrated on the Wallops C-130Q aircraft (left) and artist drawing of instrument (right).

has been fostered by EOS, will lead to an international focus for the validation of global land products; which will more readily allow data sharing and product inter-comparison between CEOS members. This transition of the EOS Core Sites to CEOS Core Sites will help maintain a long-term focus that will help quantify the accuracy of land-related climate data records composed of similar product from multiple sensors and platforms.

*d. Airborne Instrument Development*

1) AIRBORNE EARTH SCIENCE MICROWAVE IMAGING RADIOMETER (AESMIR) (E. J. Kim)

AESMIR is a passive microwave airborne imager designed from the beginning to provide a highly efficient solution for satellite calibration/validation and algorithm development applications covering nearly all components of the water cycle (snow, soil moisture/land parameters, precipitation, ocean winds, sea surface temperature, water vapor, sea ice, etc.). The key to AESMIR's utility is its coverage of all of standard imaging bands from 6.9 to 89 GHz using a single scanning package (cf. Figure 59). Also, AESMIR is unique in its capability to *simultaneously* simulate multiple satellite radiometers (including AMSR-E, Windsat, CMIS, SSMI, SSMI/S, TMI, and GPM's GMI & LRR). The microwave radiometers themselves incorporate state-of-the-art technology, including the capability to make fully-polarimetric (4-Stokes) observations—opening up new discovery opportunities. AESMIR is compatible with a variety of airborne platforms including high-altitude platforms—a capability that may open up previously unavailable science opportunities for convection/precipitation/cloud science and co-flying with synergistic instruments, as well as providing wider swath coverage for all science applications.

## 5. Project Scientist Activities

*a. Project Science Office* (M. D. King, C. S. Griner, S. M. Graham, W. H. Humberson)

The Project Science Office was established at the very beginning of the EOS Program, and Michael King was appointed Senior Project Scientist in August 1992. This office has provided numerous services to NASA management both at Headquarters and Goddard, and has been the primary day-to-day interface between the science community and NASA throughout the life of EOS.

### 1) EOS Science Leadership

The EOS Senior Project Scientist has served on various study committees, including the Science Committee of the Rebaseline and Restructure phases of the EOS Program. These activities ultimately resulted in Payload Panel meetings of EOS Principal Investigators in which recommendations were made to restructure payloads and spacecraft under constraints of a considerably reduced budget. This involved extensive interaction with scientific experts in all disciplines of Earth system science, both within NASA and in the outside scientific community, and resulted in the satellite missions and payloads that are currently flying in space or soon to be launched.

Michael King also serves as co-chair of the Investigators Working Group (IWG), a community-wide organization of the Principal Investigators and Team Leaders of all components of the EOS program that convenes every 9 months. This meeting is attended by typically 175-200 scientists and science managers, including participants from the European Space Agency and NASDA. This meeting is most informative, but involves considerable effort in finding the most breakthrough and cross-cutting science results and speakers to make the presentations. The group has been co-chaired in the past by the EOS Program Scientist at NASA Headquarters (formerly Ghassem Asrar), but is now co-chaired by Jack Kaye, Director of the Research Division in the Office of Earth Science. The Senior Project Scientist was also a member of the EOS Science Executive Committee that met once every 2 months for many years. It was this committee, made up of chairs of various committees and working groups of the IWG, that served as the Program Committee of the IWG.

### 2) Outreach Activities

The EOS Project Science Office has produced a wide variety of documents describing the EOS program, sensors, science plans, and results, and uses various avenues for conveying the Earth Science Enterprise message to the science community at large as well as the general public. These include:

- Support of a grant to the *Odyssey of the Mind* organization to sponsor an Earth Science problem. An estimated 1.5 to 2 million people internationally are exposed to NASA's Earth Science program through this avenue every


Figure 60. Opening ceremonies at Odyssey of the Mind World finals at the University of Colorado, May 22, 2002, attended by 13,000 people. The MODIS 16' blue marble globe of the world is suspended from the ceiling in the Coors Arena (photo by Todd Ulrich).

year. Figure 60 shows the Opening Ceremonies of the OM World Finals, University of Colorado, May 22, 2002, which was attended by ~13,000 people.

- Print and distribute *The Earth Observer* newsletter every 2 months to a worldwide distribution of over 6,000. This newsletter describes the latest developments on instruments, launch, Congressional appropriations, science news, and meeting announcements.
- Print and distribute *Science Posters*. In 1994, a series of 7 EOS posters was produced, one for each theme of EOS. These poster sets, now out of print, have been distributed to approximately 250,000 people and schools worldwide through our web site and conferences. They were translated to Czech by a professor in the Czech Republic and distributed to schools in that country. In 2002 we produced an entirely new set of posters oriented around air, water, land, and ice. These new posters are currently being distributed both at conferences and through web-based orders, with the web orders reaching 28,000 sets since August 15, 2002.
- NASA fact sheets and lithographs have been written, printed, and distributed at numerous conferences.
- Numerous instrument and satellite brochures have been printed and distributed, including: EOS AM-1, Terra Spacecraft, MODIS, CERES, MOPITT, ASTER, MISR, Aqua, AMSR-E, AIRS/AMSU/HSB, SORCE, and ICESat. In addition, we produced an Earth Sciences calendar for 2003.
- NASA's Earth Science Enterprise informational CD-ROM has been distrib-

uted to about 175,000 people through web-based orders and conferences since 2000. This popular CD-ROM has an accompanying Activity Guide. The CD-ROM has been translated to Portuguese by a professor in Brazil and is being distributed in that country as well as on the EOSPSO web site.

- The EOSPSO sets up a booth, distributes materials, and answers questions concerning the program at approximately 15 major scientific conferences each year such as the American Geophysical Union and the American Meteorological Society, and several general public and educational venues such as the Maryland Science Center, Andrews Air Show, and the Association for Supervisors and Curriculum Developers Conference.

3) PEER COMMUNICATIONS

The Project Science Office has edited and distributed the following substantial science reference documents to the scientific community:

- King, M. D., Ed., 1998: *EOS Science Plan: The State of Science in the EOS Program*, NASA NP-1998-12-069-GSFC, 397 pp.
- Greenstone, R., and M. D. King, Eds., 1998: *EOS Science Plan: Executive Summary*, NASA NP-1998-12-070-GSFC, 64 pp.
- King, M. D., and R. Greenstone, Eds., 1999: *1999 EOS Reference Handbook*, NASA NP-1999-08-134-GSFC, 361 pp.
- Parkinson, C. L., and R. Greenstone, Eds., 2000: *EOS Data Products Handbook, Volume 2*, NASA NP-2000-5-055-GSFC, 253 pp.
- King, M. D., J. Closs, S. Spangler, and R. Greenstone, Eds., 2003: *EOS Data Products Handbook, Volume 1*, NASA NP-2003-4-544-GSFC, 258 pp.

In addition, a pair of CDs has been produced, based on a week-long course on *Remote Sensing of the Earth's Environment from Terra* that was held in L'Aquila, Italy during August 2002. These CDs contain all PowerPoint lectures as well as all imbedded QuickTime and mpeg movies. These CDs are very popular with University Professors worldwide. Other CDs have been produced such as Terra MODIS Ocean Data, which contains MODIS Ocean File Samplers and a timer series of weekly HDF files.

4) SATELLITE IMAGERY, NATURAL HAZARDS, AND NEWS STORIES (D. D. Herring, R. B. Simmon, J. S. Allen)

The Project Science Office developed and maintains a Web site (eos.nasa.gov) that contains outreach materials, such as those outlined above, that one can view and order. In addition, the site contains considerable information and links on the EOS investigators (EOS Directory), calibration, validation, and links to sites on each of the EOS missions and instruments. There were 1,000,000 hits from 26,000 unique visitors from December 27, 2002 to January 21, 2003, indicating that even over the Christmas holidays this is a popular site for up-to-date information on the EOS program.

The most significant web presence for the Earth Science Enterprise is the Earth Observatory (earthobservatory.nasa.gov), which contains the following major elements

- Data and images, posted in thumbnails, medium sized, and full resolution.
- Feature stories on Earth system science produced roughly once per week
- Breaking news
- Missions, including satellite orbits and their locations
- Experiments
- Natural hazards (fires, dust and smoke, floods, severe storms, volcanoes, and unique imagery)

The Visible Earth (visibleearth.nasa.gov) web site is a searchable database of satellite imagery (with captions and multiple file formats) that received more than 1 million page views in its first month of operation. It currently averages about 70,000 page views per day (~2 million per month). It contains a comprehensive collection of NASA Earth images, including those from Earth orbiting satellites, selected airborne sensors, and the Space Shuttle and International Space Station. Within the next 12 months the goal is to link to all of the animations that have been produced by the Visualization & Analysis Laboratory (VAL) and the Science Visualization Studio (SVS) at Goddard (mpeg, mov, mpeg2 formats).

The Earth Observatory and Visible Earth Web sites are the #1 and #3 most popular web sites at Goddard Space Flight Center. The Earth Observatory has received numerous awards and recognitions, the most significant of which are

- 2003 *Webby* and *People's Voice Award* in the Education category
- 2002 Webby *People's Voice Award* in the Science category
- Cited by *Scientific American* as one of the 50 best science & technology web sites in 2002
- Cited by *Popular Science* as one of the 50 best science & technology web sites in 2002
- Winner of the *Society for Technical Communication's* Online Communications Competition (both Washington, DC region and international)

5) NASA'S EARTH SCIENCE NEWS TEAM (R. Gutro, K. Ramanujan)

The Earth Science News Team identifies and promotes newsworthy research among NASA-funded researchers worldwide, providing comprehensive and accurate resources to journalists covering Earth Science topics. They support NASA's Public Affairs by mining news and developing press releases, conducting and coordinating press briefings at scientific conferences, responding to media and public inquiries, producing Media Directories, Science Writers Guides for the various missions, and workshops for science journalists. The top 10 Earth Science Press Releases picked up by media worldwide since October 1, 2002 are:

6/5/03 Global Garden Grows Greener (Video)
5/26/03 Coastal Cities Turn Up the Heat on Rainfall (Video)

5/15/03 Scientists Dust off Desert Sands from the French Alps
4/23/03 Hurricane Winds Carried Ocean Salt & Plankton Far Inland
2/5/03 NASA Satellite Helps Scientists See Affects of Earthquakes in Remote Areas
1/15/03 NASA Scientists Take First "Full-Body Scan" of Evolving Thunderstorm
11.28/02 Arctic Ice Melting Faster Than Thought (Video)
10/7/02 NASA Developing Tools to Track, Predict West Nile Virus (Video)
10/1/02 Ozone Hole Splits in Half (Video)

*b. Landsat* (D. L. Williams, J. R. Irons, J. L. Barker, B. L. Markham)

Landsat 7 was/is quite different from other EOS era missions. First of all, it came into the EOS family rather late in the game, even though it was the success of the earliest Landsat missions that started the community thinking about the whole concept of Earth System Science and scientific Earth observations from space. Secondly, as a quasi-operational heritage mission with considerable baggage associated with it (e.g., users always had to pay for the data, etc.), there was no need to solicit an algorithm development team. Last, but not least, in the eyes of NASA Administrator Dan Goldin, Landsat 7 was forced on him by the Air Force who bailed out of their leadership role in the development of Landsat 7 following the fall of the Berlin wall and the resulting cuts to DoD budgets due to the "peace dividend." Goldin was not happy getting stuck with what he considered to be an overly expensive, antiquated mission, and in the style that he was famous for, he let it be known that he despised the mission and wanted to make sure only minimal funding was allocated to it. Thus, as NASA took over the mission, we had to agree to a set of demands and budget limitations (i.e., no processing to Level 1) that would have greatly affected the utility of the data for the Earth System Science user community. Thus, much of what we had to accomplish to ensure that we ended up with a mission having high scientific integrity had to be accomplished using "stealth" techniques, and Goddard's Landsat Project Science Office within the Earth Sciences Directorate provided the needed calibration and quality assessment functions.

<u>*The Landsat Mission:*</u> The ideal Landsat mission goal has always been to acquire *well-calibrated*, moderate resolution, multispectral imagery affording *systematic global coverage* of the Earth's land surfaces on a *seasonal basis* and make the data readily available for *large-scale and long-term* Earth system science and land resource management. Prior to Landsat 7, this ideal goal was never close to being realized, but largely due to the Project Science leadership role, that goal has been realized – with the possible exception of making the data available free of charge.

<u>*The Landsat Project Science Office (LPSO) Contribution*</u>: The LPSO served to ensure the scientific integrity of Landsat mission by conceiving and overseeing the development of the Image Assessment System (IAS); having sold the idea of needing an IAS, and thereby having to develop the algorithms needed to process the data to Level 1, we were able to get Level 1 processing back into the program as

the standard product for the user community. The LPSO conceived and oversaw the development of the long term data acquisition plan (LTAP); we conceived and sold the idea of formation flying with Terra (along with Piers Sellers, former Project Scientist of Terra); we stressed the need for detailed characterization and calibration of the Landsat 7 ETM+, and of reaching back in time to bring the long-ignored calibration of the Landsat 4/5 TM archive up to date; we worked with EOS upper management (Bob Price) and found the funds ($750 K) needed to initiate the salvage of a valuable, but rapidly deteriorating MSS wide band video archive containing over 30,000 scenes of data from the early to mid 1970s; we conceived the idea of under flying Landsat 5 with Landsat 7 early in the Landsat 7 mission to afford an opportunity to intercalibrate the two sensors and thereby enhance data continuity; we designed and drove the pre- and post-launch calibration procedures, making the ETM+ the "best of the best" as far as absolute calibration of Earth observation sensors goes; we fought to get a full aperture calibration panel added to the instrument design, then we successfully stiff-armed the Air Force's attempts to delete it from the design early in the development stage; we conducted rapid turnaround analyses of pre-launch data just prior to launch and identified a "fried" capacitor in the spacecraft power supply that would have compromised the mission – we caught it in time for the capacitor to be replaced on the launch pad; we fought for placement of an X-band receiving antenna at EDC, thereby ensuring direct downlink coverage of the lower 48 in case we ran into problems with the new and largely untested solid state recorder; we worked hard to sell the need for what became the NMP EO-1 technology demonstration and risk mitigation mission; we wrote the EOS-1/LandsatNext concept paper that led to what is now known as the Landsat Data Continuity Mission (LDCM); we have maintained and significantly enhanced the detailed documentation of the system and its performance via the web-based Landsat Data Users Handbook; and we have developed a very successful education (K thru college) and public outreach program (e.g., highly successful "Earth as Art," as well as videos, web pages, curricula development, training).

In developing the LTAP, we established aggressive new benchmarks such as (i) 250 scenes per day (up from 50 per day, at best, in the past), (ii) the need for a global seasonal refresh, and (iii) the need for, and incorporation of, cloud cover predictions, followed quickly by cloud cover assessment of the acquired scenes. After establishing these benchmarks, we oversaw the development of a complete end-to-end system to meet these benchmarks.

Largely as a result of our efforts, the Landsat 7 mission has established an important set of benchmarks for its successor mission with respect to:

- Sensor and system performance, characterization, and calibration
  - On-orbit characterization and calibration over mission life
- Mission operations and data acquisition
  - Archive-driven, systematic, substantially cloud-free, global coverage on a seasonal basis
- Data archival and data product distribution

- USGS archive provides non-discriminatory access
- Data products are available in consistent formats on consistent media
- Secondary distribution is unrestricted

In summary, within the LPSO, we have captured a core, veteran team of dedicated individuals who understand the instrument as well as the manufacturer, ***and*** we understand the important scientific role/contributions of ETM+ data in global change research, Earth system science, the carbon initiative, and other Earth Science Enterprise initiatives. The LPSO is the only component of the Landsat 7 Project that has not changed significantly since the Project kick-off in 1992; *we constitute NASA's in-depth corporate memory of the past, present and future Landsat Program, and thereby ensure that the scientific integrity of the mission will not be compromised.*

The quality of the data returned from the ETM+ has been spectacular! The LPSO played a significant role in ensuring that that would be the case.

*c. Terra* (K. J. Ranson, S. C. Tsay)

NASA's Terra spacecraft is providing comprehensive global measurements for quantitatively monitoring the Earth's lands, oceans, and atmosphere and acquiring many of the measurements required to advance understanding of the Earth system. Launched in December 1999, Terra has been acquiring science data since February 2000. Terra flies in a near-polar, sun-synchronous orbit that descends across the equator around 10:30 am when cloud cover over the land tends to be minimized.

Terra's orbit follows the Worldwide Reference System, along with Landsat 7 (USGS), EO-1 (NASA) and SAC-C (Argentina CONAE) all crossing the equator within 25 minutes. The selection of this orbit was made by the Terra and Landsat Project Scientists (P. J. Sellers and D. L. Williams, respectively) to facilitate joint use of the data. The EO-1 and SAC-C missions joined later. These four spacecraft comprise the "Morning Constellation." The Terra project scientist serves on a working group to facilitate communication on important aspects such as operations, maneuvers and joint use of validation and science data.

Each of the Terra instruments was developed under the supervision of a science team that also provides algorithms for analysis of the data and derivation of Earth system measurements. The science teams validate these products and use them in scientific investigations. Terra has five complementary scientific instruments: ASTER for close-up land studies, CERES for a broad view of long- and shortwave radiation, MOPITT for studies of pollution, MISR for bidirectional-reflectance studies of clouds, aerosol and land features and MODIS for global analysis of land, ocean and atmosphere properties and their interactions. The MODIS and CERES instruments extend the measurements of their heritage sensors (e.g., Advanced Very High Resolution Radiometer (AVHRR), Coastal Zone Color Scanner (CZCS), and the Earth Radiation Budget Experiment (ERBE)), but with a higher degree of calibration and characterization. The Project Science Of-

fice's role is to organize and moderate regular communication among the Terra instrument teams through regular telephone conferences, science team meetings, and organization of special issues in journals, topical workshops, and conference sessions.

Another role of the Project Scientist is to be the science liaison to the Terra Flight Operations team. This ensures that the science requirements are considered during routine operations and anomaly mitigation. Despite several anomalies to MODIS, MOPITT and some spacecraft systems, all Terra instruments are collecting high quality science data.

Early in the Terra mission, instrument-team scientists called for a series of on-orbit pitch-over maneuvers to allow Terra's instruments to view cold deep space or the sunlit lunar surface. Data from the deep-space maneuvers were required to enable CERES to confirm offsets for its long wave radiation measurements and enable MODIS to adequately characterize response with mirror scan angle. ASTER, MISR, and MODIS desired measurements of the lunar surface for radiometric calibration purposes. The maneuver required a reverse pitch during eclipse (spacecraft night) within about 33 minutes. The maneuver was controversial and the Project Scientist led the effort to gain approval of the maneuver by EOS Program, GSFC and NASA HQ Management. Working closely with the Terra FOT a series of tests, simulations, and reviews were conducted that ultimately led to approval of the maneuvers.

The first deep-space calibration maneuver was successfully performed on March 26, 2003 followed by an identical and flawless maneuver with the moon in the viewing plane of the instruments on April 14, 2003. NASA's EO-1 ALI, and Hyperion instruments and OrbView's SeaWiFS instrument acquired data of the moon around the time of Terra's maneuver. Intercomparisons with these instruments are planned. The data from the deep space and lunar maneuvers are being analyzed, and a third maneuver is planned for fall of 2003.

The amount of downloaded data from Terra's instruments is about 195 Gb of Level 0 data received each day, which represents about 850 terabytes when processed to higher-level science products. Currently, the majority of planned Terra science products are available through the EOS Data Gateway. At this point in the mission, most products are calibrated and validated and have been given the label of "validated" data. This means that a data product has been evaluated and quality checked and is considered ready for routine scientific research uses. The Project Science Office advocated for the science teams to ensure the data system had sufficient processing and reprocessing capacity to deliver highest quality data products in a timely fashion. In addition, the Project Scientist is a member of the EOS Science Working Group for Data that examines current issues involving data processing, data product distribution and data accessibility and usability, and long-term archive. The SWGD has held workshops on the first two topics and is planning a workshop on data accessibility and usability in November 2003. For the latest information on the status and availability of data from Terra

and other EOS missions, see: eosdatainfo.gsfc.nasa.gov/terra.

The scientific community now has unprecedented quantitative data sets to study the Earth as a system and answer the questions of how is the Earth changing and how will humans be affected by these changes? Terra, as the flagship observatory for NASA's Earth Observing System, is contributing new insights about our Earth. For additional information about the Terra spacecraft and links to each of the five instruments, the reader is invited to visit the Terra Project Science homepage at terra.nasa.gov.

The Terra Project Science Office is also involved in outreach and education activities. The Project Scientist gives guest lectures at conferences and schools. A video highlighting the mission's accomplishments is now under development. The Terra Project Science Office originated the Earth Science education web site, the Earth Observatory, in 1996. This site has grown to encompass all the EOS missions and has won many awards for excellence in Earth Science Education. See earthobservatory.nasa.gov.

*d. Aqua* (C. L. Parkinson, S. Platnick)

Aqua, launched on May 4, 2002 with six different Earth-observing instruments on board, the AIRS, AMSU, HSB, AMSR-E, MODIS, and CERES, is one of the key missions of the EOS program and has a heavy involvement from the Earth Sciences Directorate. This includes the Project Scientist Claire Parkinson, the Deputy Project Scientist Steve Platnick, the MODIS Science Team Leader Vince Salomonson, and science team members, associates, and other participants on each of the five Aqua Science Teams (the AIRS/AMSU/HSB Science Team, the MODIS Science Team, the CERES Science Team, the U.S. AMSR-E Science Team, and the Japanese AMSR-E Science Team).

Aqua is named for the vast amount of information it is gathering about water in the Earth/atmosphere system, including water vapor in the atmosphere, liquid and solid water in clouds, precipitation, soil moisture on the land, snow and ice cover on the land, the surface layer of the oceans, and sea ice in the oceans. The Earth Sciences Directorate is involved in EOS Aqua studies of all of those variables, with Joel Susskind using AIRS/AMSU/HSB data for studies of water vapor, Michael King and Steve Platnick using MODIS and CERES data for cloud studies, Bob Adler using AMSR-E data (along with TRMM data) for precipitation studies, Dorothy Hall, Vince Salomonson, Richard Kelly, and Al Chang using MODIS and AMSR-E data for snow and ice cover on land, Wayne Esaias and Frank Hoge using MODIS data for ocean studies, and Don Cavalieri, Joey Comiso, Dorothy Hall, Tony Liu, Thorsten Markus, and Claire Parkinson using AMSR-E and MODIS data for sea ice studies. Directorate scientists are also heavily involved in validation of the AMSR-E data products. In particular, Tom Bell is involved in precipitation validation, Peggy O'Neill and Paul Houser are involved in soil moisture validation, Jim Foster is involved in snow validation, Don Cavalieri, Joey Comiso, and Thorsten Markus are involved in sea ice validation, and Ed Kim has led the development of an airborne simulator for the AMSR-E.

The Aqua mission additionally examines non-water aspects of the environment, including atmosphere and surface temperatures and atmospheric aerosols, placing these also in the context of the global climate system. Joel Susskind is heavily involved in the atmospheric temperature retrievals from the AIRS/AMSU/HSB sounding suite; and Yoram Kaufman and Lorraine Remer lead the aerosol studies from MODIS. Additionally, Joanna Joiner leads the effort to assimilate the AIRS/AMSU/HSB data into the Data Assimilation Office (DAO) modeling efforts; Ed Masuoka leads the MODIS Science Data Support Team; and David Starr, in his role as EOS validation scientist, plays a central role in facilitating the validation activities for each of the four U.S. Aqua science teams.

Claire Parkinson was appointed Project Scientist for the EOS PM mission (later renamed the Aqua mission) in April 1993. Since that time, she has worked extensively with the five Aqua science teams, mission management, and mission operations, helping to facilitate communication, keeping an upbeat focus on the mission, and maintaining the ability of the mission to achieve its main science goals despite such occasional challenges as a contesting of the spacecraft contract, mandated downsizing to fit into a Delta II rocket, the withdrawal of the Europeans from providing two of the planned Earth-science instruments, a multitude of concerns over the main battery and other hardware just prior to launch, and frequent funding issues. As Aqua Project Scientist, she attends many meetings at GSFC and NASA Headquarters and communicates extensively through emails and, when requested, short position papers, working closely with the Aqua science team leaders. She has chaired the Aqua Science Working Group since its inception in 1996, has chaired monthly Aqua telecons since their initiation in January 2003, and is co-convening an Aqua Special Session of the Fall 2003 American Geophysical Union (AGU) meeting in San Francisco. She also served on the EOS Science Executive Committee from 1996 until its disbandment in 2000, is chief editor of the 253-page *EOS Data Products Handbook, volume 2*, published in 2000, and is the lead editor for an Aqua Special Issue of the IEEE *Transactions on Geoscience and Remote Sensing*, published in February 2003.

Dr. Parkinson has devoted considerable effort to Aqua outreach activities, for instance writing a 42-page Aqua brochure for the general public, helping to edit AIRS/AMSU/HSB and AMSR-E brochures and an Aqua Science Writers' Guide, and giving over 40 talks on Aqua in 2002 and the first 7 months of 2003, to a range of audiences including school children, teachers, the general public, scientists, and Aqua mission specialists. She helped to organize and was a participant in nine Aqua webcasts produced by the Goddard Special Project Initiatives Office, each presenting a live show on the internet describing various aspects of the mission, and she has worked with the Goddard and NASA Headquarters Public Affairs Offices on numerous press releases, and, especially in the month prior to and year after launch, has fielded many inquiries from the press regarding Aqua and referred reporters to many members of the Aqua team for more details about the mission and the expected science. She has worked with computer animators and visualizers to develop Aqua-related animations for talks by herself and others, and she works closely with Aqua Outreach Coordinator Steve Graham on

such other Aqua outreach items as an Aqua web site (aqua.nasa.gov), Aqua facts sheets, trading cards, posters, and an engineering competition for high school students. She is also on the editorial board of the Webby-award-winning Earth Observatory web site.

Steve Platnick was appointed Deputy Project Scientist for Aqua in January 2003. He has substituted for the Aqua Project Scientist at meetings she was unable to attend, has produced the official minutes for the monthly Aqua telecons, and has organized and chaired a session on clouds at the May 28-29, 2003 Aqua Science Working Group meeting.

*e. Aura* (M. R. Schoeberl, A. R. Douglass, E. Hilsenrath)

The Project Science Office acts as an interface between the Project and the instrument PIs with regard to mission science goals and engineering or budget compromises that need to be made. Aura Project Science Office also has developed the validation plan and the education/outreach effort. The Aura Project science team attends the numerous Project and Instrument meetings and reviews, presents Project status at meetings, and organizes the semi-annual science team meetings. Although the work comes in spurts, each member of the Project Science Office spends about 1/3 of their time on these activities. The Project Science Office is proposing to establish a small data center for work with the correlative data. This proposal has not been reviewed yet.

*f. SORCE* (R. F. Cahalan, D. M. Rabin)

Dr. Robert Cahalan serves as Project Scientist of SORCE. This EOS mission was launched into low Earth orbit (645 km, 40°) on an Orbital Sciences Corp. Pegasus XL at Kennedy Space Center on January 25, 2003. It carries 4 instruments that measure Total Solar Irradiance and Spectral Solar Irradiance from 1 to 2000 nm – TIM, SIM, SOLSTICE and XPS. The instruments were built at the University of Colorado's Laboratory For Atmospheric and Space Physics (LASP) in Boulder, Colorado. The SORCE Mission Operations Center is also at LASP, with whom Dr. Cahalan maintains close collaboration and partnership. Dr. Cahalan is co-convening, with SORCE PI Gary Rottman of UCO/LASP, and Judith Lean of NRL, a special SORCE session at the Fall 2003 San Francisco AGU meeting (session SH-09), immediately following the next SORCE Science Team meeting in nearby Sonoma, California. Dr. Cahalan is also lead scientist of two related missions: Solar Irradiance Gap Filler, a 2006 follow-on to SORCE, and Solar Irradiance Hitchhiker, a planned series of Shuttle flights designed to compare TIM, ACRIM, and SOLCON measurements in the laboratory and in space, to determine the absolute calibration of the Sun's total irradiance with unprecedented accuracy. Dr. Cahalan plays a key role in coordinating the efforts of the SORCE Science Team, encouraging joint efforts of the Earth and Space science communities, and formulating science requirements for future Sun-Earth missions. He has been actively involved in research and education related to solar forcing of Earth's climate, directing production of an interactive CD, a variety of printed materials and publications, and invited presentations to a variety of national and

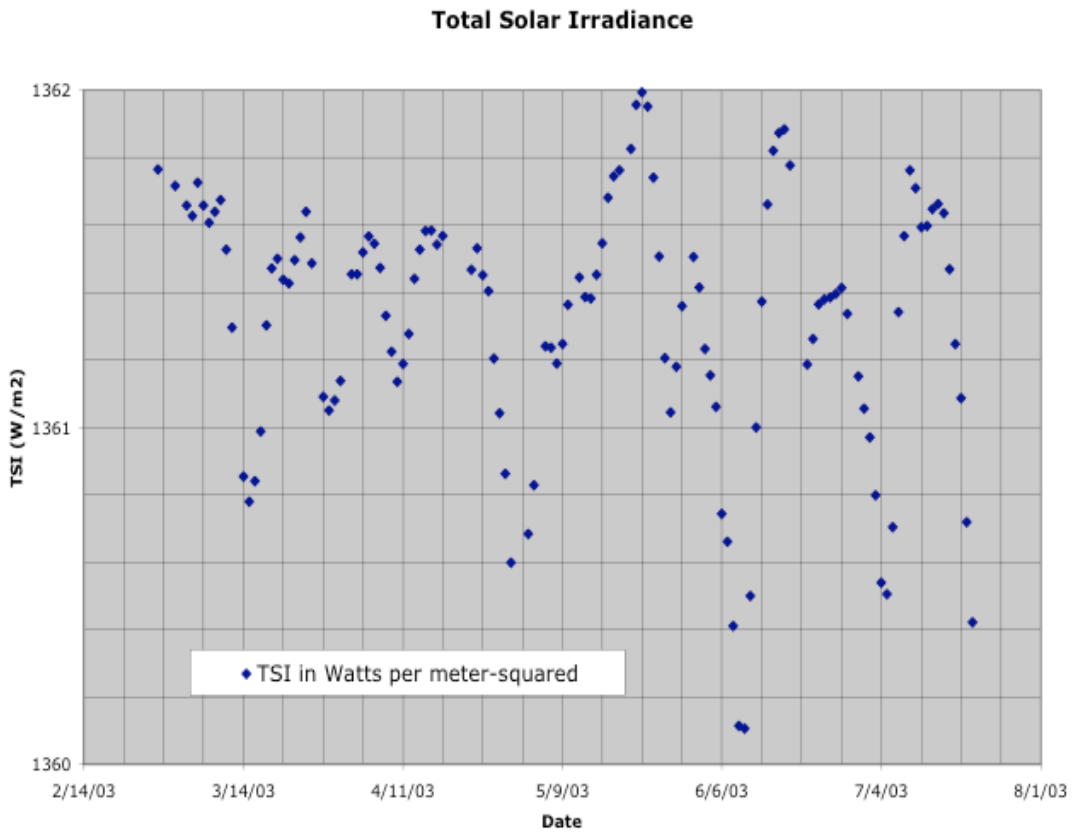


Figure 61. Total solar irradiance from February to August 2003 as derived from SORCE/TIM.

international forums, such as COSPAR, IRS, IUGG, and IGARSS. Dr. Cahalan has been a leader and innovator in climate and radiation, is a member of the International Radiation Commission, and chairs the working group on Three-dimensional Radiative Transfer.

Figure 61 shows a time series of total solar irradiance derived from the TIM instrument on SORCE from late February through lat July 2003. Not the significant drop in TSI on June 10 that corresponds to the passage of a particularly intense magnetically active region across the solar disk.

*g. ICESat* (H. J. Zwally, C. A. Shuman)

ICESat, launched on January 12, 2003, has one Earth-observing instrument on board, the Geoscience Laser Altimeter System that was developed in the Directorate under the leadership of Jim Abshire (cf. Section 1D1). This mission is another of the key missions of the EOS program and has a heavy involvement from both science and engineering at GSFC and within the Earth Sciences Directorate. This includes the Project Scientist Jay Zwally, the Deputy Project Scientist Christopher Shuman, the ICESat Science Investigator-led Processing System (I-SIPS), and science team members, associates, and contractors.

ICESat is named for its primary and secondary mission goals of polar Ice, Clouds and aerosols, and land Elevation data. The Earth Sciences Directorate is involved

in EOS studies of all of those climate variables, with Jim Spinhirne leading the studies of clouds and aerosols, David Harding focusing on land elevation and vegetation cover, Scott Luthcke assessing orbital data, David Hancock leading the in-house data processing system, and Jay Zwally and Chris Shuman focusing on ice sheet elevation data and mass balance estimates. These same Directorate scientists are also heavily involved in validation of the ICESat data products, the I-SIPS system, as well as education, outreach, and support of the NASA HQ Cryospheric Science Program.

Jay Zwally was appointed Project Scientist in 1993. Chris Shuman was appointed in April 2001 to be the Deputy Project Scientist following the move of Waleed Abdalati to NASA HQ. Since that time, they have worked to maintain the ability of the mission to achieve its main science goals despite the myriad engineering challenges of the GLAS instrument during development and testing of the instrument, an on-orbit laser failure, and funding issues. As ICESat Project Scientists, they attend many meetings at GSFC and NASA Headquarters and communicate extensively through emails and, when requested, situation reports. They also work closely with the other members of the science team; for example, they are co-convening, with Science Team Leader Bob Schutz, an ICESat Special Session of the Fall 2003 American Geophysical Union (AGU) meeting in San Francisco. Dr. Shuman has devoted considerable effort to ICEsat outreach activities, including completing a 20-page brochure for the general public and giving numerous presentations on ICESat to a range of audiences. Drs. Shuman and Zwally have worked with the Public Affairs Offices at Goddard and NASA Headquarters on press releases, and, especially in the month prior to launch, planned and participated in a press conference at the Fall AGU 2002 detailing ICESat's expected science. This reaped a bonanza of media attention for the mission including coverage on CNN and in the Washington Post. Currently, they are working with computer animators and visualizers to develop ICESat-related animations for additional media opportunities, as well as for science talks and other ICESat outreach avenues such as the main mission web site (icesat.gsfc.nasa.gov).

*h. EOSDIS* (C. A. Reber)

ESDIS is the project responsible for developing, maintaining, and operating the Earth Observing System Data and Information System (EOSDIS). Originally, the EOSDIS included ground operation of the EOS spacecraft, getting the data to the ground, data processing to higher level scientific products, data storage and archive, and data distribution to end users. Currently, ground operation is the responsibility of the Earth Science Mission Operations Project (ESMO), which takes over control about ninety days after launch of the spacecraft.

The EOSDIS Project Scientist is the prime interface and liaison between the Earth science community and the ESDIS Project, and principal advocate representing the users to the project (and vice versa). As such, he has been or is involved in:

- Understanding and interpretation of user requirements, and where appro-

priate, prioritizing these requirements to the Project.

- Providing advice and recommendations to the Project regarding resources, schedules, processes, and other activities.
- Adjudication of conflicts between requirements (where possible), and between requirements and project resources.
- Checking and testing system interfaces to the community, and providing feedback and recommendations to the Project.
- Summarizing and explaining to the community the budget of, and resource distribution by, the Project.
- Coordinating user requirements and activities to provide greater efficiencies in the use of limited EOSDIS resources.
- Developing and implementing ways to better inform users of availability of EOS data and relevant information regarding those data.
- Checking actual instantiation and characteristics prior to announcing availability of individual data sets.
- Participating in discussions and planning for future Earth sciences data systems such as "SEEDS" (formerly "New DISS"), and the NPP data system.

The scope and focus of these activities has changed over the years as the ESDIS and EOS have evolved from being primarily concerned with flight operations and data processing, through archiving, to distribution to end-users. The earlier concerns are still there for new missions, but these missions benefit greatly from experience gained on previous missions.

Two specific examples of the above are the so-called 1-on-1s initiated by the Project Scientist and the web site for informing users about EOS data.

Several years before launch of Terra, we initiated a series of visits to the home laboratories of each of the Terra and Aqua PIs or Team Leaders. These visits included pertinent, decision-making members of the ESDIS Project, as well as the Project Scientist. The goal of these get-togethers was to fully explore and understand the needs, desires, and expectations of the instrument teams, and to help them understand the similar needs, schedules, etc., of the project. These one-on-ones were in addition to larger working group meetings involving many instrument teams and the project, where more generic discussions ensued.

Sensing a need for a mechanism to provide users and potential users of data from Earth Science Enterprise missions with information on validation status, location, expected dates of availability, and access to those data, we developed a web site to do just that. The site home page at eosdatainfo.gsfc.nasa.gov is the EOS "hanging chart" that includes all Earth science missions; clicking on a mis-

sion box brings up information relating to that mission, its instruments, and its data products; e.g., Terra,

eosdatainfo.gsfc.nasa.gov/eosdata/terra/platform.html

The data product site matrix for each instrument, e.g., MISR,

eosdatainfo.gsfc.nasa.gov/eosdata/ssinc/misr_dataprod.shtml?

lists and relates the various names by which the data products have been identified, including *Product IDs*, Earth Science Data Types (*ESDTs*), and Algorithm Theoretical Basis Documents (*ATBDs*). It provides direct links to specific data product search-and-order interfaces provided by the EOS Data Gateway (EDG) system and the Distributed Active Archive Centers (DAACs); links are also provided to pages for instruments, DAAC User Services, and missions. One can also access general information about platforms, payloads, Principal Investigators, and Project Scientists. The site is not intended to be an additional interface for ordering data, but rather a guide for users to existing search-and-order systems that provide appropriate methods (e.g., geographical, time selection, subsetting, etc.) for data ordering. Over the past several months we've been averaging about 50,000 "requests" a month. (A user going to the home page, then to three subsequent pages, would count as four requests.) An article describing the site was published recently in *The Earth Observer*.

*i. ESSP* (M. L. Imhoff)

Dr. Marc Imhoff was appointed as Earth System Science Project Scientist by Dr. Mary Cleave and Dr. Ghassem Asrar in June 2000 for the purpose of helping to coordinate and manage the selection of the 3rd set of ESSP Missions. In this capacity, Dr. Imhoff helped in the restructuring of the ESSP3 Program to accommodate new procedures for mitigating risk. A two-step evaluation plan was developed in place of the previous single-phase selection process and additional funds were made available to selected ESSP Missions to better support the launch phase. Dr. Imhoff helped write the new Announcement of Opportunity and worked with the Earth Explorers Program Office (Code 470) to identify launch options for ESSP that would alleviate difficulties previously experienced by ESSP PIs. The new plan was implemented in the ESSP3 AO released in September 2000. Dr. Imhoff subsequently served as the executive secretary of the Science Review Panels for both Phase I and Phase II of the new process. Eighteen proposals were reviewed in Phase I, and the results were presented to the Associate Administrator of Earth Science in September 2001. As a result of Phase I, six missions were selected to submit more detailed proposals. The Phase II review panel was convened in April 2002, site visits to contending laboratories were made in May and June, and presentations on the final evaluation were made to the Headquarters executive panel and the Associate Administrator in late June. The selection announcements were made on July 9, 2002 listing the Orbiting Carbon Observatory (OCO) and the Aquarius missions as primary missions, and the HYDROS mission as a backup. Each of these missions was funded

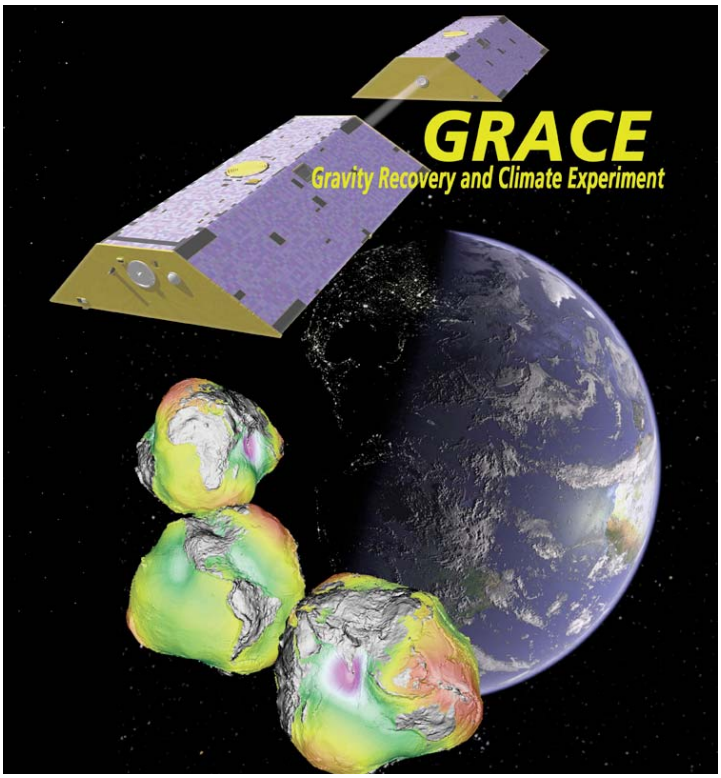


Figure 62. Front cover of GRACE Brochure, NP-2002-2-427-GSFC.

to develop plans sufficient for a risk mitigation evaluation conducted in July 2003. Final selections are pending.

Dr. Imhoff also worked with the EOS Senior Project Scientist, Dr. Michael King, to determine how the EOS Project Science Office and the ESSP Project Scientist might better serve NASA Headquarters with respect to the ESSP Program. Dr. King funded a fulltime staff person (Mr. Alan Ward) to help the ESSP Project Scientist develop a suite of information materials for ESSP that could be used by NASA Headquarters Code Y, NASA Public Affairs, and the EOS Project Science Office. Of primary concern was the fact that there had been no previous plan to produce pre-launch information materials for the ESSP's first mission – The Gravity Recovery and Climate Experiment (GRACE). As a result of this proactive approach, a brochure and a full set of information materials for the GRACE Mission were successfully produced in time for launch. The GRACE Mission brochure (Figure 62) was well received by the Associate Administrator of Earth Science, the GRACE PI, and the GRACE Science team, and has proven very popular nationally and internationally. Also as part of this effort, a fact sheet was developed for the A-Train featuring the ESSP Missions CloudSat and CALIPSO and an article about GRACE and continental water storage was produced. Mission brochures for CloudSat and CALIPSO, scheduled for launch in 2005, are under development.

## 7. References


Ackerman, A. S., O. B. Toon, D. E. Stevens, A. J. Heymsfield, V. Ramanathan, and E. J. Welton, 2000: Reduction of tropical cloudiness by soot, *Science*, **288**, 1042–1047.

Afzal, R. S., J. L. Dallas, A. Lukemire, W.A. Mamakos, A. Melak, L. Ramos-Izquierdo, B. Schröder, and A. W. Yu, 2002: Space qualification of the Geoscience Laser Altimeter System (GLAS) laser transmitters. *Conf. on Lasers and Electro-Optics*, OSA Technical Digest, Opt. Soc. Amer., Washington, DC.

Barnes, P. Y., E. A. Early, B. C. Johnson, J. J. Butler, C. J. Bruegge, S. Biggar, P. R. Spyak, and M. Pavlov, 1998: Intercomparison of reflectance measurements. *Proc. SPIE*, **3425**, 10.

Barnes, W., X. Xiong, and V. Salomonson, 2002: Status of Terra MODIS and Aqua MODIS. *Proc. IGARSS* 2002.

Bounoua, L., G. J. Collatz, P. J. Sellers, D. A. Randall, D. A. Dazlich, S. O. Los, J. A. Berry, I. Fung, C. J. Tucker, C. B. Field, and T. G. Jensen, 1999: Interactions between vegetation and climate: Radiative and physiological effects of doubled atmospheric $CO_2$. *J. Climate*, **12**, 309–324.

Bounoua, L., G. J. Collatz, S. O. Los, P. J. Sellers, D. A. Dazlich, C. J. Tucker, and D. A. Randall, 2000: Sensitivity of climate to changes in NDVI. *J. Climate*, **13**, 2277–2292.

Butler, J. J., H. Park, P. Y. Barnes, E. A. Early, C. van Eijk-Olij, A. E. Zoutman, S. van Buller-Leeuwen, and J. G. Schaarsberg, 2002: Comparison of ultraviolet bidirectional reflectance distribution function (BRDF) measurements of diffusers used in the calibration of the Total Ozone Mapping Spectrometer (TOMS). *Proc. SPIE*, **4881**, 345.

Campbell, J. R., D. L. Hlavka, E. J. Welton, C. J. Flynn, D. D. Turner, J. D. Spinhirne, V. S. Scott, and I. H. Hwang, 2002: Full-time, eye-safe cloud and aerosol lidar observation at Atmospheric Radiation Measurement program sites: Instrument and data processing. *J. Atmos. Oceanic Technol.*, **19**, 431–442.

Campbell, J. R., E. J. Welton, J. D. Spinhirne, Q. Ji, S. C. Tsay, S. J. Piketh, M. Barenbrug, and B. N. Holben, 2003: Micropulse lidar observations of tropospheric aerosols over northeastern South Africa during the ARREX and SAFARI-2000 dry season experiments. *J. Geophys. Res.*, 108, 8497, doi:10.1029/2002JD002563.

Carabajal, C. C., D. J. Harding, and J. L. Bufton, 2003: ICESat geolocation and land products validation: Laser altimetry profile and waveform matching. *Geophys. Res. Abs*, **5**, 07791, European Geophys. Soc.

Cavalieri, D. J., 2000: EOS Aqua Sea Ice Validation Program: Meltpond2000, NASA Technical Memorandum 2000-209972, National Aeronautics and Space Administration, Goddard Space Flight Center, Greenbelt, MD 20771, 31 pp., December 2000.

Cavalieri, D. J., 2002: A link between Fram Strait sea ice export and atmospheric planetary wave phase. *Geophys. Res. Lett.*, **20**, doi:10.1029/2002GL014684.

Cavalieri, D. J., C. L. Parkinson, and K. Y. Vinnikov, 2003: 30-year satellite record reveals contrasting Arctic and Antarctic decadal sea ice variability. *Geophys. Res. Lett.*, in press.

Caylor, K. K., P. R. Dowty, H. H. Shugart, and S. Ringrose, 2003: Vertical patterns of vegetation structure along the Kalahari: The importance of spatial heterogeneity in modeling system productivity. *Global Ch. Biol.*, in press.

Chang, A. T. C., J. L. Foster and D. K. Hall, 1987: Nimbus-7 SMMR derived global snow cover parameters. *Annals of Glaciology*, **9**, 39–44.

Chu. D. A., Y. J. Kaufman, C. Ichoku, L. A. Remer, D. Tanré and B. N. Holben, 2002: Validation of MODIS aerosol optical depth retrieval over land. *Geophys. Res. Lett.*, **29**, doi:10.1029/2001GL013205.

Colarco, P. R., O. B. Toon, J. S. Reid, J. M. Livingston, P. B. Russell, J. Redemann, B. Schmid, H. B. Maring, D. Savoie, E. J. Welton, J. R. Campbell, B. N. Holben, and R. Levy, 2002: Saharan dust transport to the Caribbean during PRIDE: Part 2. Transport, vertical profiles, and deposition in simulations of in situ and remote sensing observations. *J. Geophys. Res.*, in press.

Collatz, G. J., J. A. Berry, and J. S. Clark, 1998: Effects of climate and atmospheric $CO_2$ partial pressure on the global distribution of C-4 grasses: Present, past, and future. *Oecologia*, **114**, 441–454.

Collatz, G. J., M. Ribas carbo, and J. A. Berry, 1992: Coupled photosynthesis-stomatal conductance model for leaves of C4 plants. *Austral. J. Plant Physiol.*, **19**, 519–538.

Collatz, G. J., L. Bounoua, S. O. Los, D. A. Randall, I. Y. Fung, P. J. Sellers, 2000: A mechanism for the influence of vegetation on the response of the diurnal temperature range to changing climate. *Geophys. Res. Lett.*, **27**, 3381–3384.

Collins, W. D., P. J. Rasch, E. J. Welton, T. Beck, and J. D. Spinhirne, 2000: Assimilation of space-based aerosol lidar measurements for studying African dust: Methodology. *EOS Trans. Amer. Geophys. Union*, **81**, 70.

Comiso, J. C., 2000: Variability and trends in Antarctic surface temperatures from in situ and satellite infrared measurements. *J. Climate*, **13**, 1674–1696.

Comiso, J. C., D. J. Cavalieri, and T. Markus, 2003: Sea ice concentration, ice temperature, and snow depth using AMSR-E Data. *IEEE Trans. Geosci. Remote Sensing*, **41**, 243–252.

Cox, C. M. and B. F. Chao, 2002: Detection of a large-scale mass redistribution in the terrestrial system since 1998. *Science*, **297**, 831–833.

DeFries, R. S., and J. R. G. Townshend, 1994: NDVI-derived land cover classifications at a global scale. *Int. J. Remote Sens.*, **15**, 3567–3586.

DeFries, R. S., C. B. Field, I. Fung, G. J. Collatz, and L. Bounoua, 1999: Combined satellite data and biogeochemical models to estimate global effects of human-induced land cover change on carbon emissions and primary productivity. *Global Biogeochem. Cycles*, **13**, 803–815.

Denning, A. S., I. Y. Fung, and D. Randall, 1995: Latitudinal gradient of atmospheric $CO_2$ due to seasonal exchange with land biota. *Nature*, **376**, 240–243.

Denning, A. S., G. J. Collatz, C. G. Zhang, D. A. Randall, J. A. Berry, P. J. Sellers, G. D. Colello, and D. A. Dazlich, 1996: Simulations of terrestrial carbon metabolism and atmospheric $CO_2$ in a general circulation model .1. Surface carbon fluxes. *Tellus Series B-Chem. Phys. Meteor.*, **48**, 521–542.

Diner, D. J., W. A. Abdou, C. J. Bruegge, J. E. Conel, K. A. Crean, B. J. Gaitley, M. C. Helmlinger, R. A. Kahn, J. V. Martonchik, S. H. Pilorz and B. N. Holben,

2001: MISR aerosol retrievals over southern Africa during the SAFARI-2000 dry season campaign.. *Geophys. Res. Lett.*, **28**, 3127–3130.

Douglass, A. R., M. R. Schoeberl, R. B. Rood, and S. Pawson, 2003: Evaluation of transport in the lower tropical stratosphere in a global chemistry and transport model. *J. Geophys. Res.*, **108**, 4259, doi:10.1029/2002JD002696.

Dubovik, O., and M. D. King, 2000: A flexible inversion algorithm for retrieval of aerosol optical properties from sun and sky radiance measurements. *J. Geophys. Res.*, **105**, 20673–20696.

Dubovik, O., B. N. Holben, T. F. Eck, A. Smirnov, Y. J. Kaufman, M. D. King, D. Tanré and I. Slutsker, 2002: Variability of absorption and optical properties of key aerosol types observed in worldwide locations. *J. Atmos. Sci.*, **59**, 590–608.

Early, E. A., P.,Y. Barnes, B.,C. Johnson, J.,J. Butler, C.,J. Bruegge, S.,F. Biggar, P.,R. Spyak, and M.,M. Pavlov, 2000: Bidirectional reflectance round-robin in support of the Earth Observing System program. *J. Atmos. Oceanic Technol.*, **17**, 1077.

Field, C. B., J. T. Randerson, and C. M. Malmstrom, 1995: Global net primary production—Combining ecology and remote sensing. *Remote Sens. Environ.*, **51**, 74–88.

Fung, I., C. B. Field, J. A. Berry, M. V. Thompson, J. T. Randerson, C. M. Malmstrom, P. M. Vitousek, G. J. Collatz, P. J. Sellers, D. A. Randall, A. S. Denning, F. Badeck, and J. John, 1997: Carbon 13 exchanges between the atmosphere and biosphere. *Global Biogeochem. Cycles*, **11**, 507–533.

Guillevic, P., R. D. Koster, M. J. Suarez, G. J. Collatz, L. Bounoua, and S. O. Los, 2002: Influence of vegetation interannual variability on hydrological processes over land surfaces. *J. Hydrometeor.*, **3**, 617–629.

Gloersen, P., and W. B. White, 2001: Reestablishing the circumpolar wave in sea ice around Antarctica from one winter to the next. *J. Geophys. Res.*, **106**, 4391–4395.

Häkkinen, S., 1999: A simulation of thermohaline effects of a great salinity anomaly. *J. Climate*, **12**, 1781–1795.

Häkkinen, S., 2002: Surface salinity variability in the northern North Atlantic during recent decades. *J. Geophys. Res.*, **107**, 8003, doi:10.1029/2001JC000812.

Hall, D. K., G. A. Riggs, V. V. Salomonson, N. E. DiGirolamo and K. J. Bayr, 2002a: MODIS snow-cover products. *Remote Sens. Environ.*, **83**, 181–194.

Hall, D. K., R. E. J. Kelly, G. A. Riggs, A. T. C. Chang and J. L. Foster, 2002b: Assessment of the relative accuracy of hemispheric scale snow-cover maps. *Annals of Glaciology*, **34**, 24–30.

Hall, D.K., J. R. Key, K. A. Casey, G. A. Riggs, and D. J. Cavalieri, 2004: Moderate Resolution Imaging Spectroradiometer (MODIS) sea ice surface temperature product. Submitted to *IEEE Trans. Geosci. Remote Sensing.*

Hansen, J., R. Ruedy, M. Sato, M. Imhoff, W. Lawrence, D. Easterling, T. Peterson, and T. Karl, 2001: A closer look at United States and global surface temperature change. *J. Geophys. Res.*, **106**, 23,947–23,963.

Harding, D. J., M. A. Lefsky, G. G. Parker, and J. B. Blair, 2001: Laser altimeter canopy height profiles methods and validation for closed-canopies, broadleaf forests. *Remote Sens. Environ.*, **76**, 283–297.

Hoge, F. E., P. E. Lyon, R. N. Swift, J. K. Yungel, M. R. Abbott, R. M. Letelier, and W. E. Esaias, 2000: Validation of Terra-MODIS phytoplankton chlorophyll fluorescence line height. I. Initial airborne lidar results. *Appl. Opt.,* **42,** 2767–2771.

Holben, B. N., T. F. Eck, I. Slutsker, D. Tanré, J. P. Buis, A. Setzer, E. Vermote, J. A. Reagan, Y. J. Kaufman, T. Nakajima, F. Lavenu, I. Jankowiak and A. Smirnov, 1998: AERONET—A federated instrument network and data archive for aerosol characterization. *Remote Sens. Environ*., **66**, 1–16.

Holben B. N., D. Tanré, A. Smirnov, T. F. Eck, I. Slutsker, N. Abuhassan, W. W. Newcomb, J. S. Schafer, B. Chatenet, F. Lavenu, Y. J. Kaufman, J. V. Castle, A. Setzer, B. Markham, D. Clark, R. Frouin, R. Halthore, A. Karneli, N. T. O'Neill, C. Pietras, R. T. Pinker, K. Voss, and G. Zibordi, 2001: An emerging ground-based aerosol climatology: Aerosol optical depth from AERONET. *J. Geophys. Res.*, **106**, 12067–12097.

Imhoff, M. L., C. J. Tucker, W. T. Lawrence, and D. C. Stutzer, 2000: The use of multisource satellite and geospatial data to study the effect of urbanization on primary productivity in the United States. *IEEE Trans. Geosci. Remote Sens.,* **38,** 2549–2556.

Imhoff, M. L., L. Bounoua, R. DeFries, W. T. Lawrence, D. Stutzer, C. J. Tucker and T. Ricketts, 2003: The consequences of urban land transformation for net primary productivity in the United States. *Remote Sens. Environ.,* in press.

Justice C. O., L. Giglio, S. Korontzi, J. Owens, J. T. Morisette, D. Roy, J. Descloitres, S. Alleaume, F. Petitcolin, and Y. Kaufman, 2002: The MODIS fire products. *Remote Sens. Environ***., 83**, 244–262.

Kaufman, Y. J., B. N. Holben, D. Tanré, I. Slutsker, T. Eck, and A. Smirnov, 2000: Will aerosol measurements from Terra and Aqua polar orbiting satellites represent the daily aerosol abundance and properties? *Geophys. Res. Lett*., 27, 3861–3864.

Kaufman Y. J., C. Ichoku, L. Giglio, S. Korontzi, D. A. Chu, W. M. Hao, R. R. Li, and C. O. Justice, 2003: Fires and smoke observed from the Earth Observing System MODIS instrument – products, validation, and operational use. *Inter. J. Remote Sens*., **24**, 1765–1781.

Kaufman, Y. J., A. Smirnov, B. N. Holben, and O. Dubovik, 2001: Baseline maritime aerosol: Methodology to derive the optical thickness and scattering properties. *Geophys. Res. Lett*., **28**, 3251–3254.

Kaufman, Y. J., D. Tanré and O. Boucher, 2002: A satellite view of aerosols in the climate system. *Nature*, **419**, 215–223.

Kelly, R. E. J., and A. T. C. Chang, 2003: Development of a passive microwave global snow depth retrieval algorithm for SSM/I and AMSR-E data. *Radio Science,* **38**, doi: 10.1029/2002RS002648.

Kelly, R. E. J., A. T. C. Chang, L. Tsang, and J. L. Foster, 2003: A prototype AMSR-E global snow area and snow depth algorithm. *IEEE Trans. Geosci. Remote Sens.,* **41**, 230–242.

Key, J., and M. Haefliger, 1992: Arctic ice surface temperature retrieval from AVHRR thermal channels. *J. Geophys. Res.*, **97**, 5885–5893.

King, M. D., W. P. Menzel, Y. J. Kaufman, D. Tanré, B. C. Gao, S. Platnick, S. A. Ackerman, L. A. Remer, R. Pincus, and P. A. Hubanks, 2003a: Cloud and

aerosol properties, precipitable water, and profiles of temperature and humidity from MODIS. *IEEE Trans. Geosci. Remote Sens.*, **41**, 442–458.

King, M. D., S. Platnick, C. C. Moeller, H. E. Revercomb and D. A. Chu, 2003b: Remote sensing of smoke, land and clouds from the NASA ER-2 during SAFARI 2000. *J. Geophys. Res.*, **108**, 8502, doi:10.1029/2002JD003207.

Klein, A. G. and A. C. Barnett, 2003: Validation of daily MODIS snow cover maps of the Upper Rio Grande River Basin for the 2000-2001 snow year. *Remote Sens. Environ.*, in press.

Klein, A. G., and J. Stroeve, 2002: Development and validation of a snow albedo algorithm for the MODIS instrument. *Annals of Glaciology*, **34**, 45–52.

Korontzi, S., C. O. Justice, and R. Scholes R., 2003: Influence of timing and spatial extent of vegetation fires in southern Africa on atmospheric emissions. *J. Arid Environ.*, **54**, 395–404.

Koster, R. D., M. J. Suarez, and M. Heiser, 2000a: Variance and predictability of precipitation at seasonal-to-interannual timescales. *J. Hydrometeor.*, **1**, 26–46.

Koster, R. D., M. J. Suarez, A. Ducharne, M. Stieglitz, and P. Kumar, 2000b: A catchment-based approach to modeling land surface processes in a general circulation model, 1, Model structure. *J. Geophys. Res.*, **105**, 24,809–24,822.

Koster, R. D., and M. J. Suarez, 2001: Soil moisture memory in climate models. *J. Hydrometeor.*, **2**, 558–570.

Koster, R. D., and M. J. Suarez, 2003: Impact of land surface initialization on seasonal precipitation and temperature prediction. *J. Hydrometeor.*, **4**, 408–423.

Lait, L. R., et al., 2002: Ozone loss from quasi-conservative coordinate mapping during the 1999-2000 SOLVE/THESEO 2000 campaigns. *J. Geophys. Res.*, **107**, 8259, doi:10.1029/2001JD000998.

Lefsky, M. A., W. B. Cohen, D. J. Harding, G. G. Parker, S. A. Acker, and S. T. Gower, 2002: Lidar remote sensing of aboveground biomass in three biomes. *Global Ecology Biogeog.*, **1**, 393–399.

Liang, S., 2000: Narrow to broadband conversion of land surface albedo. I: Algorithms. *Remote Sens. Environ.*, **76**, 213–238.

Livingston, J. M., P. B. Russell, J. S. R eid, J. Redemann, B. Schmid, D. A. Allen, O. Torres, R. C. Levy, L. A. Remer, B. N. Holben, A. Smirnov, O. Dubovik, E. J. Welton, J. R. Campbell, J. Wang, and S. A. Christopher, 2003: Airborne sun photometer measurements of aerosol optical depth and columnar water vapor during the Puerto Rico Dust Experiment and comparison with land, aircraft, and satellite measurements. *J. Geophys. Res.*, 108, 8588, doi:10.1029/2002JD002520.

Los, S. O., C. O. Justice, and C. J. Tucker, 1994: A global 1-degrees-by-1-degrees NDVI data set for climate studies derived from the GIMMS continental NDVI data. *Inter. J. Remote Sens*, **15**, 3493–3518.

Los S. O., G. J. Collatz , P. J. Sellers, C. M. Malmstrom, H. H. Pollack, R. S. DeFries, L. Bounoua, M. T. Parris, and C. J. Tucker, 2000: A global 9-yr biophysical land surface data set from NOAA AVHRR data. *J. Hydrometeor.*, **1**, 183–199.

Los S. O., G. J. Collatz, L. Bounoua, P. J. Sellers, and C. J. Tucker, 2001: Global in-

terannual variations in sea surface temperature and land surface vegetation, air temperature and precipitation. *J. Climate*, **14**, 1535–1549.

Luthcke, S. B., C. C. Carabajal, D. D. Rowlands, and D.E. Pavlis, 2001: Improvements in spaceborne laser altimeter data geolocation. *Surv. Geophys.,* **22**, 549–559.

Luthcke, S. B., C. C. Carabajal, and D. D. Rowlands, 2002: Enhanced geolocation of spaceborne laser altimeter surface returns: parameter calibration from the simultaneous reduction of altimeter range and navigation tracking data. *J. Geodyn.,* **34**, 447–475.

Luthcke, S. B., D. D. Rowlands, D. J. Harding, J. L. Bufton, C. C. Carabajal, and T. A. Williams, 2003, ICESat laser altimeter surface return geolocation parameter calibration and validation from integrated residual analysis. *Geophys. Res. Abs.,* **5**, 13222, European Geophys. Soc.

Markowicz, K. M., P. J. Flatau, A. M. Vogelmann, P. K. Quinn, and E. J. Welton, 2003: Infrared aerosol radiative forcing at the surface and the top of the atmosphere. *Quart. J. Royal Meteor. Soc*., in press.

Markus, T. and D. J. Cavalieri, 1998: Snow depth distribution over sea ice in the Southern Ocean from satellite passive microwave data. *Antarctic Sea Ice: Physical Processes, Interactions and Variability*, Antarctic Research Series, vol. 74, pp. 19-39, American Geophysical Union, Washington, DC.

Markus, T. and D. J. Cavalieri, 2000: An enhancement of the NASA Team sea ice algorithm. *IEEE Trans. Geosci. Remote Sensing*, **38**, 1387–1398.

Maurer, E. P., J. D. Rhoads, R. O. Dubayah and D. P. Lettenmaier, 2003: Evaluation of the snow-covered area data product from MODIS. *Hydrological Processes,* **17**, 59–71.

McGill, M. J., D. L. Hlavka, W. D. Hart, E. J. Welton, and J. R. Campbell, 2003: Airborne lidar measurements of aerosol optical properties during SAFARI-2000. *J. Geophys. Res*., 108, 8493, doi:10.1029/2002JD002370.

Millar, P. S., J. M. Sirota, C. T. Field, and D. K. Mostofi, 2003: Laser pointing angle measurement system for the Geoscience Laser Altimeter. *Tech. Digest CLEO*.

Mitchell, D., J. Sauber, D. Harding, C. Carabajal, W. Krabill, S. Manizade, and J. Bufton, 2003, Expected ICESat measurement of glacier elevation change. *Geophys. Res. Abs*, **5**, 04398, European Geophys. Soc.

Myneni, R. B., S. O. Los, and C. J. Tucker, 1996: Satellite-based identification of linked vegetation index and sea surface temperature anomaly areas from 1982-1990 for Africa, Australia and South America. *Geophys. Res. Lett.*, **23**, 729–732.

Myneni, R. B., C. D. Keeling, C. J. Tucker, G. Asrar, and R. R. Nemani, 1997: Increased plant growth in the northern high latitudes from 1981 to 1991. *Nature*, **386**, 698-702.

Newman, P. A., et al., 2002: An overview of the SOLVE/THESEO 2000 campaign. *J. Geophys. Res*., **107**, 8259, doi:10.1029/2001JD001303.

Nicholson, S. E., C. J. Tucker, and M. B. Ba, 1998: Desertification, drought, and surface vegetation: An example from the West African Sahel. *Bull. Amer. Meteor. Soc.*, **79**, 815–829.

Olsen, M. A., A. R. Douglass, and M. R. Schoeberl, 2002: Estimating downward

cross-tropopause ozone flux using column ozone and potential vorticity. *J. Geophys. Res.*, **107**, 4636, doi:10.1029/2001JD002041.

Parkinson, C. L., 2000: Recent trend reversals in Arctic sea ice extents: Possible connections to the North Atlantic Oscillation. *Polar Geography*, **24**, 1–12.

Parkinson, C. L., and D. J. Cavalieri, 2002: A 21 year record of Arctic sea-ice extents and their regional, seasonal and monthly variability and trends. *Ann. Glaciology*, **34**, 441–446.

Parkinson, C. L., D. J. Cavalieri, P. Gloersen, H. J. Zwally, and J. C. Comiso, 1999: Arctic sea ice extents, areas, and trends, 1978-1996. *J. Geophys. Res.*, **104**, 20,837–20,856.

Parkinson, C. L., D. Rind, R. J. Healy, and D. G. Martinson, 2001: The impact of sea ice concentration accuracies on climate model simulations with the GISS GCM. *J. Climate*, **14**, 2606–2623.

Petitcolin, F. and E. Vermote, 2002: Land surface reflectance, emisivity and temperature from MODIS middle and thermal infrared data. *Remote Sens. Environ.*, **83**,112–134.

Platnick, S., M. D. King, S. A. Ackerman, W. P. Menzel, B. A. Baum, J. C. Riédi, and R. A. Frey, 2003: The MODIS cloud products: Algorithms and examples from Terra. *IEEE Trans. Geosci. Remote Sens.*, **41**, 459–473.

Potter, C. S., J. T. Randerson, C. B. Field, P. A. Matson, P. M. Vitousek, H. A. Mooney, and S. A. Klooster, 1993: Terrestrial ecosystem production—A process model based on global satellite and surface data. *Global Biogeochem. Cycles*, **7**, 811–841.

Privette, J. L., R. B. Myneni, Y. Knyazikhin, M. Mukelabai, Y. Tian, Y. Wang, G. Roberts, and S. Leblanc, 2002: Early spatial and temporal validation of MODIS LAI in the southern Africa Kalahari. *Remote Sens. Environ.*, **83**, 232–243.

Privette, J. L., Y. Tian, G. Roberts, R. J. Scholes, Y. Wang, K. Caylor, and M. Mukelabai, 2003: Structural characterization and relationships in Kalahari woodlands and savannas. *Global Ch. Biol.*, in press.

Proctor, J. E., and P. Y. Barnes, 1996: NIST high accuracy reference-reflectometer-spectrophotometer. *J. Res. Nat. Inst. Stand. Technol.*, **101**, 619.

Randerson, J. T., C. B. Field, I. Y. Fung, and P. P. Tans, 1999: Increases in early season ecosystem uptake explain recent changes in the seasonal cycle of atmospheric $CO_2$ at high northern latitudes. *Geophys. Res. Lett.*, **26**, 2765–2768.

Randall, D. A., D. A. Dazlich, C. Zhang, A. S. Denning, P. J. Sellers, C. J. Tucker, L. Bounoua, S. O. Los, C. O. Justice, and I. Fung, 1996: A revised land surface parameterization (SiB2) For GCMs. 3. The greening of the Colorado State University General Circulation Model. *J. Climate*, **9**, 738–763.

Remer, L. A., D. Tanré, Y. J. Kaufman, C. Ichoku, S. Mattoo, R. Levy, D. A. Chu, B. N. Holben, O. Dubovik, A. Smirnov, J. V. Martins, R. R. Li and Z. Ahmad, 2002: Validation of MODIS aerosol retrieval over ocean. *Geophys. Res. Lett.*, **29**, doi:10.1029/2001GL013204.

Reichle, R. H., J. P. Walker, R. D. Koster, and P. R. Houser. 2002: Extended versus ensemble Kalman filtering for land data assimilation. *J. Hydrometeor.*, **3**, 728–740.

Reid, J. S., J. E. Kinney, D. L. Westphal, B. N. Holben, E. J. Welton, Si-Chee Tsay, D. P. Eleuterio, J. R. Campbell, S. A. Christopher, P. R. Colarco, H. H. Jonsson, J. M. Livingston, H. B. Maring, M. L. Meier, P. Pilewskie, J. M. Prospero, E. A. Reid, L. A. Remer, P. B. Russell, D. L. Savoie, A. Smirnov, and D. Tanre´, 2003: Analysis of measurements of Saharan dust by airborne and ground-based remote sensing methods during the Puerto Rico Dust Experiment (PRIDE). *J. Geophys. Res.*, in press.

Ricketts, T., and M. Imhoff, 2003: Biodiversity, urbanization, and agriculture: locating priority ecoregions for conservation, *Conserv. Ecol.*, in press.

Riggs, G. A., D. K. Hall, and S. A. Ackerman, 1999: Sea ice extent and classification mapping with the Moderate Resolution Imaging Spectroradiometer Airborne Simulator. *Remote Sens. Environ.*, **68**, 152–163.

Rind, D., R. Healy, C. Parkinson, and D. Martinson, 1995: The role of sea ice in 2 x $CO_2$ climate model sensitivity. Part I: The total influence of sea ice thickness and extent. *J. Climate*, **8**, 449–463.

Riris, H., P. Liiva, J. Schafer, J. Nissley, J. Hirs, X. Sun, and J. B. Abshire, 2003: A system to characterize the Geoscience Laser Altimeter System (GLAS). *Tech. Digest CLEO*.

Rojstaczer, S., S. M. Sterling, and N. J. Moore, 2001: Human appropriation of photosynthesis products. *Science*, **294,** 2549–2552.

Rowlands, D. D., C. C. Carabajal, S. B. Luthcke, D. J. Harding, J. M. Sauber, and J. L. Bufton, 2000: Satellite laser altimetry: On-orbit calibration techniques for precise geolocation. *Rev. Laser Engin.*, **28**, 796–803.

Roy D. P., P. E. Lewis, and C. O. Justice, 2002: Burned area mapping using multitemporal moderate spatial resolution data – a bi-directional reflectance model-based expectation approach. *Remote Sens. Environ.*, **83**, 263–286.

Salomonson, V. V., and I. Appel, 2003: Estimating the fractional snow covering using the normalized difference snow index. Submitted to *Remote Sens. Environ.*

Salomonson, V., W. Barnes, X. Xiong, S. Kempler, and E. Masuoka, 2002: An overview of the Earth Observing System MODIS instrument and associated data systems performance. *Proc. IGARSS* 2002.

Sauber, J., G. Plafker, B. Molnia, and M. Bryant, 2000: Crustal deformation associated with glacial fluctuations in the eastern Chugach mountains, Alaska. *J. Geophys. Res.*, **105**, 8055–8077.

Scanlon, T. M., and J. D. Albertson, 2003: Inferred controls on tree/grass composition in a savanna ecosystem: Combining 16-Year NDVI data with a dynamic soil moisture model. *Water Resources Res.*, in press.

Scanlon, T. M., J. D. Albertson, K. K. Caylor and C. Williams, 2002: Determining land surface fractional cover from NDVI and rainfall time series for a savanna ecosystem. *Remote Sens. Environ.*, **82**, 376–388.

Schiff, T. F., M. W. Knighton, D. J. Wilson, F. M. Cady, J.C. Stover, and J. J. Butler, 1993: Design review of a high accuracy UV to near IR scatterometer. *Proc. SPIE*, **1995**, 121.

Schmid, B., J. Redemann, P. B. Russell, P. V. Hobbs, D. L. Hlavka, M. J. McGill, B. N. Holben, E. J. Welton, J. Campbell, O. Torres, R. A. Kahn, D. J. Diner, M. C. Helmlinger, D. A. Chu, C. Robles Gonzalez, and G. de Leeuw, 2003a: Coor-

dinated airborne, spaceborne, and ground-based measurements of massive, thick, aerosol layers during the dry season in Southern Africa. *J. Geophys. Res.*, 108, 8496, doi:10.1029/2002JD002297.

Schmid, B., D. A. Hegg, J. Wang, D. Bates, J. Redemann, P. B. Russell, J. M. Livingston, H. H. Jonsson, E. J. Welton, J. H. Seinfeld, R. C. Flagan, D. S. Covert, O. Dubovik, and A. Jefferson, 2003b: Column closure studies of lower tropospheric aerosol and water vapor during ACE-Asia using airborne sunphotometer, airborne in-situ and ship-based lidar measurements. *J. Geophys. Res.*, in press.

Schoeberl, M. R., A. R. Douglass, Z. Zhu, and S. Pawson, 2003: A comparison of the lower stratospheric age spectra derived from a general circulation model and two data assimilation systems. *J. Geophys. Res.*, **108**, 4113, doi:10.1029/2002JD002652.

Schoeberl, M. R. et al., 2002: An Assessment of the ozone loss during the 1999-2000 SOLVE/THESEO 2000 arctic campaign. *J. Geophys. Res.*, **107**, 8259, doi:10.1029/2001JD000412.

Scholes, R. J., P. R. Dowty, K. Caylor, D. A. B. Parsons, P. G. H. Frost and H. H. Shugart, 2002: Trends in savanna structure and composition on an aridity gradient in the Kalahari. *J. Veg. Sci.*, **13**, 419–428.

Sellers, P. J., C. J. Tucker, G. J. Collatz, S. O. Los, C. O. Justice, D.A. Dazlich, and D. A. Randall, 1994: A global 1-degrees-by-1-degrees NDVI data set for climate studies. 2. The generation of global fields of terrestrial biophysical parameters from the NDVI. *Int. J. Remote Sens.*, **15**, 3519–3545.

Sellers, P. J., L. Bounoua, G. J . Collatz, D. A. Randall, D. A. Dazlich, S. O. Los, J. A. Berry, I. Fung, C. J. Tucker, C. B. Field, and T. G. Jensen, 1996a: Comparison of radiative and physiological effects of doubled atmospheric $CO_2$ on climate. *Science*, **271**, 1402–1406.

Sellers, P. J., D. A. Randall, G. J. Collatz, J. A. Berry, C. B. Field, D. A. Dazlich, C. Zhang, G. D. Collelo, and L. Bounoua, 1996b: A revised land surface parameterization (SiB2) for atmospheric GCMs. 1. Model formulation. *J. Climate*, **9**, 676–705.

Sellers, P. J., S. O. Los, C. J. Tucker, C. O. Justice, D. A. Dazlich, G. J. Collatz, and D. A. Randall, 1996c: A revised land surface parameterization (SiB2) for atmospheric GCMs. 2. The generation of global fields of terrestrial biophysical parameters from satellite data. *J. Climate*, **9**, 706–737.

Sellers, P. J., B. W. Meeson, J. Closs, J. Collatz, F. Corprew, D. Dazlich, F. G. Hall, Y. Kerr, R. Koster, S. Los, K. Mitchell, J. McManus, D. Myers, K. J. Sun, and P. Try, 1996d: The ISLSCP initiative I global datasets—Surface boundary conditions and atmospheric forcings for land-atmosphere studies. *Bull. Amer. Meteor. Soc.*, **77**, 1987–2005.

Sellers, P. J., R. E. Dickinson, D. A. Randall, A. K. Betts, F. G. Hall, J. A. Berry, G. J. Collatz, A. S. Denning, H. A. Mooney, C. A. Nobre, N. Sato, C. B. Field, and A. Henderson-Sellers, 1997: Modeling the exchanges of energy, water, and carbon between continents and the atmosphere. *Science*, **275**, 502–509.

Smirnov, A., B. N. Holben, T. F. Eck, O. Dubovik and I. Slutsker, 2000: Cloud screening and quality control algorithms for the AERONET database. *Remote Sens. Environ.*, **73**, 337–349.

Spinhirne, J. D., and S. P. Palm, 1996: Space based atmospheric measurements by GLAS. *Advances in Atmospheric Remote Sensing with Lidar*, A. Ansmann, Ed., Springer, Berlin, 213–217.

Van der Werf, G. R., J. T. Randerson, G. J. Collatz, and L. Giglio, 2003: Carbon emissions from fires in tropical and subtropical ecosystems. *Global Ch. Biol*, **9**, 547–562.

Vermote, E. F., and D. P. Roy, 2002a: Land surface hot-spot observed by MODIS over central Africa. *Int. J. Remote Sens.*, **23**, 2141–2143.

Vermote E. F., N. Z. El Saleous, and C. O. Justice, 2002b: Atmospheric correction of MODIS data in the visible to middle infrared: First results. *Remote Sens. Environ.*, **83**, 97–111.

Vitousek, P. M., P. R. Ehrlich, A. H. Ehrlich, and P. A. Matson, 1986: Human appropriation of the products of photosynthesis. *BioScience* **36**, 368–373.

Welton, E. J., and J. R. Campbell, 2002: Micro-pulse lidar signals: Uncertainty analysis. *J. Atmos. Oceanic Technol.*, **19**, 2089–2094.

Welton, E. J., J. R. Campbell, J. D. Spinhirne, and V. S. Scott, 2001: Global monitoring of clouds and aerosols using a network of micro-pulse lidar systems. *Proc. SPIE*, **4153**, 151–158.

Welton, E. J., K. J. Voss, P. K. Quinn, J. R. Campbell, J. D. Spinhirne, H. R. Gordon, and J. E. Johnson, 2002: Measurements of aerosol vertical profiles and optical properties during INDOEX 1999 using micro-pulse lidars. *J. Geophys. Res.*, **107**, 8019, doi:10.1029/2000JD000038.

Wilheit, T., C. D. Kummerow, and R. Ferraro, 2003: Rainfall algorithms for AMSR-E. *IEEE Tans. Geosci. Remote Sens.*, **41**, 204–214.

Xiong, X., N. Che, F. Adimi, and W. Barnes, 2002a: On-orbit Spatial Characterizations for Terra MODIS. *Proc. SPIE* **4814**, 347-357.

Xiong, X., K. Chiang, B. Guenther, and W. Barnes, 2002b: MODIS Thermal Emissive Bands Calibration Algorithm and On-orbit Performance. *Proc. SPIE*, **4891**, 392-401.

Xiong, X., K. Chiang, J. Esposito, B. Guenther, and W. Barnes, 2003: MODIS on-orbit calibration and characterization. *Metrologia,* **40**, 89–92.

Xiong, X., J. Sun, J. Esposito, B. Guenther, and W. Barnes, 2002c: MODIS Reflective Solar Bands Calibration Algorithm and On-orbit Performance. *Proc. SPIE*, **4891**, 95-104

Zhao, Y. and A. K. Liu, 2001: Principal-component analysis of sea-ice motion from satellite data. *Ann. Glaciology*, **33**, 133–138.

Zwally, H. J., J. C. Comiso, C. L. Parkinson, D. J. Cavalieri, and P. Gloersen, 2002: Variability of Antarctic sea ice 1979-1998. *J. Geophys. Res.*, **107**, doi:10.1029/2000JC000733.

Zwally, H. J., B. Schutz, W. Abdalati, J. Abshire, C. Bentley, A. Brenner, J. Bufton, J. Dezio, D. Hancock, D. Harding, T. Herring, B. Minster, K. Quinn, S. Palm, J. Spinhirne, and R. Thomas, 2002: ICESat's laser measurements of polar ice, atmosphere, ocean, and land. *J. Geodynam.*, **34**, 405–445.